5-2023

Improving Tribological Properties of Polydopamine/ Polytetrafluoroethylene Coatings Through Incorporating Core-shell Nanoparticles and Laser Surface Texturing

Firuze Soltani-Kordshuli
University of Arkansas, Fayetteville

Improving Tribological Properties of Polydopamine/Polytetrafluoroethylene Coatings Through Incorporating Core-shell Nanoparticles and Laser Surface Texturing

A dissertation submitted in partial fulfillment
of the requirements for the degree of
Doctor of Philosophy in Engineering

by

Firuze Soltani-Kordshuli
Shiraz University
Bachelor of Science in Mechanical Engineering, 2014
Shanghai Jiao Tong University
Master of Science in Mechanical Engineering, 2017

May 2023
University of Arkansas

This dissertation is approved for recommendation to the Graduate Council.

Min Zou, Ph.D.
Committee Chair

Jingyi Chen, Ph.D.
Committee Member

Xiangbo Meng, Ph.D.
Committee Member

Paul Millet, Ph.D.
Committee Member

Han Hu, Ph.D.
Committee Member

Abstract

Polytetrafluoroethylene (PTFE) is a widely used polymer that has unique properties such as chemical and temperature resistance, corrosion resistance, low maintenance cost, and a very low coefficient of friction (COF). These distinctive properties have made PTFE a promising candidate for industrial applications where surfaces are in relative motion. PTFE can be utilized as a thin film solid lubricant to significantly reduce the friction between moving surfaces. However, PTFE coatings have low cohesion and poor adhesion to the substrate resulting in its low wear resistance. This fact limits the application of PTFE coatings in load-bearing situations. To address these limitations, an adhesive polydopamine (PDA) underlayer was used to increase PTFE coating adhesion to stainless steel substrates and the resulting coating was labeled as PDA/PTFE. To prolong the wear life of PDA/PTFE coatings on stainless steel substrates, the coating cohesion and adhesion was improved by incorporating three different low concentration of Cu-SiO_2 core-shell nanoparticles (NPs) into the PTFE coatings. Also, the Hilbert curve patterns were laser textured on both the hard stainless steel substrate and the soft PTFE coating to improve the wear life. The mechanical and tribological properties of PDA/PTFE + Cu-SiO_2 NP coatings were investigated, and the wear mechanisms of smooth and laser-textured PDA/PTFE coatings on smooth and laser-textured stainless steel substrates were analyzed. The effects of laser power and texture density on the tribological behavior of PDA/PTFE coatings were also studied.

Adding low concentrations of Cu-SiO_2 core-shell NPs into the PTFE top layer increased the wear life of PDA/PTFE coatings, prevented the global delamination inside the wear track, improved the surface morphology of the coatings, and made the coating more coherent and interconnected and less porous. Also, the adhesion of the transferred film to the counterface ball was improved

after adding the NPs. Laser texturing the Hilbert curve pattern on the surface of stainless steel substrates provided reservoirs to store the PTFE lubricant and replenish it inside the wear track. Also, laser texturing the stainless steel substrate prevented the global delamination by providing interlocking for the PTFE coating. Altogether, it significantly increased the wear life of PDA/PTFE coatings. Higher laser powers contributed to deeper and wider texture grooves, providing larger reservoirs for PTFE lubricant. Also, laser texturing the PTFE coating made it softer without changing its chemical properties, and the softer coating experienced better compaction during the tribology tests. Therefore, laser-textured PTFE coating had much longer wear life, did not experience global delamination, and showed better adhesion at higher loads during the nanoscratch tests. Overall, this dissertation provides different methods to improve the wear resistance of PTFE coatings which increases their wear life. These advancements can result in cost savings and improved performance for industries that use PTFE coatings.

Acknowledgment

I would like to thank my incredible advisor for her unconditional support and for building an efficient and beneficial research environment. This journey wouldn't have been possible without her insightful guidance and help. I would also like to thank our collaborator, Prof. Jingyi Chen's group from the department of Chemistry and Biochemistry. I am also thankful to my committee members, Prof. Jingyi Chen, Dr. Paul Millet, Dr. Xiangbo Meng, and Dr. Han Hu, for their valuable time and feedback.

I would like to thank my lab mates for their collaboration and help during the past four years, and I'd like to acknowledge the University of Arkansas for the cutting-edge facilities that enabled my research to progress.

Last but not least, I'd like to thank my mother and my siblings for their emotional support and my husband and best friend, Yeasin, for always standing by my side throughout this journey.

Dedication

I dedicate this dissertation to the soul of my father who passed away 2 months after I started my Ph.D. studies. He was my biggest support before I began this journey and my greatest inspiration during the journey.

Contents

List of papers:

Soltani-Kordshuli, F., Okyere, D., Chen, J., Miller, C., Harris, N., Afshar-Mohajer, M., Ghosh, S.K. and Zou, M., 2021. Tribological behavior of the PDA/PTFE+ Cu-SiO_2 nanoparticle thin coatings. *Surface and Coatings Technology*, *409*, p.126852. (Included as Chapter 2 of this dissertation)

Authors contribution:
Soltani-Kordshuli: writing, sample preparation, tribology testing, WCA, EDX analysis, profilometry, optical microscopy imaging; Okyere & Chen: synthesis of nanoparticles, TEM imaging, UV-vis spectrum; Miller: measurements of hardness and modulus of elasticity; Harris: analysis of porosity and PTFE particle's size; Afshar-Mohajer: SEM imaging; Ghosh: AFM imaging; Zou: supervision.

Soltani-Kordshuli, F., Harris, N. and Zou, M., 2022. Tribological behavior of polydopamine/polytetrafluoroethylene coating on laser textured stainless steel with Hilbert curves. *Friction*, pp.1-13. (Included as Chapter 3 of this dissertation)

Authors contribution:
Soltani-Kordshuli: writing, sample preparation, tribology testing, AFM, XPS, profilometry, optical microscopy imaging; Harris: developing the Hilbert curve pattern G-code; Zou: supervision.

Soltani-Kordshuli, F., Miller, C., Harris, N. and Zou, M., 2023. Laser surface texturing of both thin polytetrafluoroethylene coatings and stainless steel substrates for improving tribological properties. *Polymer Testing*, *117*, p.107852. (Included as Chapter 4 of this dissertation)

Authors contribution:
Soltani-Kordshuli: writing, sample preparation, tribology testing, AFM, XPS, EDX analysis, profilometry, optical microscopy imaging; Miller: measurements of hardness and modulus of elasticity, nanoindentation testing, SEM; Harris: developing the Hilbert curve pattern G-code, PTFE particle size analysis; Zou: supervision.

Chapter 1

Introduction

Disclaimer:

Portions of this chapter were previously published as:

Soltani-Kordshuli, F., Okyere, D., Chen, J., Miller, C., Harris, N., Afshar-Mohajer, M., Ghosh, S.K. and Zou, M., 2021. Tribological behavior of the PDA/PTFE+ Cu-SiO_2 nanoparticle thin coatings. *Surface and Coatings Technology*, *409*, p.126852.

Soltani-Kordshuli, F., Harris, N. and Zou, M., 2022. Tribological behavior of polydopamine/polytetrafluoroethylene coating on laser textured stainless steel with Hilbert curves. *Friction*, pp.1-13.

Soltani-Kordshuli, F., Miller, C., Harris, N. and Zou, M., 2023. Laser surface texturing of both thin polytetrafluoroethylene coatings and stainless steel substrates for improving tribological properties. *Polymer Testing*, *117*, p.107852.

1.1 Background and Motivation

Tribology comes from the Greek word, tribo, which means rubbing. It is the science and engineering of surfaces that are interacting with each other and includes friction, wear, and lubrication [1, 2]. Tribology is an interdisciplinary science that is used to analyze significant economic problems in the world such as reliability, maintenance, and wear of a wide range of equipment from household appliances to spacecrafts [1].

Stainless steel has several significant properties making it one of the most attractive materials in industrial applications. For example, stainless steel is corrosion-resistant, durable, easily formable, tough, recyclable, etc. [3]. These unique properties allow stainless steel to withstand high levels of stress and wear, have a high resistance to impact and distress, be a suitable candidate for high-performance or heavy-duty applications and/or in harsh or corrosive

conditions, and be easily shaped and handled into a wide range of different forms and sizes. Besides, the 100% recyclability of stainless steel provides the advantage of melting and reusing it for new products which is beneficial for industries where sustainability and environmentally friendly materials are crucial. In general, stainless steel's unique combination of properties makes it an excellent material for use in many different industrial applications including aerospace, automotive, construction, and manufacturing [3].

While stainless steel is a highly convertible material with several different desirable properties, it has a relatively high coefficient of friction (COF) which can be undesirable in some applications, specifically where rubbing and interacting are involved. Therefore, appropriate lubricants can be applied on the surface of stainless steel to reduce its COF so that its performance in different applications and systems gets improved. Applying a solid lubricant coating such as polytetrafluoroethylene (PTFE) is a common approach for reducing the COF of stainless steel.

PTFE is a well-known polymer made from carbon and fluorine atoms connected with a very strong covalent bond. As shown in Figure 1.1, PTFE has a linear structure meaning that the individual monomers are connected to each other in a straight chain and gives it a rodlike shape. In other words, the (-CF_2-CF_2-) group in the PTFE structure repeats many times to form a long-chain polymer. The backbone of this chain is made of carbon-carbon bonds that are surrounded by carbon-fluorine bonds. As shown in Figure 1.1A, the size and shape of fluorine atoms provide a continuous covering around the C-C bonds which protects them from chemical attacks. This provides a part of PTFE chemical resistance. Both carbon-carbon and carbon-fluorine bonds are super strong covalent bonds having bonding energies of 607 KJ/mol and 552 KJ/mol, respectively [4]. The linear chain structure and the strong covalent C-C and C-F bonds in PTFE

provide some of its unique properties. For example, PTFE has a high-temperature resistance that allows it to withstand temperatures up to 260°C, or 500°F, without losing its physical or chemical properties. These strong bonds make PTFE highly chemical resistant which makes it inert against most chemicals and solvents as well as UV radiation and weathering. The strong bonds also make PTFE corrosion-resistant meaning that it does not degrade over time. Besides, PTFE has a low coefficient of thermal expansion which provides its stability under temperature changes without significant expansion or contraction. Furthermore, the cylindrical structure of PTFE results in weak intermolecular forces between its molecules and the easy transfer of microscopic amount of PTFE to the counterface. Therefore, PTFE would be rubbing against itself during sliding with a very low COF, leading to its self-lubricating property. Plus, PTFE has low maintenance costs. This can eliminate the need for frequent replacements and repairs.

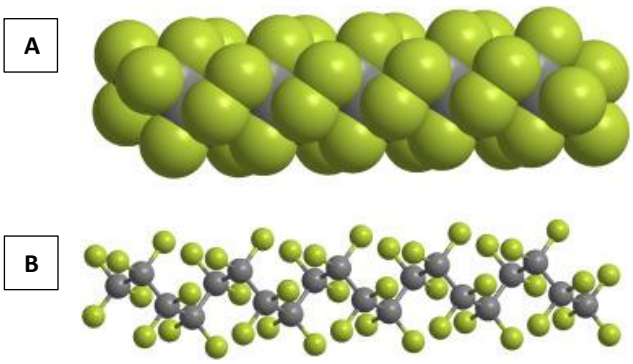

Figure 1.1: 3D chemical structure of polytetrafluoroethylene (PTFE): A) circular shape and size of atoms and B) the linear structure of the polymer. (gray spheres represent carbon atoms and green spheres represent fluorine atoms) [4].

All of the aforementioned properties make PTFE a promising candidate for a wide range of applications, including coatings, lubrications, gaskets, thermal sealing, bearings, insulations, electrical insulation, and biomedical implants [5, 6]. PTFE has been of great interest as a thin coating in several different industries. In ball bearings and polymeric gears, PTFE coatings are

used as solid lubricants for reducing the COF between surfaces [7]. It can be used as a coating on electrical cables and circuit boards due to its dielectric properties [8, 9]. PTFE coatings have clinical applications in implants, biomedical instruments, and stents because it is chemically inert [10]. Also, PTFE lubricant can be used as a coating on stainless steel to significantly decrease the COF between rubbing stainless steel surfaces in industry. When applied as a coating on stainless steel surfaces, PTFE can significantly reduce the friction between rubbing surfaces, which can improve the overall performance and lifetime of the system. For example, PTFE on stainless steel plates is commonly used in bridge bearing design to decrease the COF of stainless steel slip-style bearings [11]. In these cases, PTFE-coated stainless steel plates would degrade significantly less and therefore the whole system would have a much longer lifetime. This will eliminate the need for costly maintenance and replacements.

While PTFE has many desirable properties as a solid lubricant coating, it has relatively low wear resistance, meaning that it can be removed easily [12]. This fact limits the application of PTFE in high-load conditions. Researchers have investigated several approaches to improve the wear resistance of PTFE coatings. Incorporating nanoparticles (NPs) or fillers into the PTFE coating is a common approach that helps with reinforcing the material and improving its mechanical properties. Adding fillers such as carbon nanotubes, graphene, or metal oxides has shown significant improvement in the wear resistance of PTFE coatings [13-19]. Applying an adhesive underlayer to the surface before coating it with PTFE is another approach developed by researchers. The adhesive underlayer improves the adhesion of the PTFE to the substrate and hence improves its wear resistance [20]. Surface texturing is another approach employed for improving the wear resistance of PTFE coatings. Texturing micro or nanoscale patterns on the surface improves the adhesion of the coating and reduces the chance of wear or damage [21-23].

To elaborate, adding nanoparticles (NPs) and fillers is a common approach to improve the wear resistance of PTFE coatings. Figure 1.2 shows a schematic of NPs and/or fillers being added to PTFE coating. Although PTFE is a highly inert and thermally stable material that has excellent lubricating properties, it can be vulnerable to wear under certain conditions such as high loads or abrasive environments. Therefore, adding NPs and fillers can play a significant role by enhancing the wear resistance of PTFE coatings as NPs and fillers can provide additional reinforcement, increase hardness, and reduce friction. Also, the role of the fillers could be to improve the transfer film formation, reduce crack propagation, and improve the load-carrying capacity [13, 14, 17, 19, 24-26]. The most common NPs and fillers added to PTFE coatings include carbon nanotubes, graphene oxide, silica, alumina, and titanium dioxide. Adding a small amount of these NPs and fillers to PTFE coatings can improve their mechanical and tribological properties like hardness, scratch resistance, wear resistance, and COF. The type and concentration of the fillers are very important to be considered for coating development. It should be noted that a high concentration of hard fillers, such as SiO_2 NPs, could have negative effects on the wear behavior and friction of the films [24]. On the other hand, some NPs, such as Cu NPs, are soft, expensive, and chemically reactive, and it is desirable to use a low concentration and also make them chemically inert.

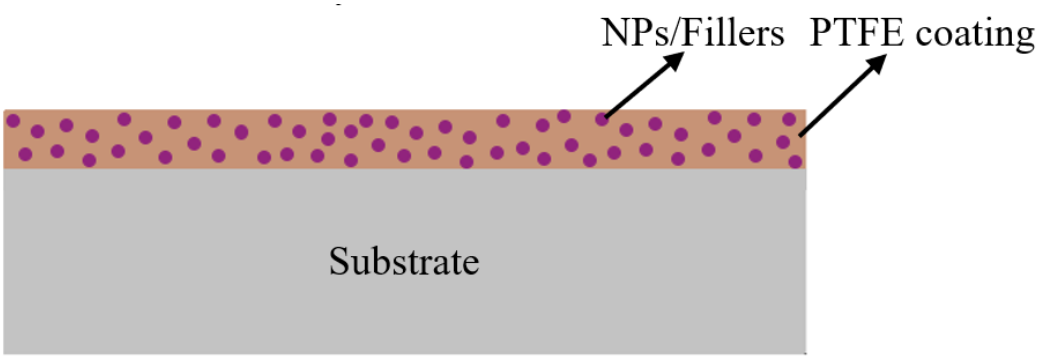

Figure 1.2: Adding NPs and/or fillers to the PTFE coating.

Even though adding NPs can improve the local wear resistance of the PTFE films, the weak adhesion of the PTFE films to the substrate can still be a leading cause of film failure [17, 24]. Polydopamine (PDA) has been used as an adhesive underlayer to increase the adhesion of PTFE to stainless steel substrates [13]. PTFE has poor adhesion to metals. On the other hand, PDA is an adaptable adhesive material that can bond to various types of surfaces, including stainless steel, by forming strong covalent bonds. Hence, depositing a thin layer of PDA on the stainless steel substrate before applying the PTFE coating significantly increases the adhesion between the two materials. PDA is a polymer that was inspired by nature and is known for its universal adhesion since it adheres to numerous organic and inorganic materials, including PTFE [27]. A group of researchers at Northwestern University discovered PDA for the first time in 2007 [28]. They reported that dopamine can polymerize in basic conditions and form a polymeric thin film on different surfaces like metals, plastics, ceramics, and glasses. The resulting film can then be further functionalized with different chemical groups or biomolecules which expands its applications in coatings, sensors, drug delivery, and tissue engineering. PDA is a self-assembled polymer that is synthesized by oxidation. It is shown that the formation of PDA happens in two simultaneous pathways: a non-covalent self-assembly in which a stable complex of (dopamine)2/5,6-dihydroxyindole (DHI) remains unpolymerized as self-assembled, and a covalent polymer oxidation in which the product of the oxidation, DHI, results in PDA formation [29]. The adhesive property of PDA might be due to the catechol functional groups in 3,4-dihydroxy-L-phenylalanine (DOPA) and the amine in lysine [30]. Figure 1.3 demonstrates the nature-inspired PDA and its polymerization and deposition process in a basic environment.

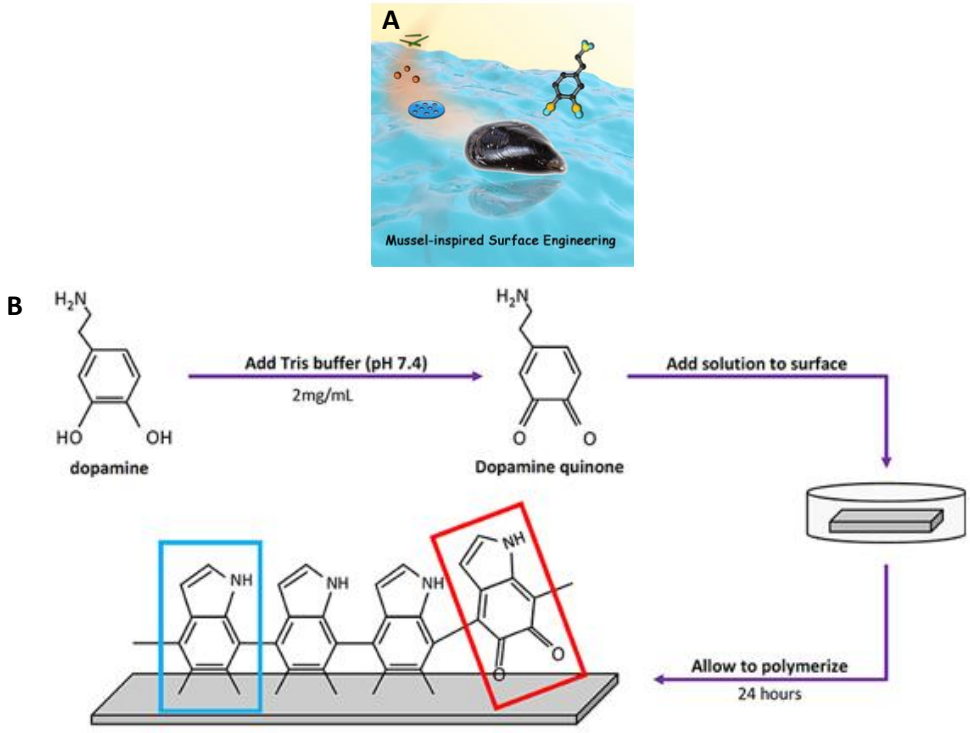

Figure 1.3: Polydopamine: A) a mussel-inspired surface modifier [31] and B) PDA polymerization and deposition process on the stainless steel [32].

Surface texturing is another approach that showed improvement in the wear resistance of solid lubricants [33]. The concept of surface texturing for improving wear resistance is fabricating micro or nanoscale textures on the surface to trap, store, and retain the solid lubricant within the texture features. Also, it increases the surface roughness which in turn increases the interlocking and resistance to tearing [34]. This will decrease the wear and prolong the lubrication lifetime. There are different ways to achieve surface texturing including chemical etching, laser surface texturing, and mechanical surface texturing (like shot peening or polishing). Depending on the material to be textured, the required application, and the designed texture pattern, the appropriate texturing method can be selected. While surface texturing using different techniques including etching and electron beam texturing has been used for several decades on the surfaces of magnetic [35] and micro-electromechanical systems (MEMS) [36]

devices, the combination of solid lubrication and texturing surfaces with laser for tribological application is relatively new [33].

Laser surface texturing has shown great promise for improving the wear resistance and COF of lubricated surfaces [37, 38]. Laser texturing enables control over the texture's shape and size. Also, it is a fast and environmentally friendly process [33] compared to other texturing methods. Laser texture characteristics such as arrangement [39], shape [40], size [41], and density [42] significantly affect the tribological behavior of laser-textured surfaces. The advantage of laser surface texturing over other surface texturing methods is its ability to create customizable texture features on the surface of materials. Adjusting the laser's parameters including energy level, pulse duration, and repetition rate allows the fabrication of various texture patterns like dimples and grooves with different sizes and shapes. In the laser surface texturing process, a laser beam with high power is applied to create microstructures on the surface of materials. During this process, the laser beam will focus on a very small area on the surface. This would heat the area locally and result in vaporizing or melting or ablating the material as shown in Figure 1.4.

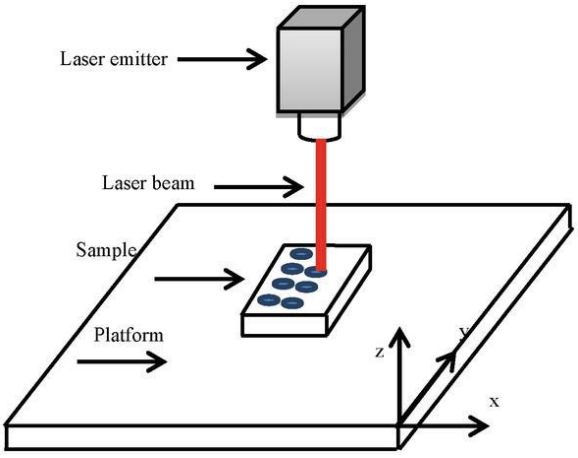

Figure 1.4: A schematic of laser surface texturing [43].

The ability of laser surface texturing to design complex patterns on the surface of different materials provides a wide range of applications for this process in industries where surface properties of the materials are important such as automotive, aerospace, and biomedical.

Using laser surface texturing, the surface properties of materials including friction, wear resistance, and hydrophobicity can be easily modified. To illustrate, laser surface texturing a metal reduces its friction and enhances its lubrication properties. Also, laser surface texturing a polymer improves its adhesion to other materials. Laser surface texturing has been successfully combined with different solid lubricants such as metal oxide coatings [44], diamond-like carbon (DLC) films [45, 46], and molybdenum disulfide (MoS_2) coatings [33, 47] and resulted in their enhanced performance in different tribological applications such as sliding contacts, rolling contacts, and cutting tools.

In general, laser surface texturing is a promising approach to improving the wear resistance of solid lubricants and this makes it a great method in different industries. However, it should be noted that laser surface texturing can be a complex and expensive process. Therefore, depending on the material properties, texture patterns, and operating conditions, careful design and optimization are necessary to obtain the desired performance and result.

In this dissertation, the wear mechanism of PDA/PTFE coatings on stainless steel substrates was investigated and different strategies were proposed for improving the wear resistance of PDA/PTFE coatings through incorporating core-shell NPs and laser surface texturing on hard stainless steel substrates and soft PTFE polymeric coatings. By shedding light on the role of surface modifications in the tribological behavior of PDA/PTFE coatings, this

dissertation contributes to the development of more effective and reliable solid lubricant coatings for industrial applications.

1.2 Literature Review

1.2.1 Tribological Properties of PTFE Coating

PTFE is well known for its tribological properties meaning its ability to reduce friction and wear between moving surfaces. PTFE can be applied as a coating on the surface of metals and other materials to provide significant tribological advantages including low COF, chemical resistance, high-temperature stability, low adhesion, and easy-release (non-sticky) properties.

Many studies have been conducted on the tribological properties of PTFE coatings. For example, Saisnith et al. studied the effect of temperature and environment on the tribological properties of PTFE coatings. In this study, they showed that the wear resistance of PTFE coatings decreases as the temperature increases [48]. In another study, Ghosh et al. investigated the impact of coating thickness on the tribological behavior of PTFE coatings. As expected, increasing the thickness of the coatings extended their wear life. This study showed that the longer wear life of thick PTFE coatings is due to the enhanced transfer film and larger contact area [49]. In a different study, Chen et al. investigated the influence of surface texturing on the tribological properties of composites consisting of graphene oxide (GO) and PTFE coatings. They confirmed that laser surface texturing considerably improved the wear life of PTFE coatings [50]. Peng et al. studied the tribological properties of PTFE coatings reinforced with black phosphorus nanoparticles. In this study, they compared the tribological behavior of thin PTFE coatings that are reinforced with either black phosphorus (BP) or ball-milled graphite nanoparticles to investigate their mechanism during reciprocating sliding tests [51]. In another

study, the impact of adding nanodiamonds to PTFE films on its tribological behavior was investigated. In this study, Lee et al. showed that, in the tested temperature ranges, adding nanodiamonds up to 2 wt.% to PTFE composite coating increases the wear resistance of the composite coating while further addition of nanodiamonds slightly decreased the wear resistance of the composite coating [25].

1.2.2 PDA Adhesive Underlayer

While PTFE suffers from low adhesion to other surfaces, another polymer called polydopamine (PDA) exists which can adhere to almost all surfaces. It was reported by Lee et al. in 2008 that PDA adheres to many organic and inorganic materials [30]. Researchers were inspired by sea mussels, which contain the same protein and attach to wet surfaces, to use PDA as a surface modifier [52]. The significant adhesion property of PDA makes it a promising choice to be used as a thin underlayer and to benefit the PTFE coating by increasing its adhesion to the surface of other materials. Indeed, PDA can be used as an anchoring agent for assisting the development of multi-layered coatings [53].

PDA was used in several studies as an adhesive layer on different surfaces for depositing functional and composite films such as ZrO_2/PDA to improve the anti-corrosion properties [54], and PDA/graphene oxide/perfluorodecyltrichlorosilane (PFDTS) to improve the tribological properties [55]. However, the reported COF in these studies was higher than in pristine PTFE coatings.

PDA has shown its ability to polymerize on stainless steel surfaces [56-59]. Developing an adhesive PDA underlayer that bonds to both stainless steel substrate and PTFE coatings resulted in improving the wear resistance of PTFE coating 500 times without affecting the low

COF of the PTFE coating [20]. Since the PDA layer has a very small thickness, it could have a significant application where thin and durable films are required [20]. It should be noted that not only thin PDA films do not affect the roughness and morphology of the top layer coating surfaces [57, 60] but also it can enhance the uniformity of the coatings by improving the hydrophilicity of the substrate [58].

Applying the PDA underlayer demonstrated significant improvement in the wear life of PTFE coatings. Several works studied the wear mechanism of different PDA/PTFE coatings on stainless steel substrates [14, 16, 19, 20, 26, 61-64]. It was shown that adding NPs to the PDA underlayer roughens the surface morphology which increased the mechanical interlocking between the PDA layer and the PTFE layer. Hence, the adhesion of PTFE coating to the PDA underlayer was improved [63, 64]. Also, adding NPs to PTFE top layer contributed to increased cohesion strength between PTFE particles, enhanced toughness within the PTFE matrix, and increased adhesion to the PDA underlayer [14, 16, 19, 26]. Compaction of PDA/PTFE coating decreased the porosity and roughness of PTFE coating, enhanced the adhesion, and increased the load-carrying capacity, as a result, prolonged the wear life of PDA/PTFE coating [62]. It was presented that the wear process of PDA/PTFE coatings consists of different stages such as plastic deformation, delamination, abrasive wear, and plowing [61]. Based on these results, in this dissertation, the PDA/PTFE coating durability will be further improved by adding Cu-SiO_2 core-shell NPs and laser surface texturing both PTFE coatings and the stainless steel substrates.

1.2.3 Incorporating Fillers and Nanoparticles

Some research studies have worked on improving the wear resistance of PTFE coatings by adding different NPs such as carbon NPs [13], nanodiamonds [25], SiO_2 NPs [24], and Au

NPs [16] to the PTFE coatings. The type and concentration of the fillers are very important to consider for coating development.

Beckford et al. incorporated SiO_2 NPs as fillers into PTFE films and showed that PTFE + SiO_2 NP composite films sustained more rubbing cycles compared to PTFE films while remaining at the same low COF [24]. SiO_2 NPs were found to enhance the development of transfer film on the counterface. Adding SiO_2 NPs to the PTFE film resulted in more fluorine in the wear track, which proved the improved adhesion of PTFE to the substrate. However, a high concentration of SiO_2 NPs was found to increase abrasive wear. In another work, the influence of adding Cu NPs as fillers in PTFE coatings was investigated [14]. It was shown that the presence of Cu NPs extended the wear life of PDA/PTFE films by 2 folds, even though the concentrations of Cu NPs were very low, at 0.01 wt%. Furthermore, the effect of incorporating PDA-coated Cu NPs into the PTFE top layer in PDA/PTFE coatings was studied, and it was illustrated that the existence of PDA-coated Cu NPs increased the adhesion of PTFE to the PDA underlayer, as well as improved the toughness of the coating [26].

Although Cu NPs improved the wear resistance of PTFE coatings, Cu is considered an expensive material. Also, it can oxidize quickly and form Cu oxide. Therefore, in this dissertation, soft Cu NPs will be coated with hard SiO_2 shells to make the NPs harder and allow using a lower concentration of Cu NPs compared to using pristine Cu NPs, while also providing a barrier to prevent the core from oxidization. Furthermore, core-shell nanostructures have been found to have novel high deformation resistance compared to nanostructures made of single materials [11-17], thus could enable even lower NP concentration. Implementing core-shell NPs enables the benefits of two different NPs to be harnessed at the same time while keeping their concentrations low.

1.2.4 Laser Surface Texturing

Laser surface texturing is a process during which different patterns or/and dimples will be textured on the surface using a laser beam. This method has better control and precision than traditional texturing methods such as sandblasting. Generally, laser surface texturing has applications in wettability [65, 66], increasing adhesion [67], enhancing wear life [68], and reducing friction [69, 70].

While laser surface texturing has been widely used to improve the wear life of different metals, it is a relatively new approach for improving the wear resistance of solid lubricant coatings. Also, there are fewer studies on the effect of laser surface texturing in dry lubricant conditions than with liquid lubrication. Wu et al. investigated the effect of the size and distance of laser-textured dimples on the wear and friction of titanium alloys under dry sliding conditions [71]. Their results showed that textured surfaces covered by molybdenum disulfide solid lubricants could reduce friction and its fluctuation compared to untextured surfaces covered with the same lubricant. In another study, AISI52100 bearing steel was textured with different densities by laser surface texturing, and it was shown that texture density could significantly affect its tribological behavior [72]. Also, Vilhena et al. illustrated that the depth and density of the laser textured dimples on steel, as well as the operating conditions such as sliding speed and lubrication mode, determined the improvement in the tribological behavior. They showed that deeper dimples and higher sliding speeds contribute to the most tribological improvements [73]. Gachot et al. textured austenitic stainless steel substrates to study the effect of laser patterns' alignment by doing dry sliding tests at different arrays of linear patterns with 0° and 90° relative alignment. They observed smaller friction for misaligned surfaces [74].

Studies showed that incorporating solid lubricant coatings with micro textures on the surface of steel [75], TiN [76], and TiCN [77] improved the wear life and wear behavior of the coatings, even for demanding tribological applications. In fact, laser surface texturing provided micro reservoirs of solid lubricants and/or micro traps of wear debris that helped improve the tribological behavior of the lubricant coating [78].

Few works have studied the combined effect of laser surface texturing and PTFE coating for improving tribological behaviors. Ye et al. investigated the effect of micro-pits textured stainless steel counter-face on the wear of alumina-PTFE nanocomposites. They suggested that, in the case of sliding against a polymeric and solid lubricant, more scattered, larger, and shallower pits would be better for reducing the wear [79]. Wang et al. examined the effect of laser parameters on the morphology of blind holes. They fabricated micro-hole array templates by laser drilling on electrophoretic deposited MoS_2-PTFE powder. They illustrated that the combination of 20% micro-hole density with MoS_2-10 wt% PTFE powder resulted in the lowest COF [21]. Fan et al. investigated the effect of double-layer textured PTFE on the Al_2O_3/Ni layered ceramics, and they observed 5 times improvement in the wear life of textured PTFE coating on the textured surface compared to smooth PTFE on the untextured surface [22]. Lu et al. examined the tribological behavior of PEO/PTFE and textured PEO/PTFE coatings on aluminum alloys under dry conditions. They observed a significantly reduced COF due to surface texturing which resulted from the compensation of the PTFE film inside the wear track [23].

All of the aforementioned studies investigated only two types of patterns: dimples and grooves in different shapes such as circular, triangle, and rectangular dimples and/or linear and wavy grooves [68]. Also, the combined effect of laser surface texturing and PTFE coating on

stainless steel substrates using an adhesive PDA underlayer has not been investigated. In the current work, mirror-finished stainless steel substrates were laser textured with a novel Hilbert curve pattern, an easily programmable space-filling pattern, and assessed the texture's effect on the wear mechanisms, wear life, and COF of PDA/PTFE coatings. Also, previous studies only investigated PTFE coatings with a thickness of more than 20 μm and texture depths of more than 50 μm on the substrates [19, 20]. Deep textures may significantly weaken the mechanical properties of the substrate and will not benefit thin coatings since the coating could not be replenished from the deep valleys of the textures. It is hypothesized that fabricating laser textures on stainless steel substrates with a shallow Hilbert curve pattern could improve the wear life of thin PDA/PTFE coatings. This texture pattern has not been studied for tribological performance before. In the current work, the effects of the laser texture density (texture area coverage) and laser power (LP) were studied to evaluate the effect of shallow Hilbert curve textures on the friction and wear of thin PDA/PTFE coatings.

Also, the effect of laser texturing the PTFE coating is a completely new approach that needs further detailed investigation. All of the previous studies have investigated the effect of laser texturing the substrate on the wear mechanism of PTFE coating. Here, laser texturing the PTFE will be studied to provide a detailed understanding of the relation between coating surface topography and its tribological behavior. This dissertation provides a comprehensive study on the effect of laser texturing with low laser power on the surface topography and wear mechanism of PTFE coatings.

1.3 Research Goals and Objectives

The goal of this dissertation research is to prolong the wear life of PDA/PTFE coatings on stainless steel substrates by improving coating cohesion and adhesion to the substrate so that industrial applications where load bearings are applied can benefit from the very low COF of PTFE without suffering from its low wear resistance. This goal will be accomplished by incorporating Cu-SiO_2 core-shell NPs into the PTFE layer and applying laser texturing to stainless steel substrates and PTFE coatings. The detailed objectives to meet this goal are:

- Investigating and understanding the wear mechanism of PDA/PTFE + Cu-SiO_2 core-shell NP coatings and identifying an optimal concentration of Cu-SiO_2 core-shell NPs to be incorporated into the PTFE top layer.
- Understanding the effect of laser surface texturing the stainless steel substrates on the tribological behavior of PDA/PTFE coatings and determining an optimum laser power for texturing the surface of stainless steel substrates.
- Assessing the effect of laser texturing the surface of soft PTFE coating on the tribological behavior of PDA/PTFE coatings and examining whether laser texturing changes the chemical composition of the PTFE polymer.

Chapter 2 of this dissertation focuses on the tribological behavior of the PDA/PTFE + Cu-SiO_2 core-shell NP thin coatings. Cu-SiO_2 core-shell NPs have been incorporated into the PTFE top layer of PDA/PTFE coatings, as shown in Figure 1.5, in three different concentrations. Then, the mechanical and tribological properties of the PDA/PTFE + Cu-SiO_2 NP thin coatings were studied and results are reported in this chapter [15].

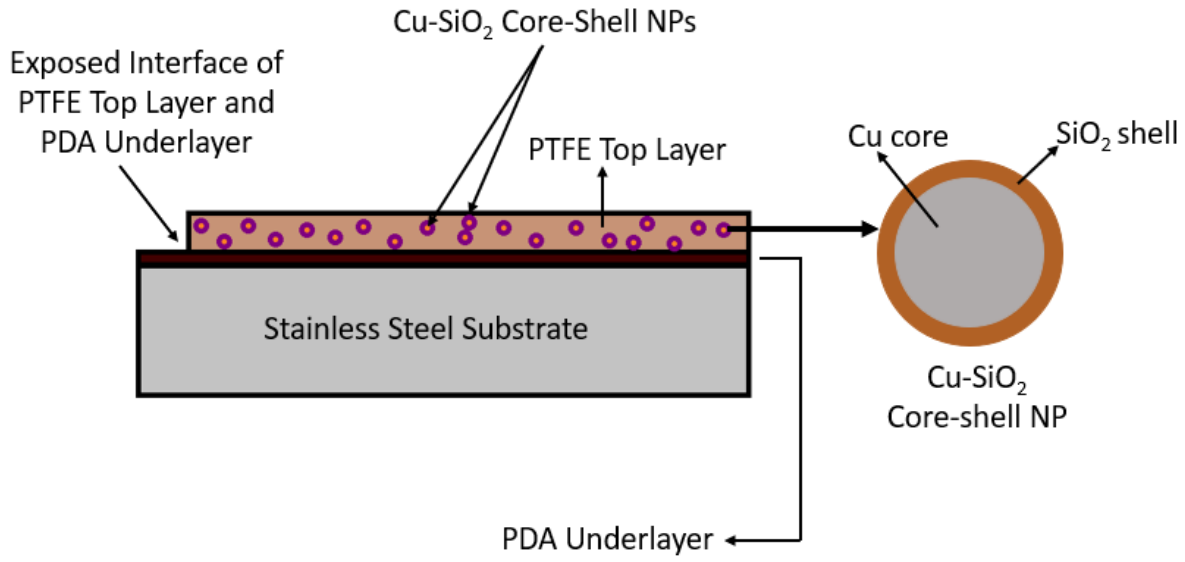

Figure 1.5: Incorporating Cu-SiO_2 core-shell NPs into the PTFE top layer of PDA/PTFE thin coatings.

Chapter 3 of this dissertation is about the tribological properties of PDA/PTFE coatings on laser-textured stainless steel with Hilbert curve patterns. Applying four different laser powers and two different texture densities, Hilbert curve patterns (Figure 1.6A) were laser textured on the surface of stainless steel substrates and then PDA/PTFE was coated on laser-textured stainless steel as shown in Figure 1.6B. The effect of laser power and texture density on the wear and friction of PDA/PTFE coatings was investigated and reported in chapter 3 [80].

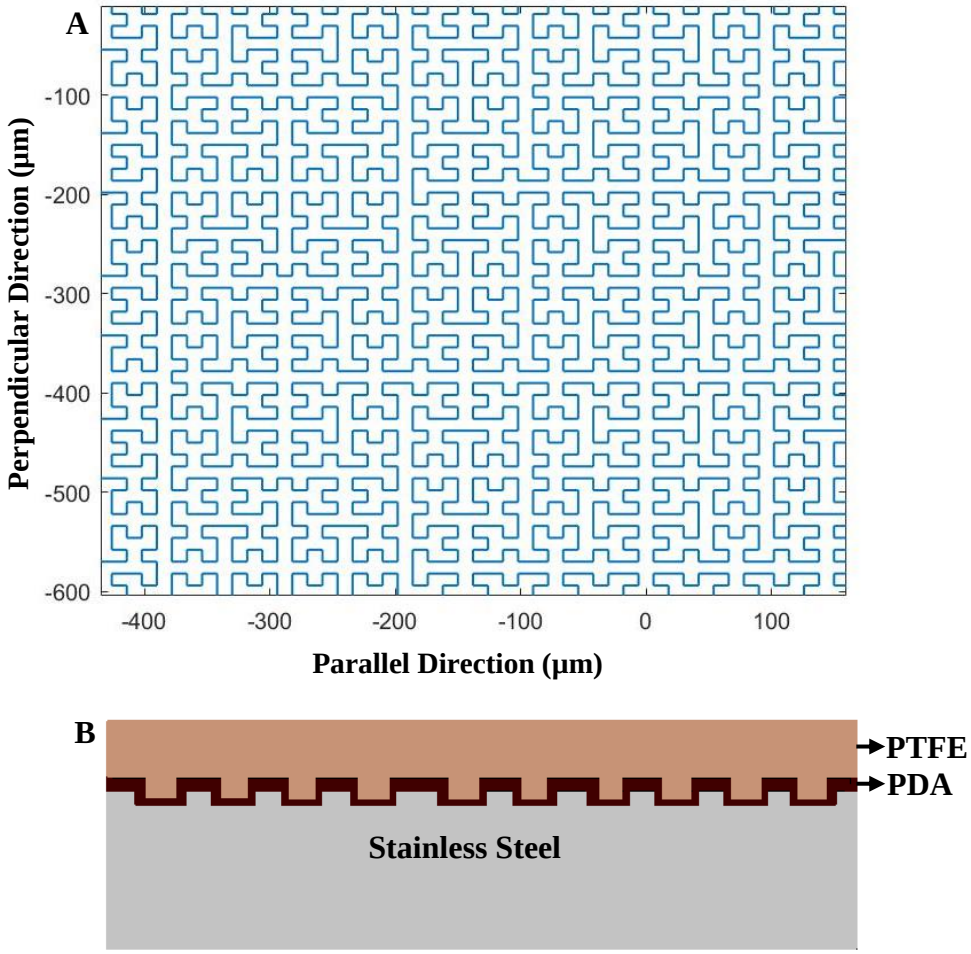

Figure 1.6: A) Mathematical image of the Hilbert curve pattern and B) PDA/PTFE coatings on the laser-textured stainless steel substrate.

In chapter 4 of this dissertation, the laser surface texturing of both thin PTFE coatings and stainless steel substrates for improving tribological properties is reported. In this chapter, four types of samples with smooth and laser-textured PTFE on the smooth and laser-textured substrates were fabricated and their tribological and mechanical behavior was investigated. Figure 1.7 shows the sample types that were studied in chapter 4 [81].

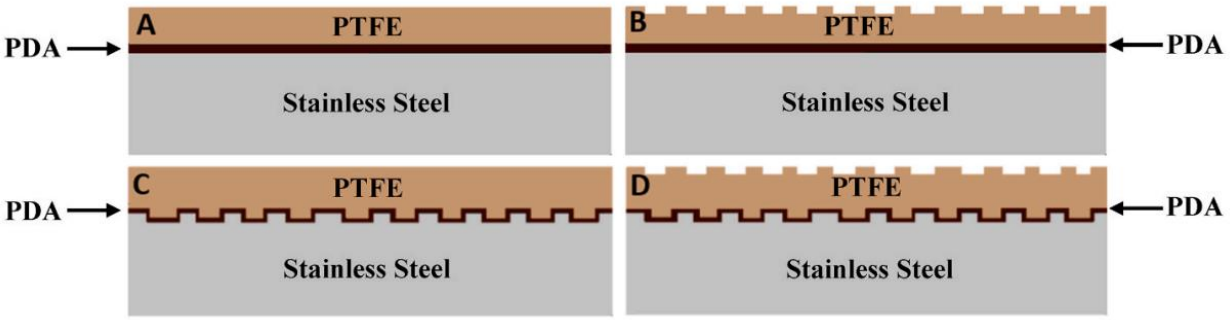

Figure 1.7: Schematic of PDA/PTFE coatings with smooth and laser-textured PTFE top layer on smooth and laser-textured stainless steel substrate: A) smooth PTFE on the smooth substrate, B) smooth PTFE on the laser-textured substrate, C) laser-textured PTFE on the smooth substrate, and D) laser-textured PTFE on the laser-textured substrate.

A ball-on-disk configuration was used in chapters 2-4 to study the tribological behavior of the PDA/PTFE coatings. As shown in Figure 1.8, a chrome steel ball was used as the counterface in a reciprocating sliding movement on the surface of the PTFE coating.

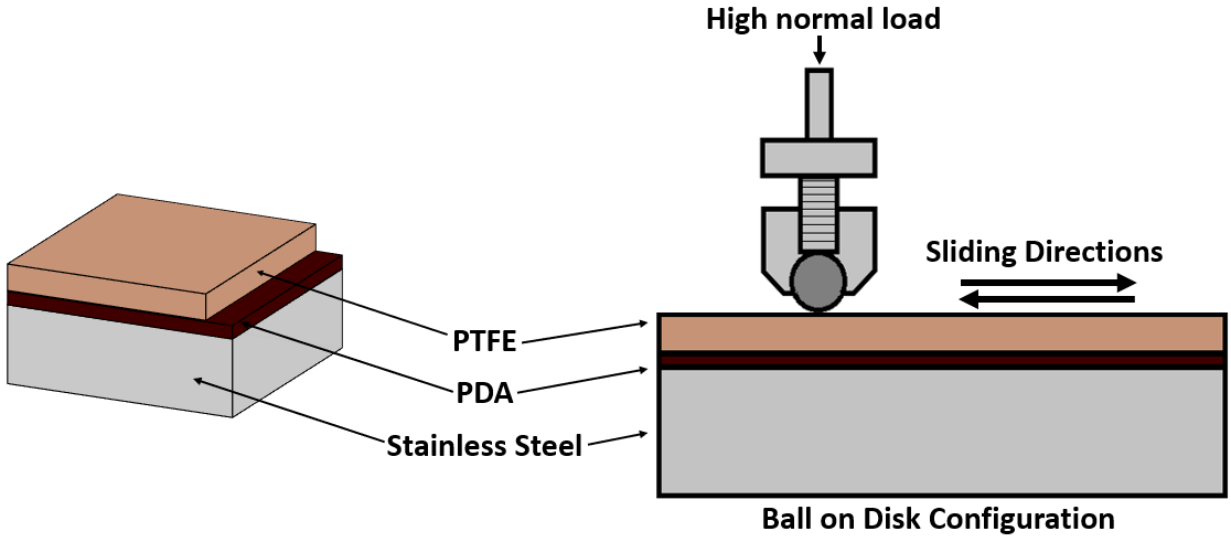

Figure 1.8: Schematic of ball-on-disk configuration test setup (not-to-scale).

1.4 Fabrication and Characterization Instruments

In this section, an overview of the instruments and devices employed in this dissertation is presented in Figures 1.9 to 1.19.

An AutoMet 250 Grinder-Polisher (Buehler, IL, USA) was applied to mirror-polish the stainless steel substrates (Figure 1.9). An A-series femtosecond laser micromachining system (32-Oxford Laser A5 Femtosecond, Oxford Lasers Ltd., UK) was used to texture Hilbert curve patterns on the polished stainless steel substrates (Figure 1.10).

A digital rocking bath was used at a rocking rate of 25 rpm and a rocking angle of 7° to deposit PDA on stainless steel substrates (Figure 1.11). A dip coater (KSV Dip Coater, MD, USA) was used to coat PTFE on the PDA deposited stainless steel substrate (Figure 1.12).

Figure 1.9: Buehler AutoMet 250 Grinder-Polisher.

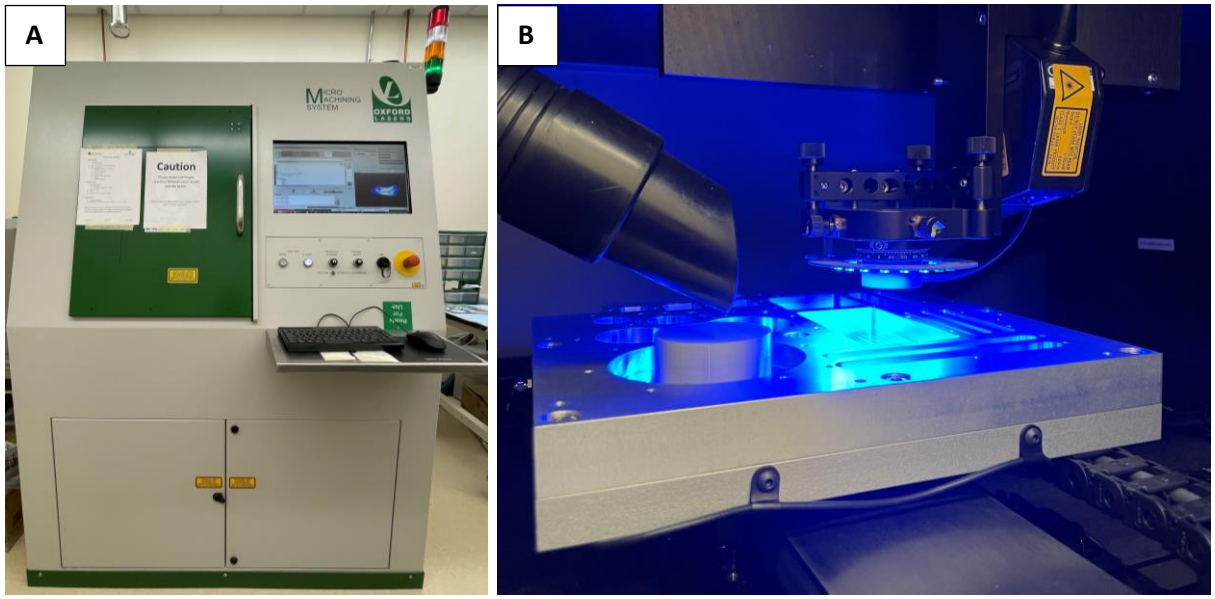

Figure 1.10: Oxford Laser A5 Femtosecond: A) view of the complete instrument and B) the laser beam inside the chamber.

A stylus profilometry (Dektak 150, Bruker Nano Surfaces) was used to measure the thickness of PTFE coatings (Figure 1.13). An atomic force microscopy (Dimension Icon, Bruker) was used to image the topography and measure the surface roughness of PTFE coatings (Figure 1.14).

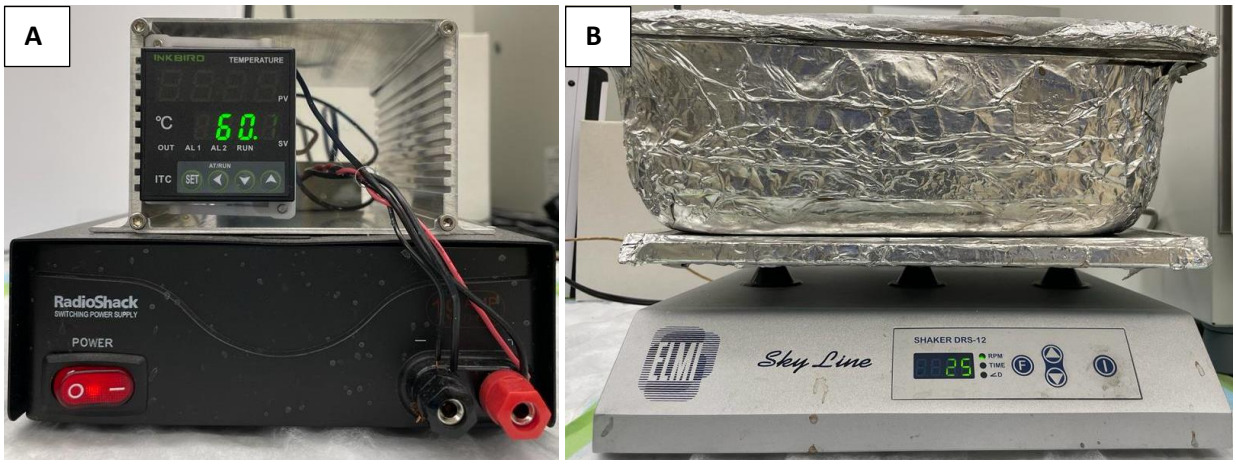

Figure 1.11: PDA deposition system: A) the thermostat panel and B) the rocking bath.

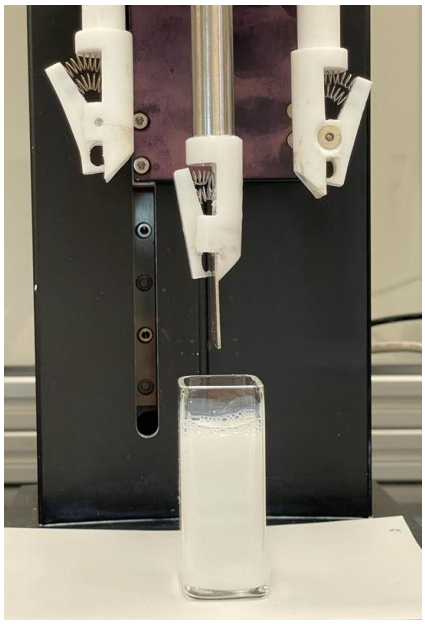

Figure 1.12: KSV Dip coater.

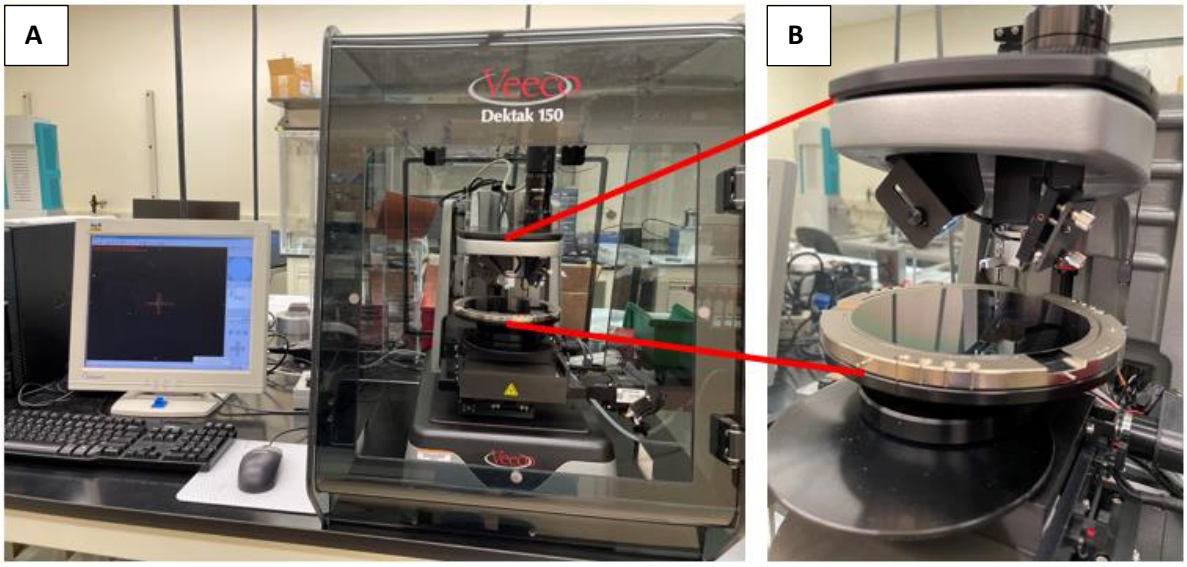

Figure 1.13: Dektak stylus profilometer: A) the complete view of the instrument and B) the close-up view of the profilometer tip.

A tribometer (UMT, Bruker) was used to perform tribology tests including durability (wear life), progressive wear, and scratch tests (Figure 1.15). A nanoindenter (TriboIndenter, Hysitron) was used to measure the hardness and modulus of elasticity of PTFE coatings, perform indentation, and load-controlled scratch tests (Figure 1.16).

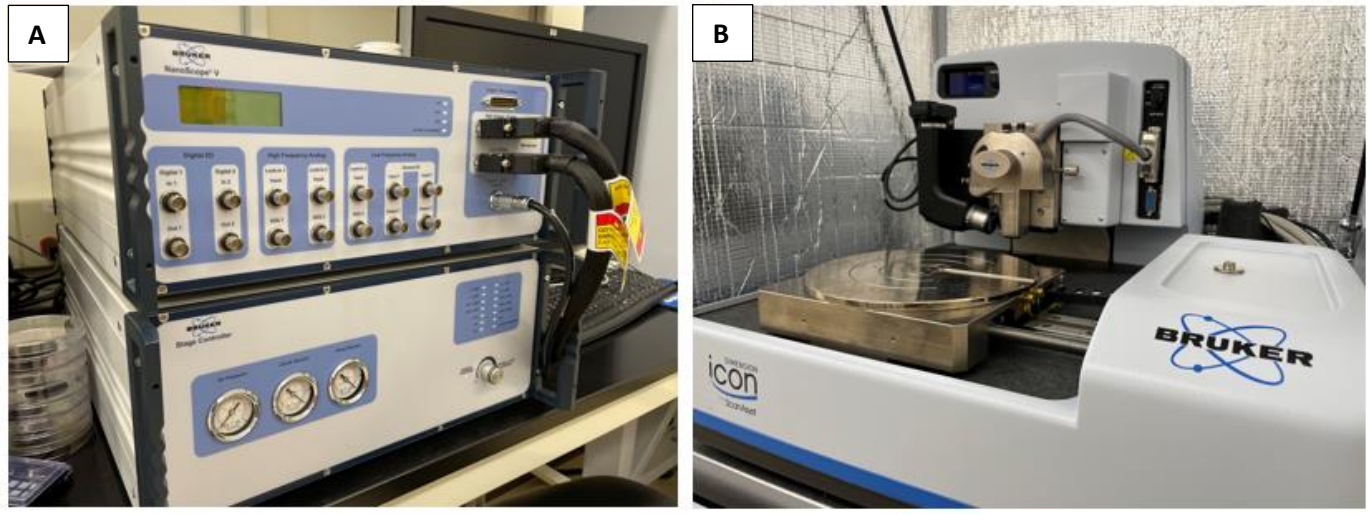

Figure 1.14: Atomic force microscopy (AFM): A) the nanoscope stage controller and B) the AFM tip and sample stage.

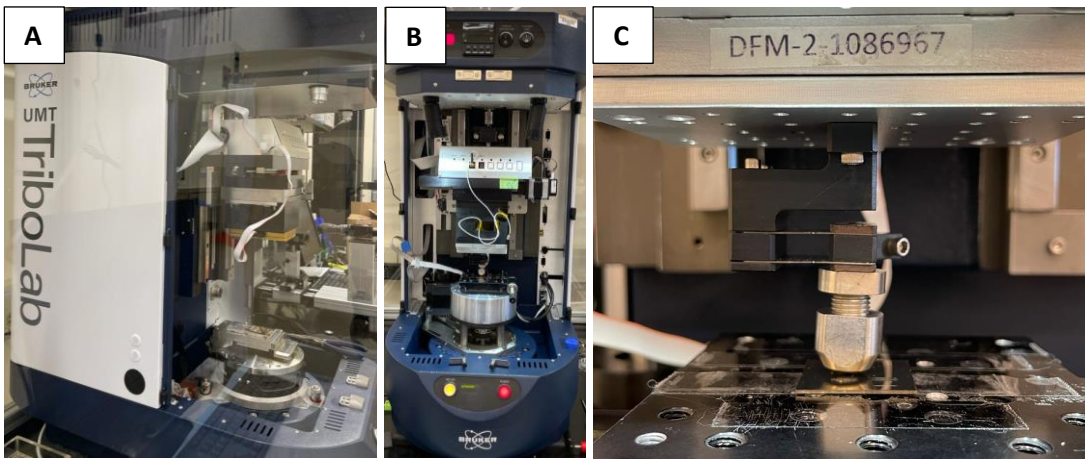

Figure 1.15: Bruker UMT TriboLab: A) side view, B) front view, and C) ball-on-disk configuration.

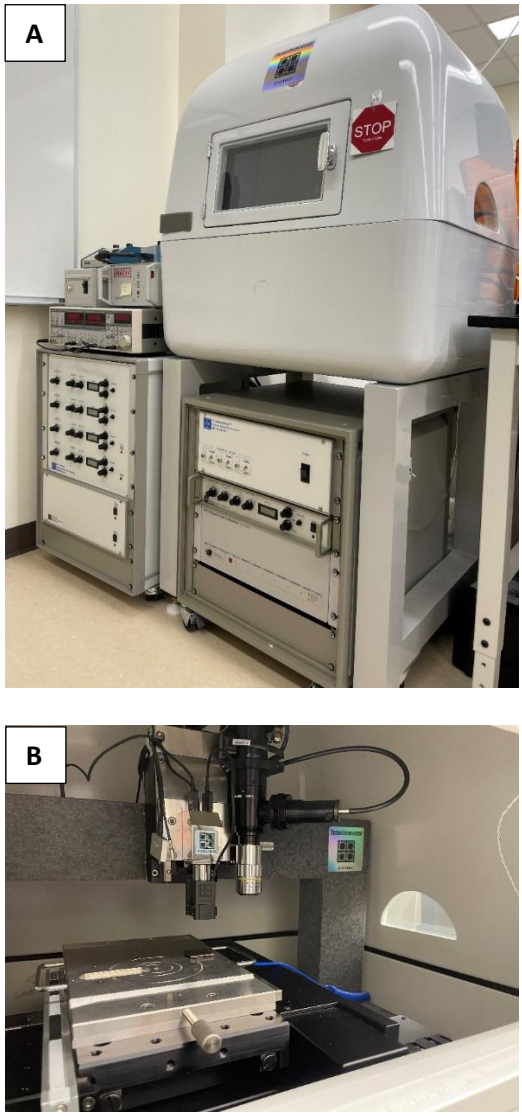

Figure 1.16: Hysitron TriboIndenter: A) photo of the complete instrument and B) the indenter inside the chamber.

A 3D laser scanning confocal microscopy (VK-X260, Keyence Corporation) was applied to measure the wear tracks and counterface balls after durability tests, and the textured patterns on the stainless steel substrates (Figure 1.17). A scanning electron microscopy (SEM) (VEGA 3, TESCAN) was used to characterize the microscale topography of the PTFE coatings (Figure 1.18). Also, Energy-dispersive X-ray spectroscopy (EDS) (XL-30, Phillips/FEI) was employed to image and map the elements on the wear tracks after the durability tests (Figure 1.18).

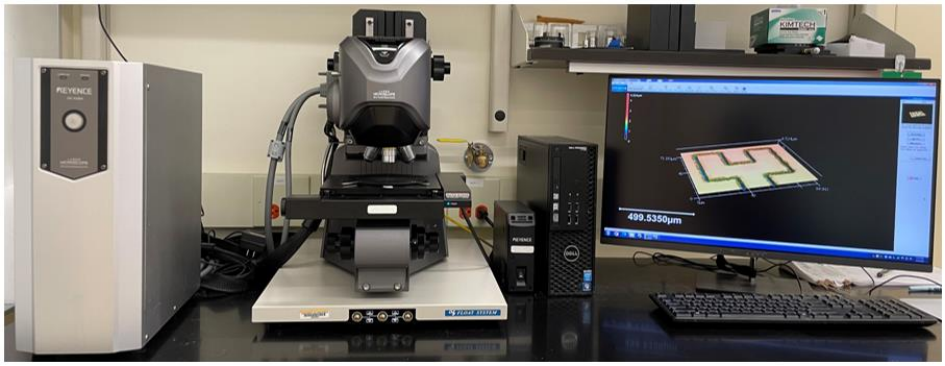

Figure 1.17: Keyence 3D laser scanning confocal microscopy.

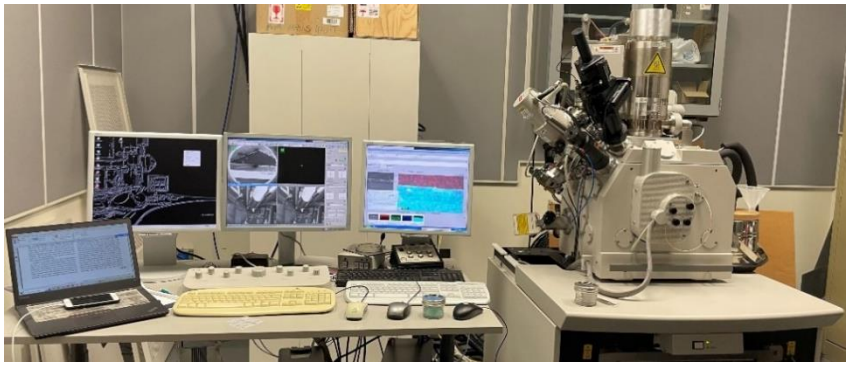

Figure 1.18: Scanning Electron Microscopy (SEM).

A goniometer (OCA 15, DataPhysics Instruments) was used to measure the water contact angle on the surface of PTFE coatings (Figure 1.19).

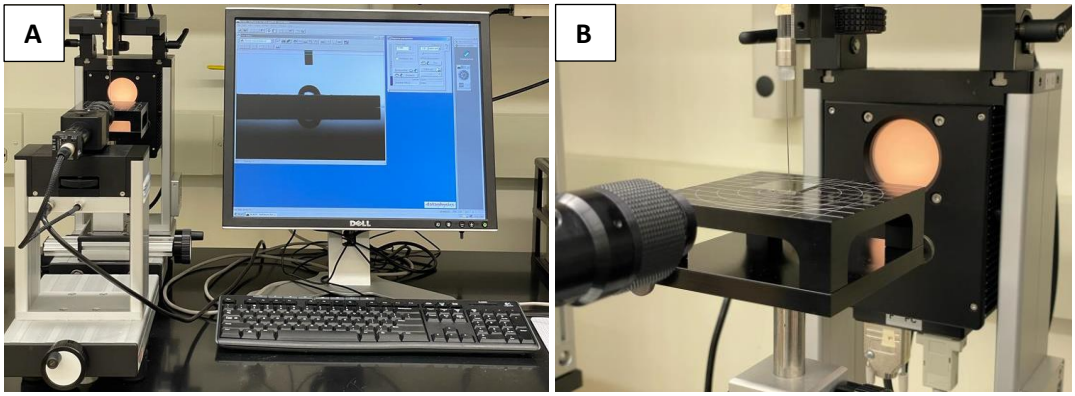

Figure 1.19: Water Contact Angle (WCA) measurement: A) a complete view of the instrument and B) a close-up view of the water dispenser.

References

[1] B. Bhushan, *Introduction to tribology*. John Wiley & Sons, 2013.

[2] G. W. Stachowiak and A. W. Batchelor, *Engineering tribology*. Butterworth-heinemann, 2013.

[3] N. Baddoo, "Stainless steel in construction: A review of research, applications, challenges and opportunities," *Journal of constructional steel research,* vol. 64, no. 11, pp. 1199-1206, 2008.

[4] L. W. McKeen, *Fluorinated coatings and finishes handbook: The definitive user's guide*. William Andrew, 2015.

[5] E. Dhanumalayan and G. M. Joshi, "Performance properties and applications of polytetrafluoroethylene (PTFE)—a review," *Advanced Composites and Hybrid Materials,* vol. 1, no. 2, pp. 247-268, 2018.

[6] H. Unal, A. Mimaroglu, U. Kadıoglu, and H. Ekiz, "Sliding friction and wear behaviour of polytetrafluoroethylene and its composites under dry conditions," *Materials & Design,* vol. 25, no. 3, pp. 239-245, 2004.

[7] X.-D. Yuan and X.-J. Yang, "A study on friction and wear properties of PTFE coatings under vacuum conditions," *Wear,* vol. 269, no. 3-4, pp. 291-297, 2010.

[8] Z. Xia, A. Wedel, and R. Danz, "Charge storage and its dynamics in porous polytetrafluoroethylene (PTFE) film electrets," *IEEE transactions on dielectrics and electrical insulation,* vol. 10, no. 1, pp. 102-108, 2003.

[9] D. N. Light and J. R. Wilcox, "Process considerations in the fabrication of fluoropolymer printed circuit boards," *IEEE Transactions on Components, Packaging, and Manufacturing Technology: Part A,* vol. 18, no. 1, pp. 118-126, 1995.

[10] F.-H. Su, Z.-Z. Zhang, and W.-M. Liu, "Study on the friction and wear properties of glass fabric composites filled with nano-and micro-particles under different conditions," *Materials Science and Engineering: A,* vol. 392, no. 1-2, pp. 359-365, 2005.

[11] "Low Frictional Resistance of PTFE: A Benefit in Bridge Bearing Design." https://www.ipolymer.com/blog/low-frictional-resistance-of-ptfe-a-benefit-in-bridge-bearing-design/ (accessed 2016).

[12] C. Donnet and A. Erdemir, "Solid lubricant coatings: recent developments and future trends," *Tribology Letters,* vol. 17, no. 3, pp. 389-397, 2004.

[13] J.-Y. Lee, D.-P. Lim, and D.-S. Lim, "Tribological behavior of PTFE nanocomposite films reinforced with carbon nanoparticles," *Composites Part B: Engineering,* vol. 38, no. 7-8, pp. 810-816, 2007.

[14] S. Beckford, L. Mathurin, J. Chen, and M. Zou, "The influence of Cu nanoparticles on the tribological properties of polydopamine/PTFE+ Cu films," *Tribology Letters,* vol. 59, no. 1, pp. 1-9, 2015.

[15] F. Soltani-Kordshuli *et al.*, "Tribological behavior of the PDA/PTFE+ Cu-SiO2 nanoparticle thin coatings," *Surface and Coatings Technology,* vol. 409, p. 126852, 2021.

[16] S. Beckford, L. Osborn, M. Zou, J. Cai, and J. Chen, "Tribological study of PTFE/Au nanoparticle composite thin films," in *International Joint Tribology Conference,* 2011, vol. 54747, pp. 1-3.

[17] S. Beckford, J. Cai, J. Chen, and M. Zou, "Use of Au nanoparticle-filled PTFE films to produce low-friction and low-wear surface coatings," *Tribology Letters,* vol. 56, no. 2, pp. 223-230, 2014.

[18] D. Choudhury, C. Miller, and M. Zou, "Tribological performance of PDA/PTFE+ graphite particle coatings on 60NiTi," *Applied Surface Science,* vol. 527, p. 146731, 2020.

[19] S. Beckford, J. Cai, R. A. Fleming, and M. Zou, "The effects of graphite filler on the tribological properties of polydopamine/PTFE coatings," *Tribology Letters,* vol. 64, no. 3, pp. 1-10, 2016.

[20] S. Beckford and M. Zou, "Wear resistant PTFE thin film enabled by a polydopamine adhesive layer," *Applied surface science,* vol. 292, pp. 350-356, 2014.

[21] A. Wang, J. Xia, Z. Yang, and D. Xiong, "A novel assembly of MoS2-PTFE solid lubricants into wear-resistant micro-hole array template and corresponding tribological performance," *Optics & Laser Technology,* vol. 116, pp. 171-179, 2019.

[22] H. Fan, Y. Su, J. Song, H. Wan, L. Hu, and Y. Zhang, "Design of “double layer” texture to obtain superhydrophobic and high wear-resistant PTFE coatings on the surface of Al2O3/Ni layered ceramics," *Tribology International,* vol. 136, pp. 455-461, 2019.

[23] C. Lu, P. Shi, J. Yang, J. Jia, E. Xie, and Y. Sun, "Effects of surface texturing on the tribological behaviors of PEO/PTFE coating on aluminum alloy for heavy-load and long-performance applications," *Journal of Materials Research and Technology,* vol. 9, no. 6, pp. 12149-12156, 2020.

[24] S. Beckford, Y. Wang, and M. Zou, "Wear-resistant PTFE/SiO2 nanoparticle composite films," *Tribology Transactions,* vol. 54, no. 6, pp. 849-858, 2011.

[25] J.-Y. Lee and D.-S. Lim, "Tribological behavior of PTFE film with nanodiamond," *Surface and Coatings Technology,* vol. 188, pp. 534-538, 2004.

[26] S. Beckford, L. Mathurin, J. Chen, R. A. Fleming, and M. Zou, "The effects of polydopamine coated Cu nanoparticles on the tribological properties of polydopamine/PTFE coatings," *Tribology International,* vol. 103, pp. 87-94, 2016.

[27] H. Li *et al.*, "Synthesis and catalytic performance of polydopamine supported metal nanoparticles," *Scientific reports,* vol. 10, no. 1, pp. 1-7, 2020.

[28] H. Lee, S. Dellatore, W. Miller, and P. Messersmith, "Mussel-Inspired Surface Chemistry for Multifunctional Coatings. science 2007, 318 (5849), 426–430," ed: DOI.

[29] S. Hong, Y. S. Na, S. Choi, I. T. Song, W. Y. Kim, and H. Lee, "Non-covalent self-assembly and covalent polymerization co-contribute to polydopamine formation," *Advanced Functional Materials,* vol. 22, no. 22, pp. 4711-4717, 2012.

[30] H. Lee, "Bioadhesion of mussels and geckos: Molecular mechanics, surface chemistry, and nanoadhesives," Northwestern University, 2008.

[31] Z. Wang *et al.*, "Mussel-inspired surface engineering for water-remediation materials," *Matter,* vol. 1, no. 1, pp. 115-155, 2019.

[32] A. Tyo, S. Welch, M. Hennenfent, P. Kord Fooroshani, B. P. Lee, and R. Rajachar, "Development and characterization of an antimicrobial polydopamine coating for conservation of humpback whales," *Frontiers in Chemistry,* vol. 7, p. 618, 2019.

[33] T. Hu, Y. Zhang, and L. Hu, "Tribological investigation of MoS2 coatings deposited on the laser textured surface," *Wear,* vol. 278, pp. 77-82, 2012.

[34] C. Miller, D. Choudhury, and M. Zou, "The effects of surface roughness on the durability of polydopamine/PTFE solid lubricant coatings on NiTiNOL 60," *Tribology Transactions,* vol. 62, no. 5, pp. 919-929, 2019.

[35] R. Ranjan, D. Lambeth, M. Tromel, P. Goglia, and Y. Li, "Laser texturing for low-flying-height media," *Journal of Applied Physics,* vol. 69, no. 8, pp. 5745-5747, 1991.

[36] K. Komvopoulos, "Adhesion and friction forces in microelectromechanical systems: mechanisms, measurement, surface modification techniques, and adhesion theory," *Journal of adhesion science and technology,* vol. 17, no. 4, pp. 477-517, 2003.

[37] A. Kovalchenko, O. Ajayi, A. Erdemir, G. Fenske, and I. Etsion, "The effect of laser surface texturing on transitions in lubrication regimes during unidirectional sliding contact," *Tribology International,* vol. 38, no. 3, pp. 219-225, 2005.

[38] L. Mourier, D. Mazuyer, F. Ninove, and A. Lubrecht, "Lubrication mechanisms with laser-surface-textured surfaces in elastohydrodynamic regime," *Proceedings of the Institution of Mechanical Engineers, Part J: Journal of Engineering Tribology,* vol. 224, no. 8, pp. 697-711, 2010.

[39] S.-C. Vlădescu, A. Ciniero, K. Tufail, A. Gangopadhyay, and T. Reddyhoff, "Looking into a laser textured piston ring-liner contact," *Tribology International,* vol. 115, pp. 140-153, 2017.

[40] J. Bressan and J. Williams, "Mathematical slip-line field solutions for ploughing a hard particle over a softer material," *Wear,* vol. 267, no. 11, pp. 1865-1872, 2009.

[41] S. P. Mishra and A. A. Polycarpou, "Tribological studies of unpolished laser surface textures under starved lubrication conditions for use in air-conditioning and refrigeration compressors," *Tribology International,* vol. 44, no. 12, pp. 1890-1901, 2011.

[42] A. Kovalchenko, A. Erdemir, O. Ajayi, and I. Etsion, "Tribological behavior of oil-lubricated laser textured steel surfaces in conformal flat and non-conformal contacts," *Materials Performance and Characterization,* vol. 6, no. 2, pp. 1-23, 2017.

[43] N. Jeyaprakash, C.-H. Yang, and D. R. Kumar, "Laser Surface Modification of Materials," in *Practical Applications of Laser Ablation*: IntechOpen London, UK, 2020.

[44] S. Yuan *et al.*, "In-situ fabrication of gradient titanium oxide ceramic coating on laser surface textured Ti6Al4V alloy with improved mechanical property and wear performance," *Vacuum,* vol. 176, p. 109327, 2020.

[45] D. He, S. Zheng, J. Pu, G. Zhang, and L. Hu, "Improving tribological properties of titanium alloys by combining laser surface texturing and diamond-like carbon film," *Tribology international,* vol. 82, pp. 20-27, 2015.

[46] N. Yasumaru, K. Miyazaki, and J. Kiuchi, "Control of tribological properties of diamond-like carbon films with femtosecond-laser-induced nanostructuring," *Applied Surface Science,* vol. 254, no. 8, pp. 2364-2368, 2008.

[47] Y. Liu, J. Li, S. Yi, X. Ge, X. Chen, and J. Luo, "Enhancement of friction performance of fluorinated graphene and molybdenum disulfide coating by microdimple arrays," *Carbon,* vol. 167, pp. 122-131, 2020.

[48] V. Saisnith and V. Fridrici, "A study of the wear damage of a PTFE coating: The effects of temperature and environment on its mechanical and tribological properties," *Wear,* vol. 480, p. 203946, 2021.

[49] S. K. Ghosh, C. Miller, D. Choudhury, J. A. Goss, and M. Zou, "The effects of PTFE thickness on the tribological behavior of thick PDA/PTFE coatings," *Tribology Transactions,* vol. 63, no. 3, pp. 575-584, 2020.

[50] Z. Chen, Z. Wu, J. Sun, C. Mao, and F. Su, "Improved load-bearing capacity and tribological properties of PTFE coatings induced by surface texturing and the addition of GO," *Tribology Letters,* vol. 69, pp. 1-15, 2021.

[51] S. Peng, Y. Guo, G. Xie, and J. Luo, "Tribological behavior of polytetrafluoroethylene coating reinforced with black phosphorus nanoparticles," *Applied Surface Science,* vol. 441, pp. 670-677, 2018.

[52] J. H. Waite and M. L. Tanzer, "Polyphenolic substance of Mytilus edulis: novel adhesive containing L-dopa and hydroxyproline," *Science,* vol. 212, no. 4498, pp. 1038-1040, 1981.

[53] Y. Han *et al.,* "Self-adhesive lubricated coating for enhanced bacterial resistance," *Bioactive Materials,* vol. 6, no. 8, pp. 2535-2545, 2021.

[54] J. Ou, J. Wang, Y. Qiu, L. Liu, and S. Yang, "Mechanical property and corrosion resistance of zirconia/polydopamine nanocomposite multilayer films fabricated via a novel non-electrostatic layer-by-layer assembly technique," *Surface and interface analysis,* vol. 43, no. 4, pp. 803-808, 2011.

[55] J. Ou, L. Liu, J. Wang, F. Wang, M. Xue, and W. Li, "Fabrication and tribological investigation of a novel hydrophobic polydopamine/graphene oxide multilayer film," *Tribology Letters,* vol. 48, no. 3, pp. 407-415, 2012.

[56] M. Muhammad *et al.*, "Enhancing the corrosion resistance of Q235 mild steel by incorporating poly (dopamine) modified h-BN nanosheets on zinc phosphate-silane coating," *Surface and Coatings Technology,* vol. 390, p. 125682, 2020.

[57] L. Wen *et al.*, "Antibacterial properties of Ag/TiO 2/PDA nanofilm on anodized 316L stainless steel substrate under illumination by a normal flashlight," *Journal of materials science,* vol. 55, no. 22, pp. 9538-9550, 2020.

[58] S. Zhang, X. Liang, G. M. Gadd, and Q. Zhao, "Advanced titanium dioxide-polytetrafluorethylene (TiO2-PTFE) nanocomposite coatings on stainless steel surfaces with antibacterial and anti-corrosion properties," *Applied Surface Science,* vol. 490, pp. 231-241, 2019.

[59] F. Elmi, E. Valipour, and S. Ghasemi, "Synthesis of anticorrosion nanohybrid films based on bioinspired dopamine, L-cys/CNT@ PDA through self-assembly on 304 stainless steel in 3.5% NaCl," *Bioelectrochemistry,* vol. 126, pp. 79-85, 2019.

[60] D. Gan *et al.*, "Mussel-inspired contact-active antibacterial hydrogel with high cell affinity, toughness, and recoverability," *Advanced Functional Materials,* vol. 29, no. 1, p. 1805964, 2019.

[61] Y. Zhao and M. Zou, "Experimental investigation of the wear mechanisms of thin PDA/PTFE coatings," *Progress in Organic Coatings,* vol. 137, p. 105341, 2019.

[62] S. K. Ghosh *et al.*, "Improving the tribological performances of PDA+ PTFE nanocomposite coatings by hot compaction," *Tribology Transactions,* no. just-accepted, pp. 1-12, 2021.

[63] A. Abe, D. Choudhury, and M. Zou, "Improved tribological performance of PDA/PTFE thin coatings with silica nanoparticles incorporated into the PDA underlayer," *Journal of Tribology,* pp. 1-22, 2021.

[64] D. Choudhury, I. I. Niyonshuti, J. Chen, J. A. Goss, and M. Zou, "Tribological performance of polydopamine+ Ag nanoparticles/PTFE thin films," *Tribology International,* vol. 144, p. 106097, 2020.

[65] A. Riveiro *et al.*, "Influence of laser texturing on the wettability of PTFE," *Applied Surface Science,* vol. 515, p. 145984, 2020.

[66] I. Singh, S. M. George, A. Tiwari, J. Ramkumar, and K. Balani, "Influence of laser surface texturing on the wettability and antibacterial properties of metallic, ceramic, and polymeric surfaces," *Journal of Materials Research,* vol. 36, no. 19, pp. 3985-3999, 2021.

[67] A. Cunha *et al.*, "Femtosecond laser surface texturing of titanium as a method to reduce the adhesion of Staphylococcus aureus and biofilm formation," *Applied Surface Science,* vol. 360, pp. 485-493, 2016.

[68] B. Mao, A. Siddaiah, Y. Liao, and P. L. Menezes, "Laser surface texturing and related techniques for enhancing tribological performance of engineering materials: A review," *Journal of Manufacturing Processes,* vol. 53, pp. 153-173, 2020.

[69] E. Gualtieri, A. Borghi, L. Calabri, N. Pugno, and S. Valeri, "Increasing nanohardness and reducing friction of nitride steel by laser surface texturing," *Tribology International,* vol. 42, no. 5, pp. 699-705, 2009.

[70] G. Boidi, I. Tertuliano, F. Profito, W. De Rossi, and I. Machado, "Effect of laser surface texturing on friction behaviour in elastohydrodynamically lubricated point contacts under different sliding-rolling conditions," *Tribology International,* vol. 149, p. 105613, 2020.

[71] Z. Wu, Y. Xing, P. Huang, and L. Liu, "Tribological properties of dimple-textured titanium alloys under dry sliding contact," *Surface and Coatings Technology,* vol. 309, pp. 21-28, 2017.

[72] X. Li, Y. Li, Z. Tong, Q. Ma, Y. Ni, and G. Dong, "Enhanced lubrication effect of gallium-based liquid metal with laser textured surface," *Tribology International,* vol. 129, pp. 407-415, 2019.

[73] L. Vilhena, B. Podgornik, J. Vižintin, and J. Možina, "Influence of texturing parameters and contact conditions on tribological behaviour of laser textured surfaces," *Meccanica,* vol. 46, no. 3, pp. 567-575, 2011.

[74] C. Gachot *et al.*, "Dry friction between laser-patterned surfaces: role of alignment, structural wavelength and surface chemistry," *Tribology letters,* vol. 49, no. 1, pp. 193-202, 2013.

[75] L. Rapoport *et al.*, "Friction and wear of MoS2 films on laser textured steel surfaces," *Surface and Coatings Technology,* vol. 202, no. 14, pp. 3332-3340, 2008.

[76] C. G. Guleryuz and J. E. Krzanowski, "Mechanisms of self-lubrication in patterned TiN coatings containing solid lubricant microreservoirs," *Surface and Coatings Technology,* vol. 204, no. 15, pp. 2392-2399, 2010.

[77] A. Voevodin and J. Zabinski, "Laser surface texturing for adaptive solid lubrication," *Wear,* vol. 261, no. 11-12, pp. 1285-1292, 2006.

[78] I. Etsion, "State of the art in laser surface texturing," *J. Trib.,* vol. 127, no. 1, pp. 248-253, 2005.

[79] J. Ye, H. Zhang, X. Liu, and K. Liu, "Low wear steel counterface texture design: a case study using micro-pits texture and alumina–PTFE nanocomposite," *Tribology Letters,* vol. 65, no. 4, pp. 1-12, 2017.

[80] F. Soltani-Kordshuli, N. Harris, and M. Zou, "Tribological behavior of polydopamine/polytetrafluoroethylene coating on laser textured stainless steel with Hilbert curves," *Friction,* Research Article 2022, doi: 10.1007/s40544-022-0671-0.

[81] F. Soltani-Kordshuli, C. Miller, N. Harris, and M. Zou, "Laser surface texturing of both thin polytetrafluoroethylene coatings and stainless steel substrates for improving tribological properties," *Polymer Testing,* vol. 117, p. 107852, 2023.

Chapter 2

Tribological Behavior of the PDA/PTFE + Cu-SiO_2 Nanoparticle Thin Coatings

2.1 Abstract

Cu-SiO_2 core-shell nanoparticles (NPs) were added to the polytetrafluoroethylene (PTFE) top layer of polydopamine (PDA)/PTFE thin coatings to improve the durability of the coatings. Three very low weight percentages of Cu-SiO_2 NPs (0.005 wt%, 0.0075 wt%, 0.01 wt%) were added to a PTFE dispersion, which was then used to dip-coat the PTFE + Cu-SiO_2 NPs onto PDA-coated stainless steel substrates to form PDA/PTFE + Cu-SiO_2 NP thin coatings. The resulting thin coatings were less porous and had smaller surface roughness compared to PDA/PTFE thin coatings, revealing the effect of Cu-SiO_2 NPs in making more compact thin coatings with interconnected PTFE fibrils. The compaction of the coatings led to improved adhesion and durability of the PDA/PTFE + Cu-SiO_2 NP thin coatings.

2.2 Introduction

Polytetrafluoroethylene (PTFE) is a popular solid lubricant due to its remarkable properties such as high-temperature resistance, low maintenance cost, superior chemical resistance, and low coefficient of friction (COF) [1, 2]. However, PTFE has low wear resistance and its capacity for load-bearing is low [3, 4], which prevent its use as a thin coating for many practical applications. Therefore, it is important to enhance the wear resistance of PTFE thin coatings. In this regard, some studies have been performed by adding nanoparticles (NPs) such as nanodiamond [5], carbon NPs [6], SiO_2 NPs [3], and Au NPs [4] to the PTFE films. For example, Beckford et al. incorporated SiO_2 NPs as fillers in PTFE film and showed that PTFE +

SiO_2 NP composite films sustained more rubbing cycles compared to PTFE films while remained at the same low COF [3]. SiO_2 NPs have been found to enhance the development of a transfer film on the counterface. Adding SiO_2 NPs to the PTFE film resulted in more fluorine in the wear track, which proved the improved adhesion of PTFE to the substrate. In another study, Beckford et al. added a small concentration of Au NPs into PTFE films to improve the wear resistance [4]. Au NPs were selected because of their excellent tribological properties as well as higher hardness than PTFE for improving mechanical properties. It was shown that incorporating a small concentration, 0.06%, of Au NPs into the PTFE film improved the wear resistance of the composite film by up to two times and decreased the COF by up to 50%. Also, the delamination of PTFE film was mitigated after adding Au NPs.

Even though adding NPs improved the local wear resistance of the PTFE films, the weak adhesion of the PTFE films to the substrate was still a leading cause of film failure [3, 4]. Beckford et al. investigated the effect of polydopamine (PDA) adhesive layer, bonding to both stainless steel substrate and PTFE film, on the wear resistance and friction of PTFE film [7]. They observed that the number of rubbing cycles withstood by PDA/PTFE films was 500 times more than that by PTFE films alone while maintaining the same low COF. They also studied the combined influence of using Cu NPs as fillers in PTFE films and PDA as an adhesive underlayer [8]. They showed that the presence of Cu NPs extended the wear life of PDA/PTFE films by 2 folds, even though the concentrations of Cu NPs were very low, at 0.01 wt%. Furthermore, they investigated the effect of incorporating PDA-coated Cu NPs into the PTFE in PDA/PTFE coatings [9]. They confirmed that the existence of PDA-coated Cu NPs increased the adhesion of PTFE to the PDA underlayer, as well as improving the toughness of the coating.

The role of the fillers could be to improve the transfer film formation, reduce crack propagation, and improve the load-carrying capacity [3-6, 8-10]. The type and concentration of the fillers are very important to consider for coating development. It should be noted that a high concentration of hard fillers, such as SiO_2 NPs, could have negative effects on the wear behavior and friction of the films [3]. On the other hand, some NPs, such as Cu NPs, are soft, expensive, and chemically reactive, and it is desirable to use a low concentration and make them chemically inert. We hypothesize that coating the soft Cu NPs with hard SiO_2 shells could make the NPs harder and allow a lower concentration of Cu NPs to be used compared to using pristine Cu NPs, while also provide a barrier to prevent the core from oxidization. Furthermore, core-shell nanostructures have been found to have novel high deformation resistance compared to nanostructures made of single materials [11-17], thus could enable even lower NP concentration.

In this study, we incorporated Cu-SiO_2 core-shell NPs into the PTFE top layer of PDA/PTFE coatings at three very low concentrations: 0.005 wt%, 0.0075 wt%, and 0.01 wt%, with two being lower than all previous studies. The tribological behavior of coatings was examined by applying a high normal load of 2 N to accelerate the testing to failure. The morphology, durability, scratch resistance, and hardness of the PDA/PTFE + Cu-SiO_2 NP thin coatings were investigated. This study demonstrated that adding the much-reduced concentration of Cu-SiO_2 NPs into the PTFE top layer could still improve the durability of PDA/PTFE thin coatings up to two times at a much higher contact pressure.

2.3 Experimental Methods

2.3.1 Cu-SiO_2 NP Synthesis and Characterization

2.3.1.1 Chemicals

Copper (II) 2,4-pentanedionate ($Cu(acac)_2$, 98%), 1-octadene (ODE, 90%), tri-n-octylphosphine (TOP, 90%), tetraethoxysilane (TEOS, 98%), and sodium hydroxide (NaOH, 98%) were purchased from Alfa Aesar. Oleylamine (OLAM, 70%), poly(oxythylene nonylphenyl ether) (Igepal CO-520), dopamine hydrochloride (DA, 99%), and tris(hydroxymethyl)aminomethane (Trizma base, > 99%) were acquired from Sigma-Aldrich. Hexanes (ACS grade) were ordered from Fischer Scientific. Formic acid (99%) was purchased from BDH. Sulfuric acid (ACS grade, 98%) was acquired from J.T. Baker. All chemicals were used as received. Ultrapure water was used in all reactions and purification processes.

2.3.1.2 Synthesis of Cu NPs

Cu NPs were synthesized using a scaled-up protocol of our previously established procedure [18]. Briefly, $Cu(acac)_2$ (524 mg, 0.2 mmol) was added into a 250 mL three-neck round-bottom flask containing 40 mL of ODE and 10 mL of OLAM. The reaction was protected under nitrogen using a Schlenk line setup with a magnetic stirrer and attached to a condenser that was cooled by water. After removing air from the reaction flask, 10 mL of TOP was added, followed by heating the reaction mixture to 220 °C. During this period, a small amount of CO produced by reacting formic acid and sulfuric acid 10 mL each was introduced to the reaction mixture for 10 s when the reaction temperature reached 200 °C. The reaction continued for 20 min at 220 °C. After cooling down, the Cu NP product was purified by adding 25 mL of ethanol

and toluene mixture at a ratio of 4:1 and centrifuged at 8000 rpm for 5 min. This purification step was repeated twice. The pellet of the purified Cu NPs was dispersed in toluene and kept for future use.

2.3.1.3 Synthesis of Cu-SiO_2 Core-shell NPs

The as-prepared Cu NPs were used for fabricating the Cu-SiO_2 core-shell NPs following a sol-gel process in a water/oil microemulsion method that we established previously [18]. 1.2 mL of Igepal CO-520 was added to a 50 mL three-neck round-bottom flask containing 20 mL of hexane, followed by adding 45 μL of TEOS. Immediately after, 15 mg of Cu NPs in 2 mL of toluene was transferred into the reaction mixture, and then 140 μL of 20 mM NaOH was added to the reaction mixture as a catalyst. The reaction proceeded for 48 h at the ambient temperature. After the chemical reaction, the product was purified using 30 mL of ethanol and collected by centrifuging at 11,000 rpm for 30 min. Additional purification was carried out using 15 mL of ethanol three times. The final product was dispersed in water and stored for future use.

2.3.2 Sample Fabrication

Stainless steel 316 substrates (McMaster-Carr) were shaped into 25.4 mm × 25.4 mm squares with 2 mm thickness and cleaned in deionized (DI) water with detergent, acetone, and isopropyl alcohol for 20 min each in an ultrasonic bath. The PDA adhesive underlayer was then deposited on the substrates. In this step, 25 mL of DI water was brought to 60 °C. Also, its pH was adjusted to 8.5 by adding 0.025 g tris (hydroxymethyl) aminomethane (T1503) (Sigma Aldrich) in a digital rocking bath at a rocking rate of 25 rpm and rocking angle of 7°. Then, the clean substrates were settled in the buffer solution, and 0.04 g of DA (Sigma Aldrich) was added.

The process of PDA deposition was allowed to continue for 45 min. Immediately after the PDA deposition, the samples were rinsed using DI water and then dried with nitrogen gas.

Cu-SiO_2 core-shell NPs dispersion was mixed in an ultrasonic bath with 60 wt% aqueous PTFE dispersion (Teflon Dispersion DISP30, Fuel Cell Earth) to obtain 3 different weight percentages of Cu-SiO_2 core-shell NPs at 0.005 wt%, 0.0075 wt%, and 0.01 wt%. Next, the resulting PTFE + Cu-SiO_2 dispersion was deposited on the PDA underlayer with a dip coater, setting the dipping speed and withdrawing speed at 10 mm/min and the soaking time at 1 min. In this step, part of the PDA-coated stainless steel substrates was not dip-coated with PTFE so that PTFE coating thickness could be measured from the exposed interface of PDA and the PTFE coatings. Four different PTFE top layer dipped with 0 wt%, 0.005 wt%, 0.0075 wt%, and 0.01 wt% Cu-SiO_2 core-shell NPs were labeled as PDA/PTFE, PDA/PTFE + 0.005 wt% NP, PDA/PTFE + 0.0075 wt% NP, PDA/PTFE + 0.01 wt% NP, respectively. Three samples in each group were fabricated.

Finally, the samples were heat-treated using three steps: first, heated at 120 °C so that the water from the coating could evaporate, then heated at 300 °C so that the surfactant could evaporate, and last, heated at 372 °C so that PTFE particles sinter together. The samples were heated for four min during each of the three steps without any cooling time between them.

2.3.3 Tribological Testing

The tribological performance of PDA/PTFE and PDA/PTFE + Cu-SiO_2 NP coatings was measured from durability tests with a tribometer (UMT-3) (Bruker) adopting a linear reciprocating motion in a configuration of ball-on-plate. The counterfaces were Cr steel balls with a diameter of 6.35 mm (McMaster-Carr), and the plates were various PDA/PTFE coated

316 stainless steel substrates. Tests were performed at a 2 N normal load, a 5 mm stroke length, a 10 mm/s sliding speed, and with a failure specification of a frictional force larger than 0.6 N (failure COF threshold of 0.3). The Hertzian contact pressure corresponding to the 2 N normal load was 615 MPa when not considering the effect of the PDA/PTFE thin coating. Also, scratch tests were conducted on the samples with the longest durability to investigate the coating adhesion strength. The scratch load was linearly increased from 0.5 N to 18 N with a 0.1 mm/s sliding speed and at a 10 mm scratch testing length.

2.3.4 Sample Characterization

A transmission electron microscope (TEM) (JEOL JEM-1011) was used to image the Cu and Cu-SiO_2 NPs. The Cu concentration of the samples was determined using inductively coupled plasma mass spectrometry (ICP-MS) (iCAP Q, Thermo Scientific). Hydrodynamic diameter and zeta-potential of the samples were analyzed by dynamic light scattering (ZetaPALS, Brookhaven Instruments). UV-Vis spectra were obtained using a UV-Vis spectrophotometer (Cary 50, Agilent).

The topography and surface roughness of the PDA/PTFE and PDA/PTFE + Cu-SiO_2 NP coatings were studied by an atomic force microscope (AFM) (Dimension Icon, Bruker). A ScanAsyst air AFM tip (Bruker) having a 0.4 N/m spring constant was used to perform the AFM study. Root mean square roughness (R_q) was reported based on the average measured from six random areas of 60 µm × 60 µm on each sample.

3D laser scanning confocal microscopy (VK-X260, Keyence Corporation) was employed to inspect the counterface balls and wear tracks after the durability tests. Counterface balls and

wear tracks were imaged in order to observe the transferred films on the balls and the wear mechanisms.

Scanning electron microscopy (SEM) (VEGA 3, TESCAN) was used to characterize the microscale topography of the PTFE top layer at different magnifications. Energy-dispersive X-ray spectroscopy (EDS) (XL-30, Phillips/FEI) was employed to image and map the elements on the wear tracks after the durability tests. Samples were sputtered with a thin layer of gold prior to SEM measurements.

A stylus profilometer (Dektak 150, Bruker Nano Surfaces) was used to measure the thickness of the PTFE top layer. Thickness was measured from line scans with a scan length of 6,000 mm and a scan duration of 60 seconds on 4 different lines across the interface between PDA and PDA/PTFE. The resulting average thickness of the PTFE top layer was reported in Table 2.1. The stylus profilometer with scan lengths of 2,000 mm and scan durations of 60 seconds was employed to evaluate the profile of the wear tracks after the durability tests.

Water contact angles (WCAs) were determined by dropping a 3 ml water droplet on three different places on each sample using a goniometer (OCA 15, DataPhysics Instruments), and the average contact angles are reported.

Nanoindentation was conducted to determine the hardness and modulus of elasticity of the PDA/PTFE thin coatings. Five load-controlled indentations were performed on each sample with a 50 mN maximum load, 2.5 mN/s loading and unloading rates, and a holding time of 2.5 s. The indentations were performed using a 1 mm spheroconical diamond tip.

Table 2.1: Coating composition and characterization results.

Coating composition	Average roughness of PTFE top layer (RMS) (nm)	Average thickness of PTFE top layer (µm)	Average diameter of PTFE fibrils (µm)	Porosity of PTFE top layer (%)
PDA/PTFE	26.57 ± 1.85	1.18 ± 0.13	0.200 ± 0.006	18.10 ± 0.63
PDA/PTFE + 0.005 wt% Cu-SiO_2 NP	23.09 ± 0.67	1.05 ± 0.01	0.218 ± 0.010	16.40 ± 0.54
PDA/PTFE + 0.0075 wt% Cu-SiO_2 NP	21.46 ± 3.72	1.17 ± 0.15	0.230 ± 0.008	15.85 ± 1.50
PDA/PTFE + 0.01 wt% Cu-SiO_2 NP	20.21 ± 1.48	1.04 ± 0.01	0.243 ± 0.022	12.68 ± 1.52

2.4 Results and Discussion

2.4.1 NP Characterizations

The as-synthesized Cu NPs were a mixture of 80 % NPs and 20 % nanorods (Figure 2.1A). The average diameter of the Cu NPs was 82 ± 8.3 nm. The Cu nanorods had an average length of 204.0 ± 12.2 nm and an average diameter of 66.2 ± 3.6 nm. The absorbance spectrum of the as- synthesized Cu sample exhibited a peak at 584 nm corresponding to the extinction peak of Cu NPs. The broad tail in the longer wavelength mainly corresponds to the extinction of Cu nanorods and possibly self-assembled Cu nanostructures (Figure 2.1B). After the SiO_2 coating process, the average diameter of the Cu-SiO_2 NPs was 93.1 ± 9.8 nm, and the average size of the Cu-SiO_2 nanorods was 210.8 ± 13.5 nm by 73.4 ± 3.1 nm (Figure 2.1C). The slight increase in the size of the Cu-SiO_2 sample suggests a SiO_2 coating thickness of ~ 5.6 nm for the

Cu NPs and ~ 3.5 nm for the Cu nanorods, respectively. The variation of SiO_2 coating thickness is likely due to the surface area difference between the NPs and nanorods with a ratio of ~ 0.4:1. The absorbance of the Cu-SiO_2 NPs was slightly shifted to 592 nm due to the SiO_2 coating, and the broad band at 650 – 750 nm corresponds to the dispersed Cu-SiO_2 nanorods (Figure 2.1D).

2.4.2 Surface Properties

AFM images of the PDA/PTFE and the PDA/PTFE + Cu-SiO_2 NP coatings shown in Figure 2.2 all demonstrated spindle-like microstructures, which were formed during the annealing process [19]. The higher resolution AFM images on the right revealed that there are small pores between the spindle-like microstructures, and adding NPs to the PTFE top layer decreased the pore size and resulted in a smoother interconnected network of PTFE fibrils. This can be explained by the lower softening temperature of PTFE facilitated by the NPs and the lower melting point of the NPs, similar to our previous findings [4, 8, 9]. Table 2.1 and Figure 2.3 shows that the surface roughness and porosity decreased with increasing concentration of Cu-SiO_2 NPs based on three measurements.

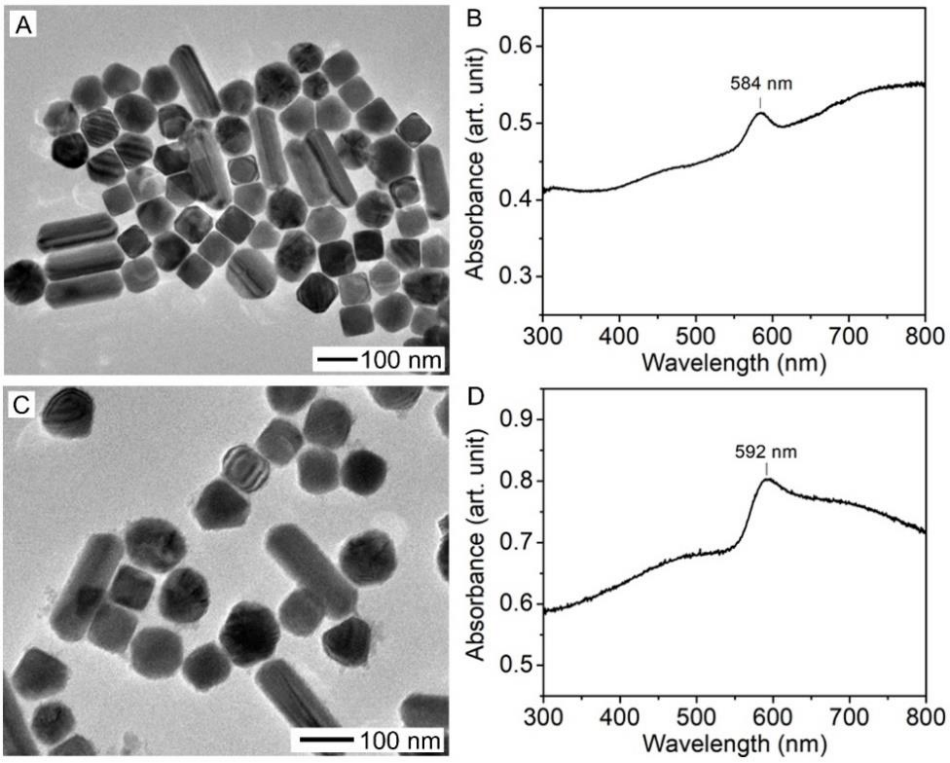

Figure 2.1: Characterization of the as-synthesized Cu nanostructures and Cu-SiO_2 nanostructures: A) TEM image of the Cu nanostructures showing a mixture of 80% NPs and 20% nanorods, B) UV–vis spectrum of the sample in (A) suspended in toluene, C) TEM image of the Cu-SiO_2 nanostructures obtained after the sample was coated with SiO_2 shells, and D) UV–vis spectrum of the sample in (C) suspended in water.

The WCAs of PDA/PTFE and PDA/PTFE + Cu-SiO_2 NP coatings were measured and reported in Figure 2.3B. *t*-Tests confirmed that there were no statistically significant differences in the average WCA among the various coatings. Several factors could affect WCA, including porosity, surface roughness, heterogeneity, and material surface energy [20]. Based on the studies done by Troger et al. [21], porosity decreased the WCA of PTFE membranes. As the AFM images shown in Figure 2.2, the PDA/PTFE coating was more porous than the PDA/PTFE + Cu-SiO_2 NP coatings. However, the roughness values of PDA/PTFE + Cu-SiO_2 NP coatings were smaller than that of the PDA/PTFE coating. Due to these competing effects, all coatings showed similar WCAs.

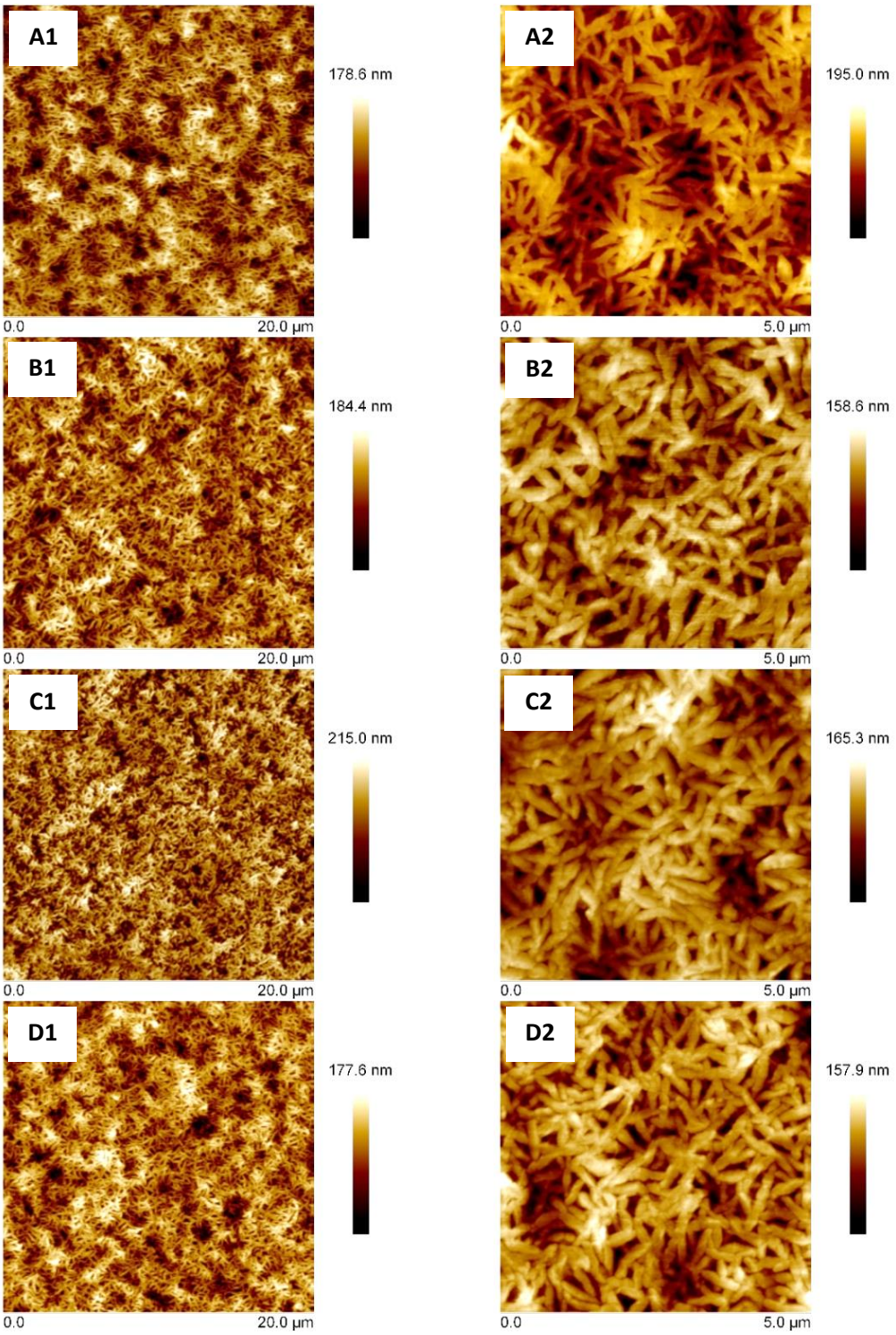

Figure 2.2: Overview and zoom-in AFM images of the coatings: A1 and A2) PDA/PTFE, B1 and B2) PDA/PTFE + 0.005 wt% Cu-SiO_2 NP, C1 and C2) PDA/PTFE + 0.0075 wt% Cu-SiO_2 NP, and D1 and D2) PDA/PTFE + 0.01 wt% Cu-SiO_2 NP.

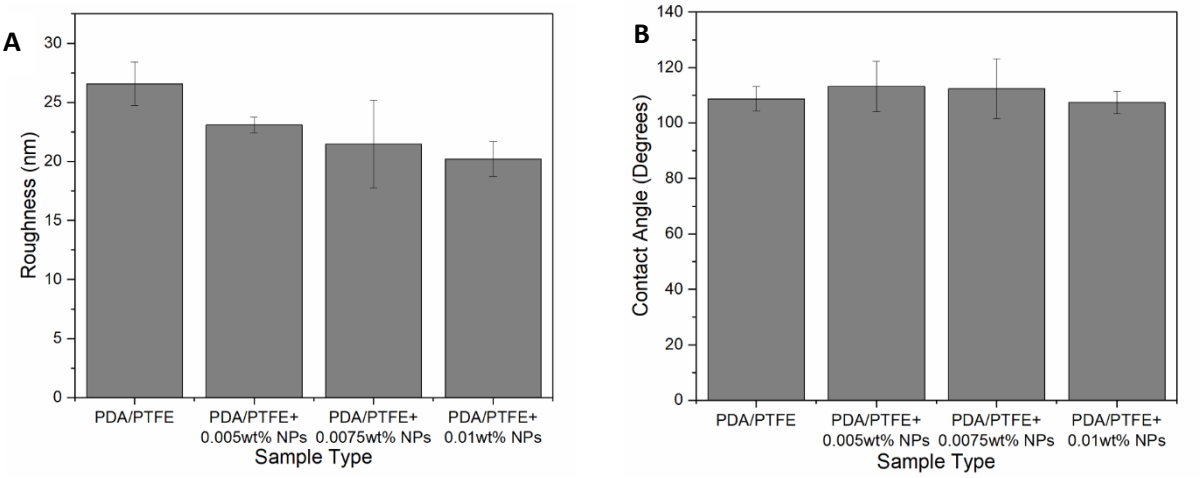

Figure 2.3: Average roughness and water contact angle of the PDA/PTFE and PDA/PTFE + Cu-SiO_2 NP thin coatings: A) average roughness and B) water contact angle.

The SEM images of the surfaces of the PDA/PTFE and PDA/PTFE + Cu-SiO_2 NP coatings in Figures 2.4A1-D1 clearly showed that the PDA/PTFE coating had a higher porosity than the other coatings. A complimentary MATLAB program was developed to estimate the porosity and fibril diameter of each coating using the very high resolution SEM images in Figures 2.4A2-D2. It was found that the percentage of porous areas decreased with increasing concentration of Cu-SiO_2 NPs, while the average fibril diameter increased with increasing concentration of Cu-SiO_2 NPs (See Figure 2.5), supporting the fact that the inclusion of Cu-SiO_2 NPs reduced the porosity and increased PDA/PTFE particle connectivity. The information revealed from the SEM images verified the conclusions drawn from the AFM images.

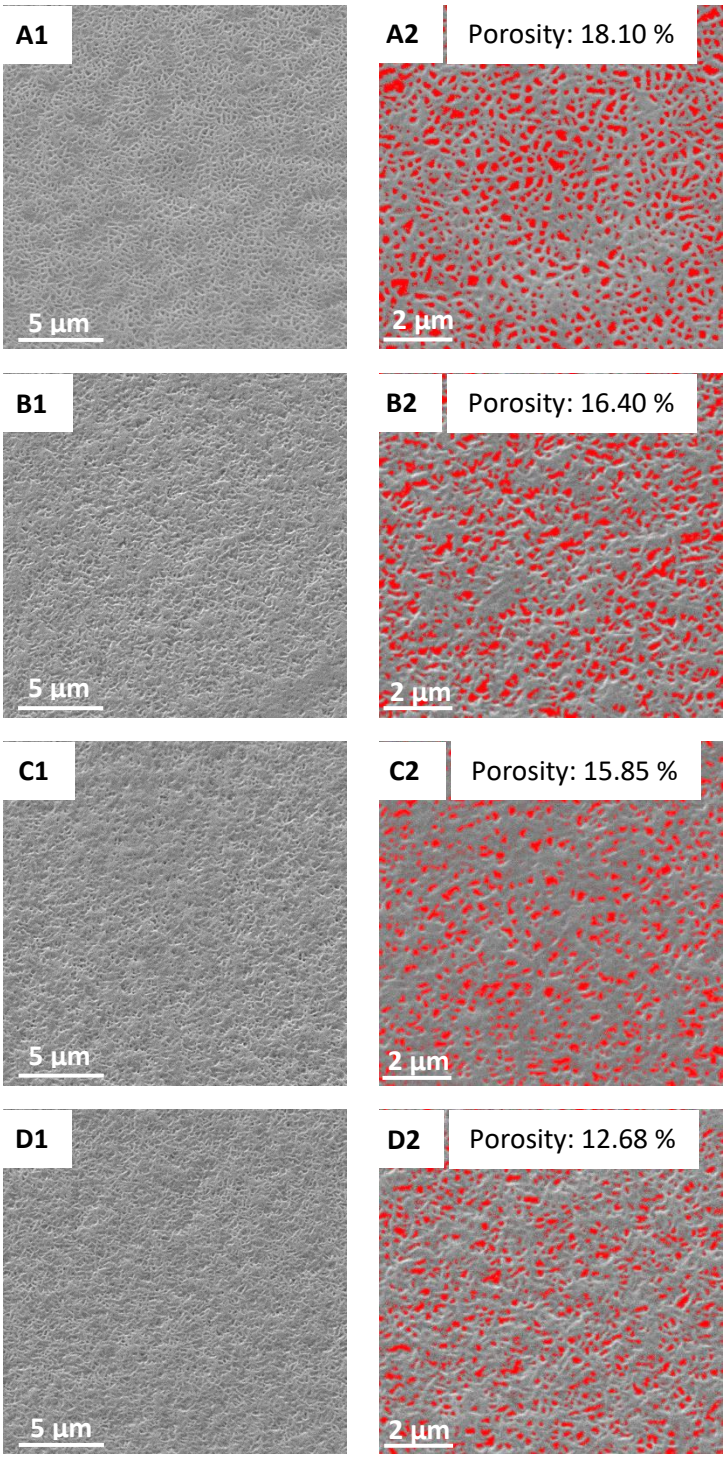

Figure 2.4: SEM images and percentage porous areas shown in red of PTFE top layer on PDA/PTFE coatings: A1 and A2) PDA/PTFE, B1 and B2) PDA/PTFE + 0.005 wt% Cu-SiO_2 NP, C1 and C2) PDA/PTFE + 0.0075 wt% Cu-SiO_2 NP, and D1 and D2) PDA/PTFE + 0.01 wt% Cu-SiO_2 NP.

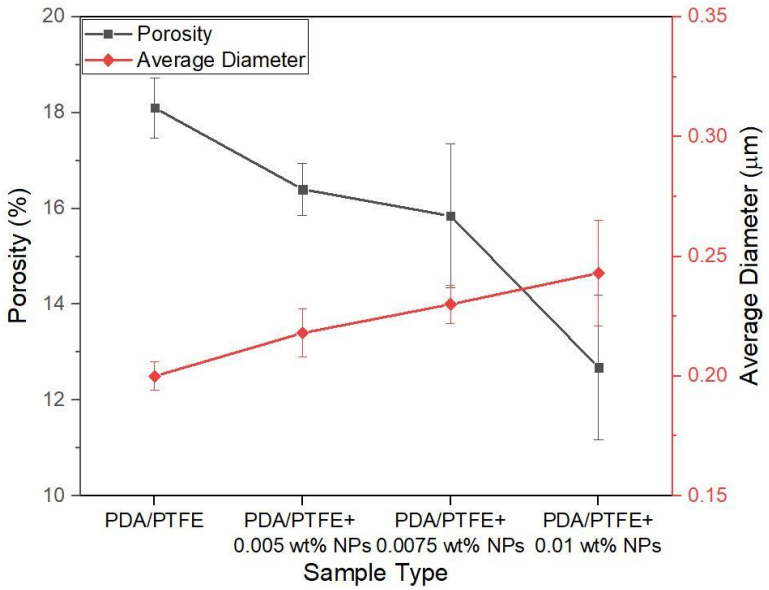

Figure 2.5: Porosity of PTFE top layer and the average diameter of PTFE fibrils for PDA/PTFE and PDA/PTFE + Cu-SiO_2 NP thin coatings.

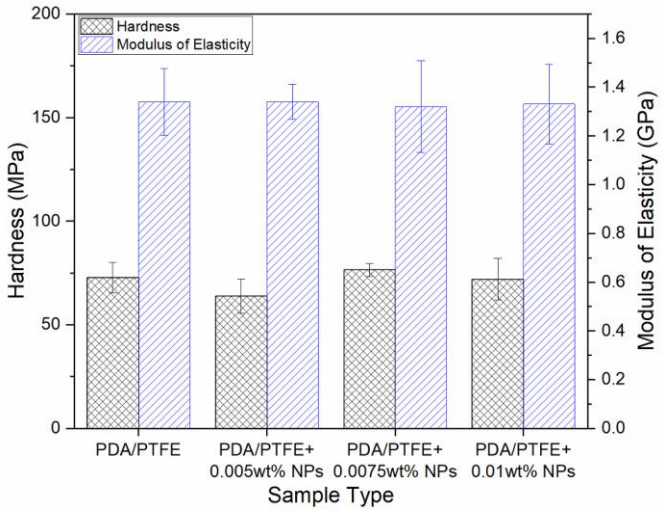

Figure 2.6: Hardness and modulus of elasticity of PDA/PTFE and PDA/PTFE + Cu-SiO_2 NP thin coatings.

The modulus of elasticity and hardness of the top layer of the PDA/PTFE and PDA/PTFE + Cu-SiO_2 NP coatings were measured and illustrated in Figure 2.6. PDA/PTFE coatings had an average hardness of 70 ± 5 MPa and an average modulus of elasticity of 1.330 ± 0.008 GPa. Adding Cu-SiO_2 NPs into PTFE top layer did not cause a notable change in the modulus of

elasticity or hardness of PDA/PTFE coatings. This is due to the very low percentage of Cu-SiO_2 NPs in the coating.

2.4.3 Tribological Properties

The average durability of the PDA/PTFE and PDA/PTFE + Cu-SiO_2 NP coatings are summarized in Figure 2.7A. It can be seen that incorporating Cu-SiO_2 NPs into PDA/PTFE thin coatings, even at very low concentrations, increased the durability up to 2.0 times, and the PDA/PTFE + 0.0075 wt% Cu-SiO_2 NP showed the longest wear life of approximately 300 cycles. The COF versus the number of testing cycles for PDA/PTFE coatings was presented in Figure 2.7B. The initial COF of PDA/PTFE coating was very low at 0.01, but it increased sharply yet sporadically during the first 50 cycles. Similar transitions of COF from low to high at the beginning of tribological tests were also observed in our previous study on the wear mechanisms of thin PDA/PTFE coatings [22], which explained the transition in the context of the PTFE coating microstructures and wear mechanisms. The relatively low COF at the beginning of the test was due to the counterface ball rubbing on the loosely connected PTFE nanoparticles with a low resistance to motion. As the test progressed, local coating delamination/spalling occurred from adhesive wear after the loosely connected PTFE nanoparticles were plowed away or compacted. The COF stabilized when most of the PTFE topcoat had delaminated, and the ball had reached the robust PTFE and PDA interface, which provided more resistance to the ball movement and a higher COF. Since the PTFE + Cu-SiO_2 NP coatings had more cohesive networks, they reached a compacted state sooner, and thus the transition took less time and the remaining coating was thicker. Following this transition, the COF had a moderate and gradual increase until reaching 150 cycles, after which a sharp increase could be observed. This sharp increase in COF corresponded to the failure of the coating. The

COF of PDA/PTFE + Cu-SiO_2 NP coatings experienced a similar trend. However, PDA/PTFE + Cu-SiO_2 NP coatings had longer wear lives, and the sharp increase occurred later due to thicker remaining coating.

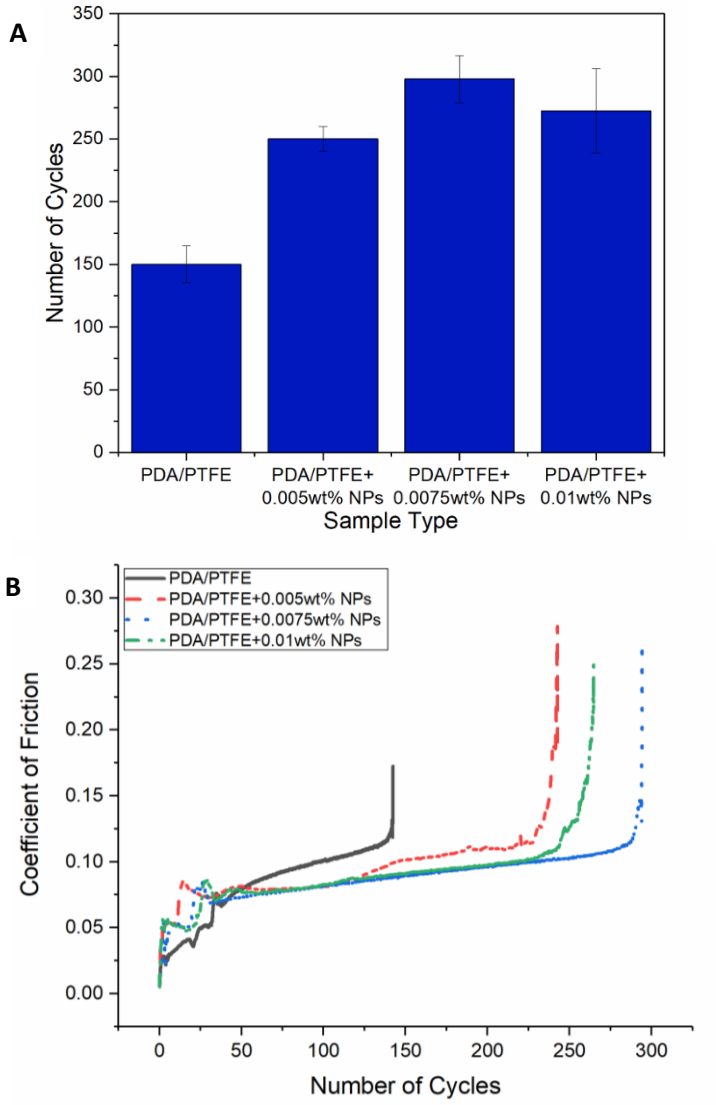

Figure 2.7: Average durability and coefficient of friction of PDA/PTFE and PDA/PTFE + Cu-SiO_2 NP thin coatings: A) Average durability and B) coefficient of friction versus the number of testing cycles.

To understand the coating failure mechanisms, optical images of the wear tracks on the PDA/PTFE and PDA/PTFE + Cu-SiO_2 NP coatings and the transfer film on the counterface balls

after the durability tests were taken and are shown in Figure 2.8. In the wear track optical images for PDA/PTFE + Cu-SiO_2 NP samples, a thin, white line inside the wear tracks was observable, which corresponded to the exposed stainless steel substrate, suggesting abrasive coating failure. In contrast, the white part inside the wear track for PDA/PTFE sample was much wider, suggesting the failure of PDA/PTFE was associated with global delamination along the wear track. Therefore, it can be concluded that adding a small amount of NPs improved the coating adhesion to the substrate through the anchoring effect of the NPs. As shown in Figure 2.8A2-D2, the amount of PTFE transferred to the counterface balls from PDA/PTFE + Cu-SiO_2 NP coatings were more than that from PDA/PTFE coating, indicating adding Cu-SiO_2 NPs improved the adhesion of the PTFE transfer films to the counterface. This can also be explained by the anchoring effect provided by the NPs [3]. As a result, the coatings lasted longer during the durability tests.

To analyze the delamination failure process of the PDA/PTFE samples further, several tribology tests were executed with different numbers of cycles from 130 to 170 on the PDA/PTFE coatings. Figure 2.9 showed the optical images of the wear tracks in low and high magnifications, the balls after the durability tests, and the profiles of the wear tracks. As the optical images of the wear tracks illustrated, the failure of PDA/PTFE coatings was associated with PTFE global delamination, which was evident by the exposed substrate polishing lines that are perpendicular to the sliding direction, even at 130 testing cycles. This was further supported by the wear track profiles in Figure 2.9F, which showed flat wear tracks at the PDA/PTFE interface in the center of the wear track and the large pileup height at the two sides of the wear track. Also, optical images of the ball after the durability tests showed a large amount of loose,

transferred PTFE. These observations proved that the PDA/PTFE coating did not adhere well to the substrate and thus was not wear-resistant.

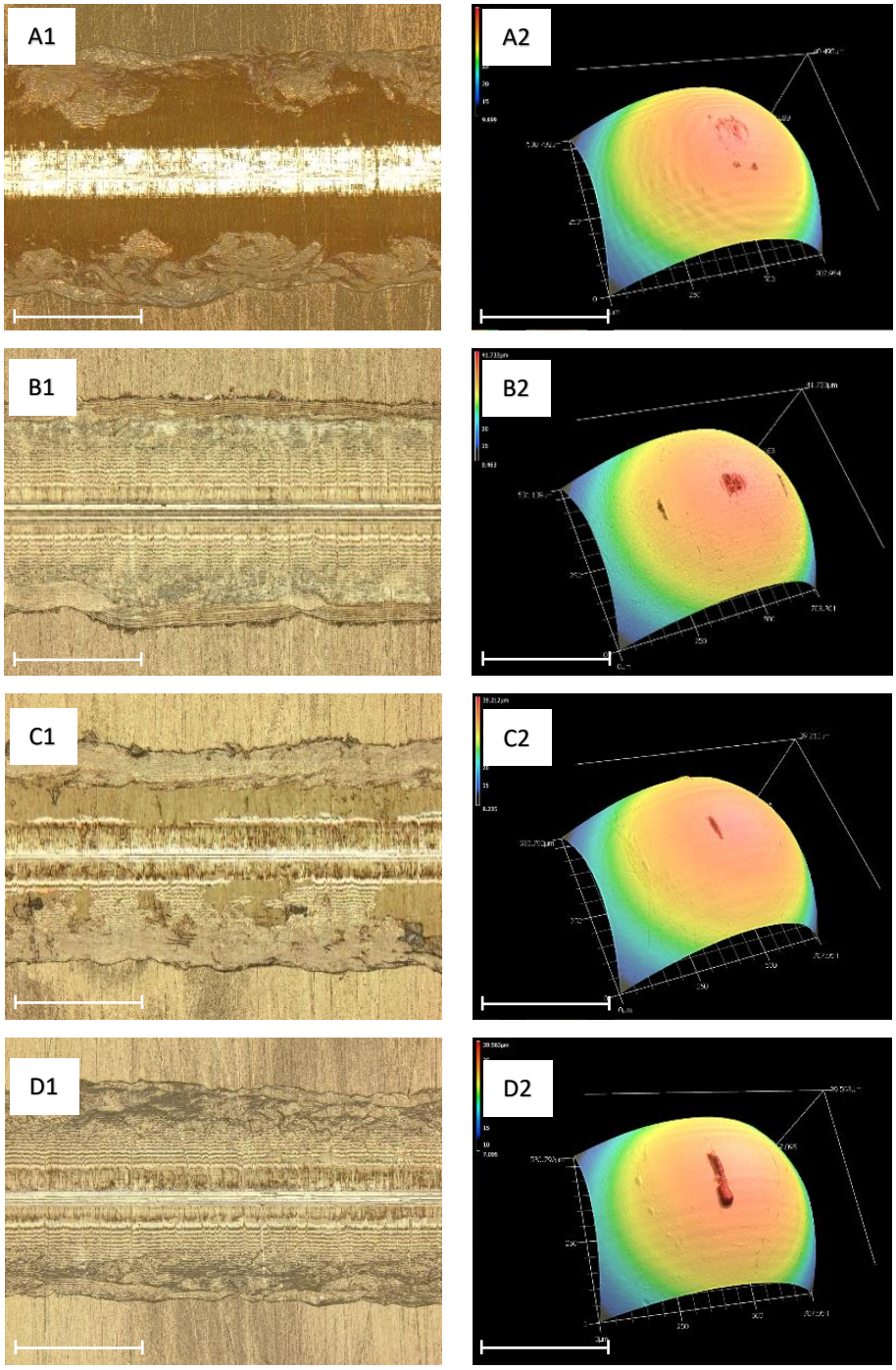

Figure 2.8: Optical images of the wear tracks and the balls after durability tests: A1 and A2) PDA/PTFE, B1 and B2) PDA/PTFE + 0.005 wt% Cu-SiO_2 NP, C1 and C2) PDA/PTFE + 0.0075 wt% Cu-SiO_2 NP, and D1 and D2) PDA/PTFE + 0.01 wt% Cu-SiO_2 NP (scale bars = 200 µm).

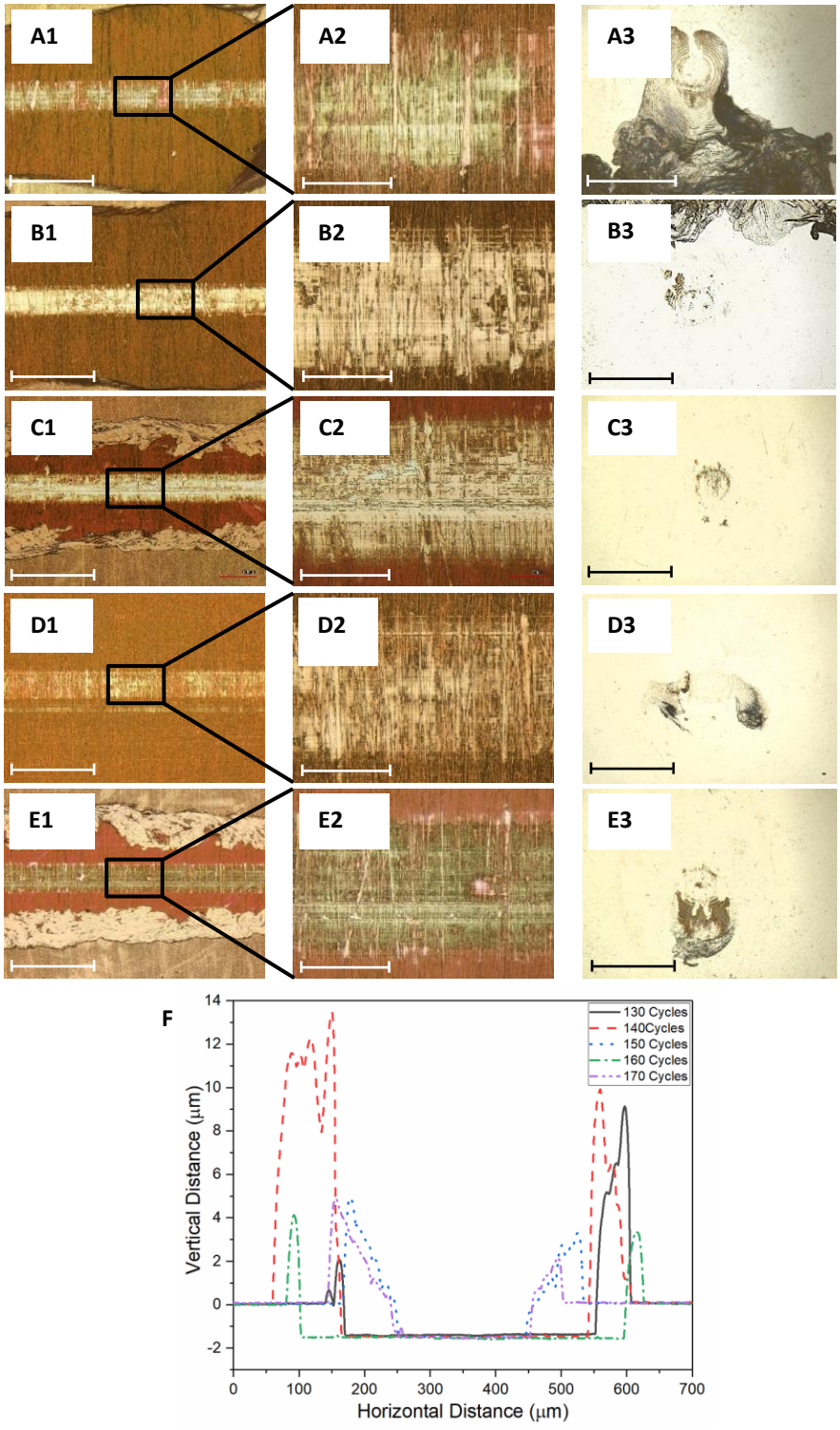

Figure 2.9: Failure analysis of PDA/PTFE coatings after tribological test at different cycles. Optical images of the wear tracks and the balls after: A1-A3) 130 cycles, B1-B3) 140 cycles, C1-C3) 150 cycles, D1-D3) 160 cycles, and E1-E3) 170 cycles (scale bars on A1-E1 and A3-E3 = 200 µm, and scale bars on A2-E2 = 50 µm). F) The profiles of the wear tracks shown on (A1-E1).

In order to confirm that PDA/PTFE thin coating failed after 150 testing cycles, EDS analysis was performed on the PDA/PTFE coating associated with the 150-cycle test. Figure 2.10A illustrated the SEM image of the wear track, and Figures 2.10B and C showed the EDS line profiles and elemental maps of Fluorine (F) and Chromium (Cr) corresponding to Figure 2.10A, respectively. As shown in Figure 2.10B and C, the element of F, which represents PTFE, was essentially absent in the wear track, proving the global delamination failure of the PTFE. In contrast, the element of Cr, which represents the substrate, was substantially increased in the wear track and proved the exposure of the substrate inside the wear track.

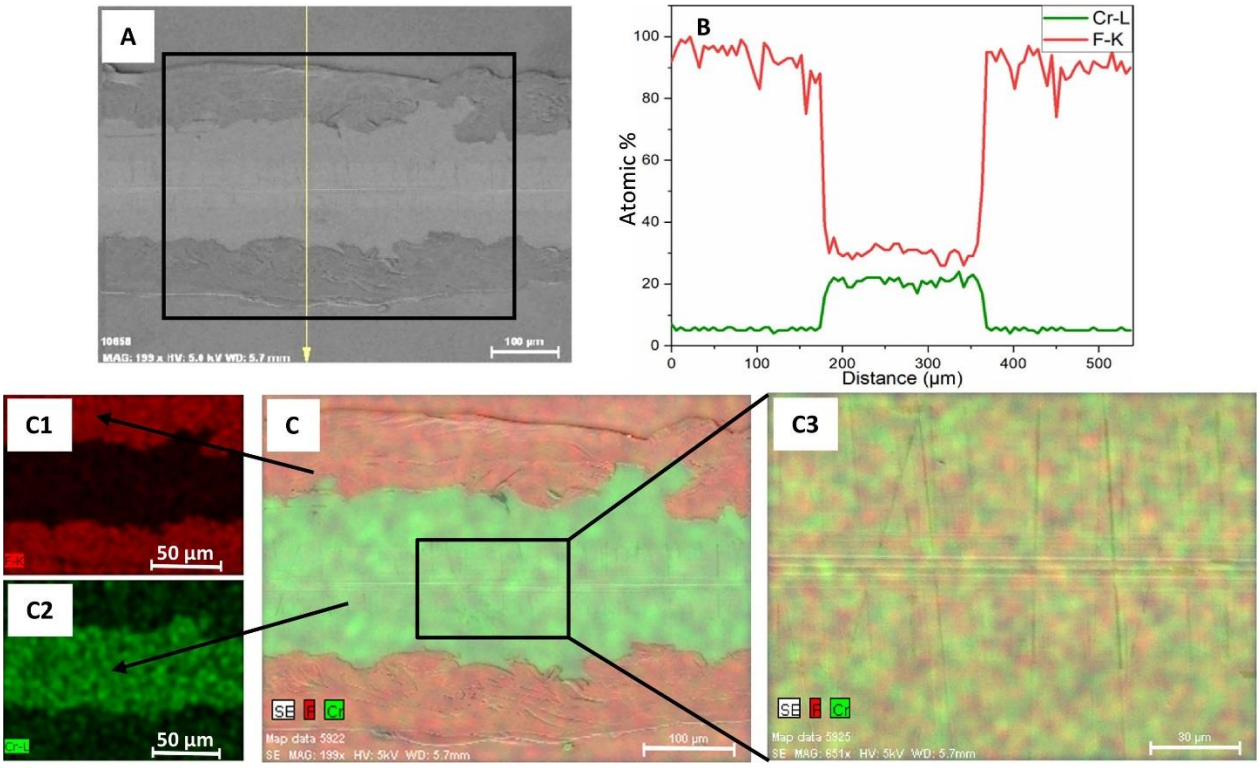

Figure 2.10: SEM image and EDS analysis of the wear track after 150-cycle test on PDA/PTFE coating: A) SEM image (scale bar = 100 µm), B) EDS line profiles of Cr and F along the yellow line in (A), and C and C1-2) EDS map of both F and Cr, only F, and only Cr of the area inside box in (A), respectively (scale bars on C, and C1-C2 = 100 µm, and 50 µm, respectively), C3) EDS map of the area inside the box in (C) (scale bar = 30 µm).

Figure 2.11 shows the comparisons of the profiles of the wear tracks on the PDA/PTFE and PDA/PTFE + Cu-SiO_2 NP thin coatings after the durability tests. It can be seen that both the wear track depths and width of the PDA/PTFE + Cu-SiO_2 NP coatings were smaller, and the shape of the wear track was also different from that of the PDA/PTFE coating. These results were due to the existence of Cu-SiO_2 NPs, which increased the coating adhesion to the substrate and coating cohesion, thus preventing global delamination and large-scale removal of the coating from inside the wear track to the borders. In addition, there were small grooves at the center of the wear track profiles of the PDA/PTFE + Cu- SiO_2 samples, most likely due to the abrasion from the Cu-SiO_2 NPs. In contrast, the wear track profile of PDA/PTFE sample was flat, suggesting the failure was due to the global delamination of PTFE rather than abrasion, as previously mentioned.

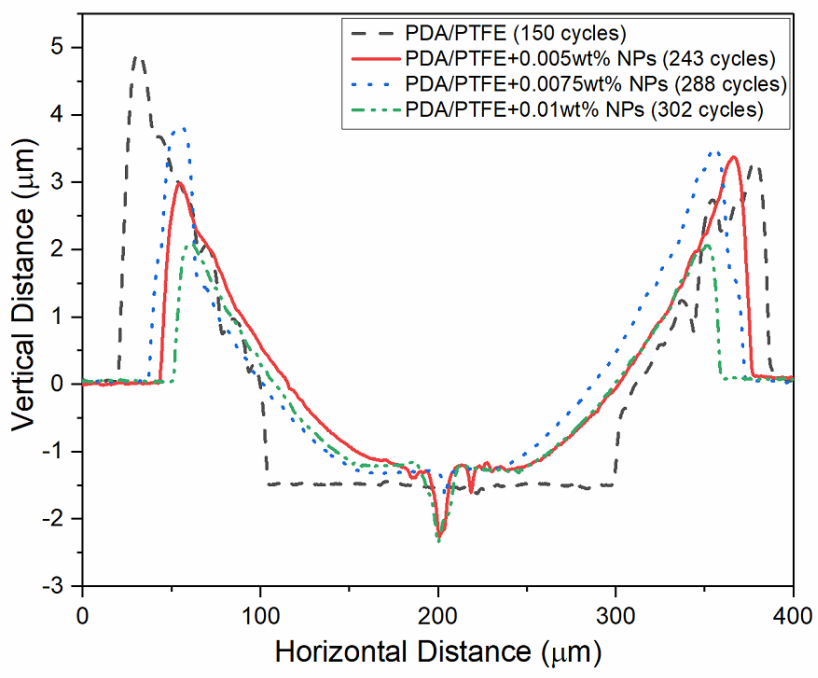

Figure 2.11: Profiles of the wear tracks on PDA/PTFE and PDA/PTFE + Cu-SiO_2 NP coatings.

Figure 2.12 shows the scratch test results for PDA/PTFE and PDA/PTFE + 0.0075 wt% NP coatings. The Optical images of the scratch wear tracks of the two coatings were shown in Figures 2.12B and C, respectively. For both coatings, the width of the wear track increased as the normal load increased, as expected. At the beginning of the scratch test, the COF of the coatings was high. As the load increased, the COF decreased as the coatings were smoothened due to compaction. Further increasing the normal load caused the counterface balls to penetrate the coatings, resulting in plowing at a distance of 2 mm (Figure 2.12B2) and 0.5 mm (Figure 2.12C2) for the PDA/PTFE and PDA/PTFE + 0.0075 wt% NP coatings, respectively. This caused an abrupt increase in the COFs in their corresponding COF graphs (Figure 2.12A). For the PDA/PTFE coating, as the load continued to increase, the COF continued to increase until the coating delaminated at 3.5 mm when the counterface reached the coating-substrate interface. The delaminated PTFE was displaced by the counterface ball to the sides and the end of the wear track. The image of the counterface chrome ball after the test showed no transferred PTFE (Figure 2.12B4).

In comparison, the COF of PDA/PTFE + 0.0075 wt% NP coating was significantly higher than that of the PDA/PTFE coating at the beginning of the test due to the existence of NPs, which provided stronger coating cohesion and thus a higher resistance to shear. The better cohesion also delayed the counterface ball penetrating the coating. However, when the normal load further increased, part of the substrate started to be exposed, as shown in the light spots in Figure 2.12C2, thus the COF started to increase gradually until the end of the test. The oblique lines in the wear track of PDA/PTFE + 0.0075 wt% NP revealed that NPs were pinned on the substrate and thus provided an anchoring effect to the coating to resist friction and shear.

Furthermore, transfer films were formed on the counterface ball as shown in Figure 2.12C4, also facilitated by the anchoring effect of the NPs [3].

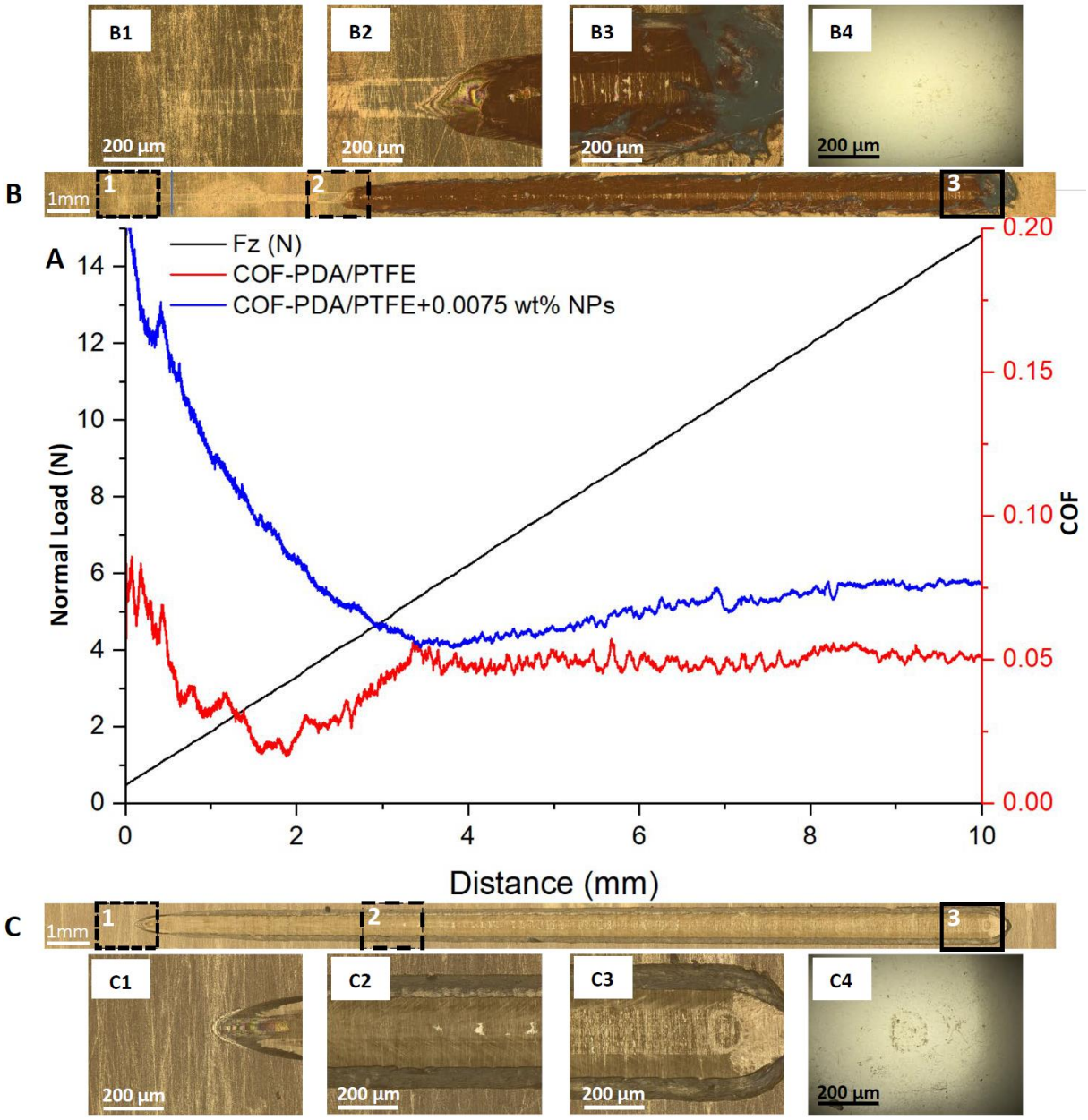

Figure 2.12: Scratch test results on PDA/PTFE and PDA/PTFE + 0.0075 wt% Cu-SiO_2 NP thin coatings: A) Applied normal load and coefficient of friction as a function of sliding distance, and optical pictures of representative wear tracks and balls after the test for B) PDA/PTFE and C) PDA/PTFE + 0.0075 wt% Cu-SiO_2 NP; B1-B3) the area inside boxes 1-3, respectively, shown on (B), and C1-C3) the area inside boxes 1-3, respectively, shown on (C).

2.5 Conclusion

Incorporating low concentrations of Cu-SiO_2 NPs in the PTFE layer increased the wear life of PDA/PTFE thin coatings. PDA/PTFE + 0.0075 wt% NP coating was seen to have twice the durability of PDA/PTFE. The surface morphology of the PDA/PTFE coatings with Cu-SiO_2 NPs was improved as indicated by less porous, more coherent, and interconnected coatings with lower roughness. Adding low concentrations of Cu-SiO_2 NPs into the PTFE layer prevented global delamination during the durability tests. The NPs also helped the PTFE transfer films to adhere more strongly to the counterface. All these aspects resulted in improving the wear life of PDA/PTFE + Cu-SiO_2 NP coatings.

CRediT Authorship Contribution Statement

Firuze Soltani-Kordshuli: Methodology, Formal analysis, Investigation, Writing – original draft, Visualization, Project administration. **Deborah Okyere:** Investigation. **Jingyi Chen:** Writing – review & editing. **Charles Miller:** Investigation, Writing – review & editing. **Nathaniel Harris:** Software. **Mahyar Afshar-Mohajer:** Investigation. **Sujan K. Ghosh:** Investigation. **Min Zou:** Conceptualization, Supervision, Validation, Writing – review & editing, Funding acquisition.

Declaration of Competing Interest

The authors declare that they have no known competing financial interests or personal relationships that could have appeared to influence the work reported in this paper.

2.6 Acknowledgments

This work was supported by the National Science Foundation under Grants CMMI-1563227 and OIA-1457888. Any opinions, findings, and conclusions or recommendations expressed in this material are those of the authors and do not necessarily reflect the views of the National Science Foundation. The authors thank the Electron Optics Facility (EOF) of the University of Arkansas for equipment use. ICP-MS measurements were carried out at the Arkansas Mass Spectrometry facility, which is supported by the Arkansas Biosciences Institute.

References

[1] H. Unal, A. Mimaroglu, U. Kadıoglu, H. Ekiz, Sliding friction and wear behaviour of polytetrafluoroethylene and its composites under dry conditions, Mater. Des. 25 (2004) 239-45.

[2] D. L. Burris, W. G. Sawyer, Improved wear resistance in alumina-PTFE nanocomposites with irregular shaped nanoparticles, Wear 260 (2006) 915-918.

[3] S. Beckford, Y. Wang, M. Zou, Wear-resistant PTFE/SiO_2 nanoparticle composite films, Tribol. Trans. 54 (2011) 849-858.

[4] S. Beckford, J. Cai, J. Chen, M. Zou, Use of Au nanoparticle-filled PTFE films to produce low-friction and low-wear surface coatings, Tribol. Lett. 56 (2014) 223-230.

[5] J. Lee, D. Lim, Tribological behavior of PTFE film with nanodiamond, Surf. Coat. Tech. 188 (2004) 534-538.

[6] J. Lee, D. Lim, D. Lim, Tribological behavior of PTFE nanocomposite films reinforced with carbon nanoparticles, Comp. Part B: Eng. 38 (2007) 810-816.

[7] S. Beckford, M. Zou, Wear resistant PTFE thin film enabled by a polydopamine adhesive layer, Appl. Surf. Sci. 292 (2014) 350-356.

[8] S. Beckford, L. Mathurin, J. Chen, M. Zou, The influence of Cu nanoparticles on the tribological properties of polydopamine/PTFE Cu films, Tribol. Lett. 59 (2015) 11.

[9] S. Beckford, L. Mathurin, J. Chen, R. A. Fleming, M. Zou, The effects of polydopamine coated Cu nanoparticles on the tribological properties of polydopamine/PTFE coatings, Tribol. Int. 103 (2016) 87-94.

[10] S. Beckford, J. Cai, R. A. Fleming, M. Zou, The effects of graphite filler on the tribological properties of polydopamine/PTFE coatings, Tribol. Lett. 64 (2016) 42.

[11] J. G. Steck, M. Afsher Mohajer, Q. Sun, X. Meng, M. Zou, Fabrication and tribological characterization of deformation-resistant nano-textured surfaces produced by two-photon lithography and atomic layer deposition, Tribol. Int. 132 (2019) 75-84.

[12] J. G. Steck, R. A. Fleming, J. A. Goss, M. Zou, Deformation and fatigue resistance of Al/a-Si core-shell nanostructures subjected to cyclic nanoindentation, Appl. Surf. Sci. 433 (2018) 617-626.

[13] R. A. Fleming, M. Zou, Nanostructure-textured surfaces with low friction and high deformation resistance, Tribol. Trans. 61 (2018) 80-87.

[14] R. A. Fleming, M. Zou, The effects of confined core volume on the mechanical behavior of Al/a-Si core-shell nanostructures, Acta Mater. 128 (2017) 149-159.

[15] R. A. Fleming, M. Zou, Material dimensionality effects on the nanoindentation behavior of Al/a-Si core-shell nanostructures, Appl. Surf. Sci. 412 (2017) 96-104.

[16] W. Tidwell, D. Scott, H. Wang, R. A. Fleming, M. Zou, Nanoindentation study of deformation-resistant Al/a-Si core-shell nanostructures, Acta Mater. 59 (2011) 6110-6116.

[17] B. Morton, H. Wang, R. A. Fleming, M. Zou, Nanoscale surface engineering with deformation-resistant core-shell nanostructures, Tribol. Lett. 42 (2011) 51-58.

[18] C. C. Crane, F. Wang, J. Li, J. Tao, Y. Zhu, J. Chen, Synthesis of copper–silica core–shell nanostructures with sharp and stable localized surface plasmon resonance, J. Phys. Chem. C. 121 (2017) 5684-5692.

[19] Y. Jiang, D. Choudhury, M. Brownell, A. Nair, J. Goss, M. Zou, The effects of annealing conditions on the wear of PDA/PTFE coatings, Appl. Surf. Sci. 481(2019) 723-735.

[20] Membrane Materials, in: Y. Osada, T. Nakagawa (Eds.), Membr. Sci. Tech., 2006, pp. 40-104.

[21] J. Tröger, K. Lunkwitz, K. Grundke, W. Bürger, Determination of the surface tension of microporous membranes using wetting kinetics measurements, Coll. Surf. A: Physicochem. Eng. Asp. 134 (1998) 299-304.

[22] Y. Zhao and M. Zou, Experimental investigation of the wear mechanisms of thin PDA/PTFE coatings, Prog. Org. Coat. 137(2019) 105341.

Chapter 3

Tribological Behavior of Polydopamine/Polytetrafluoroethylene Coating on Laser Textured Stainless Steel with Hilbert Curves

3.1 Abstract

Shallow Hilbert curve patterns with easily programmable texture density were selected for laser texturing of stainless steel substrates. Two different texture path segment lengths (12 and 24 μm) and four different laser power percentages (5%, 10%, 15%, and 20%) were investigated. The textured and smooth substrates were coated with thin polydopamine/polytetrafluoroethylene (PDA/PTFE) coatings for tribological property assessment. The effects of texture density (texture area coverage) and laser power on the durability and friction of the coated surfaces were studied. Laser texturing the substrates improved the coating durability up to 25 times, reduced the friction coefficient, and prevented coating global delamination. The textures fabricated with a laser power of 15% and a texture path segment length of 12 μm yielded the best coating durability. The textures provided the interlocking for the PTFE coating and thus prevented its global delamination. Furthermore, the PTFE inside the texture grooves replenished the solid lubricant worn away in the wear track and prolonged the coating wear life.

3.2 Introduction

Controlling the coefficient of friction (COF) between two rubbing surfaces is of great importance in achieving an efficient mechanical movement [1]. Solid lubricant coatings reduce the COF between two surfaces while still supporting the applied load. One such example is

polytetrafluoroethylene (PTFE). PTFE is a useful solid lubricant because it is chemically inert, has high-temperature resistance, and has low maintenance costs [2]. PTFE coatings have a wide range of applications for minimizing COF in mechanical parts. However, pristine PTFE coatings have low wear resistance and low load-bearing performance because of their poor adhesion to the working surfaces. This fact limits applications where thin PTFE coatings can be applied [3].

Several studies have enhanced the wear behavior of thin PTFE coatings [4-6]. Using an adhesive polydopamine (PDA) underlayer that bonds to both substrate and PTFE coatings is an excellent approach that resulted in improving the wear resistance of thin PTFE coating 500 times without affecting its COF [4]. Since the PDA layer is very thin and could attach to all types of material surfaces [7, 8], it could be added as an adhesive underlayer to boost the durability of thin PTFE films without significantly increasing the total film thickness [4].

Surface texturing is another approach for improving the wear resistance under dry sliding contact [9-13]. Studies showed that applying MoS_2 and graphite coatings on microtextured surfaces of steel [14, 15], TiN [16], and TiCN [17] improved the durability of the coatings even for demanding tribological applications. A few studies also reported the combined effect of laser surface texturing and PTFE coating for improving tribological performance. Wang et al. [18] laser-drilled micro-hole array into laser-clad Fe-based alloy coatings on carbon steel and then deposited MoS_2-PTFE powders by electrophoretic deposition. They showed that the combination of 20% micro hole density with MoS_2-10 wt% PTFE powders resulted in the lowest COF. Fan et al. [19] investigated the effect of textured spray-coated PTFE on the micro-dimple-textured Al_2O_3/Ni layered ceramic substrate. They observed 5 times improvement in the durability of textured PTFE coating on the textured substrate compared to smooth PTFE on the untextured substrate. Lu et al. [20] coated PTFE by vacuum impregnation on smooth and laser textured

plasma electrolytic oxidization (PEO) treated 2024 aluminum alloy. They examined the tribological behavior of the samples and observed significantly improved durability due to the surface textures. The textures provided reservoirs for PTFE to compensate for the PTFE inside the wear track.

The aforementioned studies only investigated PTFE coatings with a thickness of more than 20 μm and texture depths of more than 50 μm [18-20]. Deep textures may significantly weaken the mechanical properties of the substrate and will not benefit thin coatings since the coating could not be replenished from the deep valleys of the textures. Also, these studies only investigated the effect of circular dimples that were as large as 50 μm in diameter [18-20]. There is no previous study that combined laser texturing stainless steel substrates with PDA/PTFE coatings. We hypothesize that fabricating laser textures on stainless steel substrates with a shallow Hilbert curve pattern could improve the durability of thin PDA/PTFE coatings. A Hilbert curve is a bidirectional type of space-filling curve that can be defined by its path segment length (Figure 3.1). The texture density can be easily adjusted by changing the path segment length within an arbitrary texture area and the bidirectional nature of the curve could minimize the direction sensitivity of the tribological performance. The curve consists of one continuous line, which allows a laser to continuously cut the curve without turning on and off the laser between line segments, which may lead to inconsistency in the cut pattern at the beginning and end of the line segments. This texture pattern has not been studied for tribological performance before. In the current work, the effects of the laser texture density (texture area coverage) and laser power (LP) were studied to evaluate the effect of shallow Hilbert curve textures on the friction and wear of thin PDA/PTFE coatings.

3.3 Experimental Methods

3.3.1 Sample Fabrication

316 stainless steel substrates (McMaster-Carr) were chosen as the substrate for laser texturing and coating deposition because it is a material commonly used in ball bearings. Square-shaped substrates (25.4 mm × 25.4 mm) of 2.5 mm thickness were polished with sandpaper grit 320 (Buehler, IL, USA), 6 μm polycrystalline diamond suspension (Buehler, IL, USA), and 0.06 μm amorphous colloidal silica suspension (Buehler, IL, USA) for 3, 12, and 15 min, respectively, to obtain a mirror-finished surface. Then samples were rinsed with water and wiped with acetone.

An A-series femtosecond laser micromachining system (32-Oxford Laser A5 Femtosecond, Oxford Lasers Ltd., UK) was used to texture Hilbert curve patterns on the polished stainless steel substrates. The laser is a diode-pulsed solid-state femtosecond laser (Carbide CB1-05, Light Conversion, Inc.) with a wavelength of 515 nm, a pulse length of 290 fs, and the maximum average laser power of > 5 W at 60 kHz per wavelength. A custom MATLAB script was used to generate the Hilbert curve patterns and export the curve path as G-code for the femtosecond laser system to execute. The laser power (LP) and laser texture density (the ratio of textured area to the total area of the substrate) were varied. Four laser powers of 5%, 10%, 15%, and 20% of the measured maximum laser power of 2.6 W were applied with a laser frequency of 600 Hz and an R.A. divider of 1,200. These laser parameters were chosen because they allow the generation of shallow grooves with less laser debris. Also, they provide the desired textured area density, making it easy for coating thin PDA/PTFE films inside the texture grooves. The path segment lengths of the Hilbert curves were set to 12 and 24 μm, respectively, for achieving

different laser texture densities. Samples were labeled as P(X, Y), where X is the texture path segment length in μm, and Y is the laser power in the percentage of 2.6 W.

Table 3.1: Sample types with different texture path segment lengths and different laser power having different texture densities. All samples were textured with a laser frequency of 600 Hz and an R. A. divider of 1,200.

Sample type	Substrate	Laser texture path segment length (μm)	Laser power (% of 2.6 W)	Texture density (Area coverage %)
P(0, 0)	Polished stainless steel (SS)	0	0	0
P(12, 5)	Laser textured SS	12	5	19.21 ± 6.8
P(12, 10)	Laser textured SS	12	10	32.03 ± 5.2
P(12, 15)	Laser textured SS	12	15	44.01 ± 7
P(12, 20)	Laser textured SS	12	20	51.56 ± 5.9
P(24, 5)	Laser textured SS	24	5	9.23 ± 3.2
P(24, 10)	Laser textured SS	24	10	17.18 ± 2.7
P(24, 15)	Laser textured SS	24	15	24.00 ± 3.2
P(24, 20)	Laser textured SS	24	20	27.69 ± 3.5

Next, smooth and laser textured stainless steel substrates were cleaned by washing sequentially in deionized (DI) water with detergent, then in acetone, followed by in isopropanol in a sonication bath, each with a duration of 20 min. PDA/PTFE coatings were then deposited on the clean substrate according to our published research [4]. Briefly, 0.04 g of dopamine hydrochloride (DA, Sigma Aldrich) was dissolved into 25 mL of DI water, and 0.025 g of tris (hydroxymethyl) aminomethane (T1503, Sigma Aldrich) was added to it to obtain a pH of 8.5. Smooth and laser textured stainless steel substrates were placed in the above solution in a rocking bath to deposit PDA adhesive underlayer with 25 rpm rocking rate and 7° rocking angle at 60 °C for 45 min. The stainless steel substrates were then dip-coated with an aqueous PTFE dispersion (Teflon Dispersion DISP30, Fuel Cell Earth) with 60 wt% of PTFE. The dipping and withdrawal speed was 10 mm/min, and soaking time was 1 min. A small area on the top portion of the samples was not coated by PTFE to create a height step for PTFE thickness measurements.

Immediately after the PTFE coating, samples were heated at 120, 300, and 372 °C, each for 4 min to drive off water and surfactant, and sinter the PTFE particles respectively.

3.3.2 Sample Characterization

The surface roughness of the smooth and laser textured stainless steel substrates, the profiles of the Hilbert curve texture grooves on stainless steel, and the PDA-coated stainless steel substrates were measured using a 3D laser scanning confocal microscope (VK-X260, Keyence Corporation). The counterface and the wear tracks from the durability tests were also imaged by it. The surface roughness and topography of the PDA/PTFE coatings on smooth and laser textured stainless steel substrates, as well as the profiles of texture grooves on PDA/PTFE-coated stainless steel substrates, were measured using an atomic force microscope (AFM, Dimension Icon, Bruker) with a ScanAsyst air AFM tip (Bruker) having a 0.4 N/m spring constant.

The PTFE layer thickness was measured using a stylus contact profilometer (Dektak 150, Bruker Nano Surfaces) at three different locations over the intersection between the PDA layer and PTFE layer, and the average value was reported. The scan length was 2000 μm and the scan duration was 60 s. The profiles of the wear tracks were also measured by the stylus profilometer. X-ray photoelectron spectroscopy (XPS) was applied (PHI Versaprobe XPS system, Physical Electronics) to measure the elements and chemical states inside the wear tracks.

A custom MATLAB script was used to calculate the texture density of the Hilbert curve textures from images obtained by the 3D laser scanning confocal microscope. At least 5 images were sampled for each parameter combination.

3.3.3 Tribological Tests

Durability tests were run on smooth and laser textured stainless steel substrates coated with PDA/PTFE using a tribometer (UMT-3, Bruker). All tests were conducted in a linear reciprocating motion with a ball-on-plate configuration. Cr steel balls (McMaster-Carr) having diameters of 6.35 mm were used as counterfaces. A normal load of 2 N was applied during the test with a stroke length of 5 mm and a sliding speed of 10 mm/s. The failure standard was set to friction forces larger than 0.65 N, which is equivalent to a failure COF threshold of 0.325. Neglecting the impact of PDA/PTFE coating and laser textured grooves, the Hertzian contact pressure that corresponds to 2 N normal load on stainless steel was 615 MPa. All tests were run at room temperature and relative humidity of 30%. These testing parameters were chosen to accelerate the test to failure time.

3.4 Results and Discussion

3.4.1 Surface Texture Characterization

Table 3.1 shows the sample types and the corresponding laser power, texture path segment length, and texture density on the stainless-steel substrates. Texture density was calculated based on optical images as the ratio of the textured area to the total area of the substrate using a custom MATLAB script. At least 5 images were sampled for each parameter combination. The texture density was controlled by using two different path segment lengths of the Hilbert curves and varying the laser power. It can be seen that increasing the path segment length decreased the texture density while increasing the laser power increased the texture density due to the wider texture grooves generated with higher laser power.

The line plots from the Hilbert curve mathematical model and the optical images of the laser textured Hilbert curves on stainless steel substrates with path segment lengths of 12 and 24 µm are shown in Figures 3.1A and B, respectively. The effects of laser power on the fabricated texture densities are presented in Figure 3.2. It is shown that increasing the laser power resulted in deeper and wider texture grooves. Wider texture grooves resulted in larger texture area coverage. Also, higher laser powers resulted in more debris generated around the texture grooves, which could have a detrimental effect on the tribological performance.

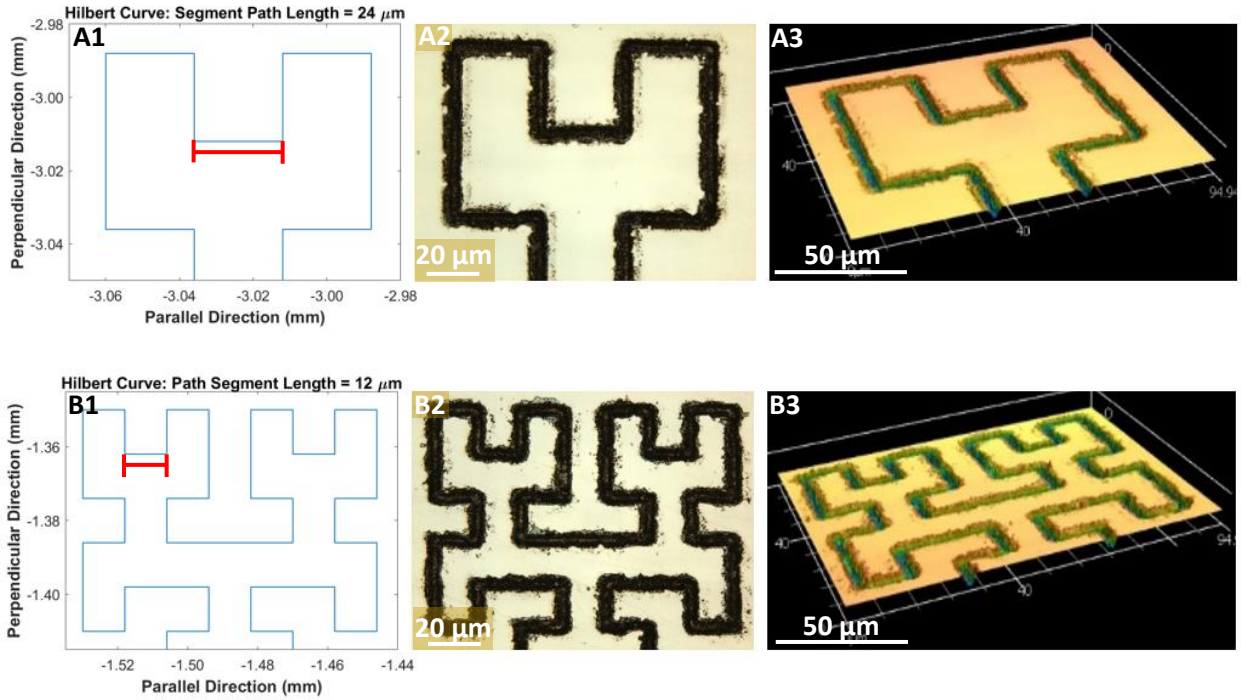

Figure 3.1: Line plots from the mathematical models of Hilbert curves and the top-down and 3D oblique-angle views of the optical images of laser textured Hilbert curves on polished stainless steel surfaces with two texture path segment lengths of (A) 24 µm and (B) 12 µm. Red lines in (A1) and (B1) represented the texture path segment length.

Figure 3.3A illustrates the average texture density associated with each texture path segment length and laser power. It can be seen that reducing the texture path segment length and increasing laser power increased the average texture density and average surface roughness

because of wider and deeper texture grooves. The smooth stainless steel had a smaller average surface roughness than laser textured stainless steel. Substrates with higher texture density had a larger average surface roughness than substrates with lower texture density. The average depth and width of texture grooves with different laser powers are demonstrated in Figure 3.4. As expected, the texture path segment length could not affect the groove size. The depth of the texture grooves increased with the laser power. It was 0.3 μm when the laser power was 5% and increased to 1.8 μm when the laser power 20%. Similarly, the width of the texture grooves increased with the laser power from 2.5 μm for 5% laser power to 4.4 μm for 20% laser power. It was shown that the selected laser parameters resulted in shallow texture grooves (< 2 μm) compared to textured depths reported in previous studies that were larger than 50 μm [18-20]. Deep texture grooves could hamper the lubrication recovery since solid lubricant would get stuck inside the grooves.

Figure 3.5 illustrates the surface topography profiles of laser textured grooves on stainless steel, the PDA deposited stainless steel, and PDA/PTFE coated stainless steel measured by Dektak. As shown, the depth of the grooves decreased in each step after depositing PDA and PTFE coatings, indicating the PDA and PTFE were successfully deposited inside the texture grooves. The measured average thickness of the PTFE coatings based on the difference in height between the exposed PDA layers outside the textured area and the PDA/PTFE coatings was at 1.65 ± 0.098 μm but the average difference between the depth of the textured grooves of the PDA deposited stainless steel and that of the PDA/PTFE coated stainless steel was less than 0.75 μm. This difference indicates that the PTFE thickness inside the texture grooves was less than the thickness of PTFE on the smooth area. Furthermore, the difference in the texture groove depths fabricated using different laser power before and after coating PTFE indicated that deeper

and wider texture grooves fabricated using higher laser powers had more PTFE stored. The profile of textured grooves on P(12, 5) became almost flat after coating with PDA/PTFE,

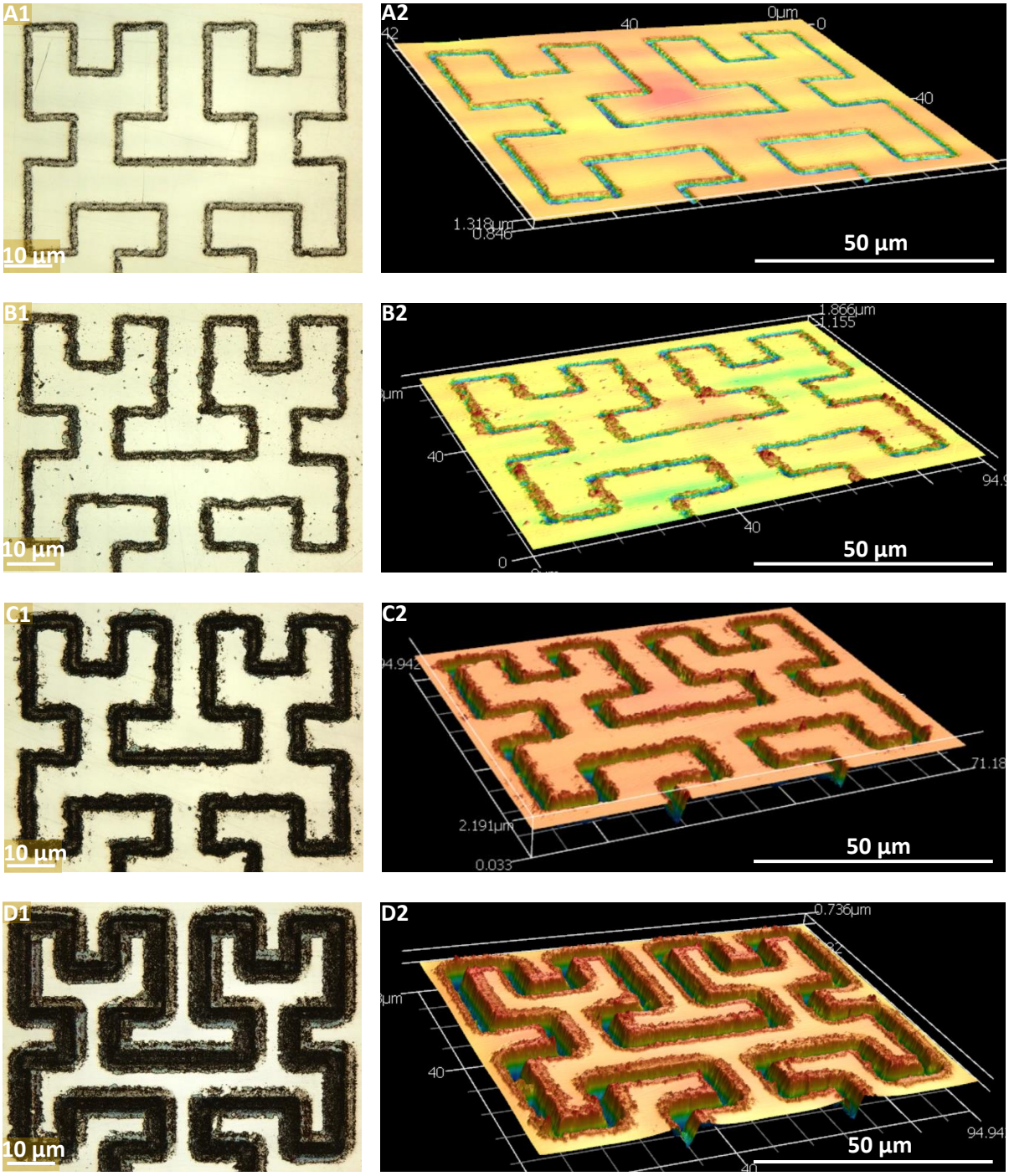

Figure 3.2: Effect of different laser powers on the Hilbert curve textures: (A) LP = 5%, (B) LP = 10%, (C) LP = 15%, and (D) LP = 20%.

indicating it is easier to fill the shallowest grooves. This can also be seen in the average surface roughness data illustrated in Figure 3.6. It is shown that the average surface roughness of PDA/PTFE coatings on P(12, 5) and P(24, 5) was similar to the average surface roughness of the coatings on smooth stainless steel, P(0, 0). As discussed above, the texture groove profile of PDA/PTFE on these two laser textured surfaces was almost flat resulting in an average surface roughness similar to that on smooth surfaces. Coating PDA/PTFE increased the average surface roughness of the remaining textures due to the additional roughness introduced by the PDA/PTFE coating. As the laser power increased, the surface roughness of PDA/PTFE coatings also increased due to the deeper grooves cannot be filled by the thin PDA/PTFE coatings. PDA/PTFE coatings on laser textured surfaces with 12 μm texture path segment lengths had a larger roughness value than those on laser textured surfaces with 24 μm texture path segment lengths fabricated with the same laser power because of the existence of more textured grooves underneath the coatings.

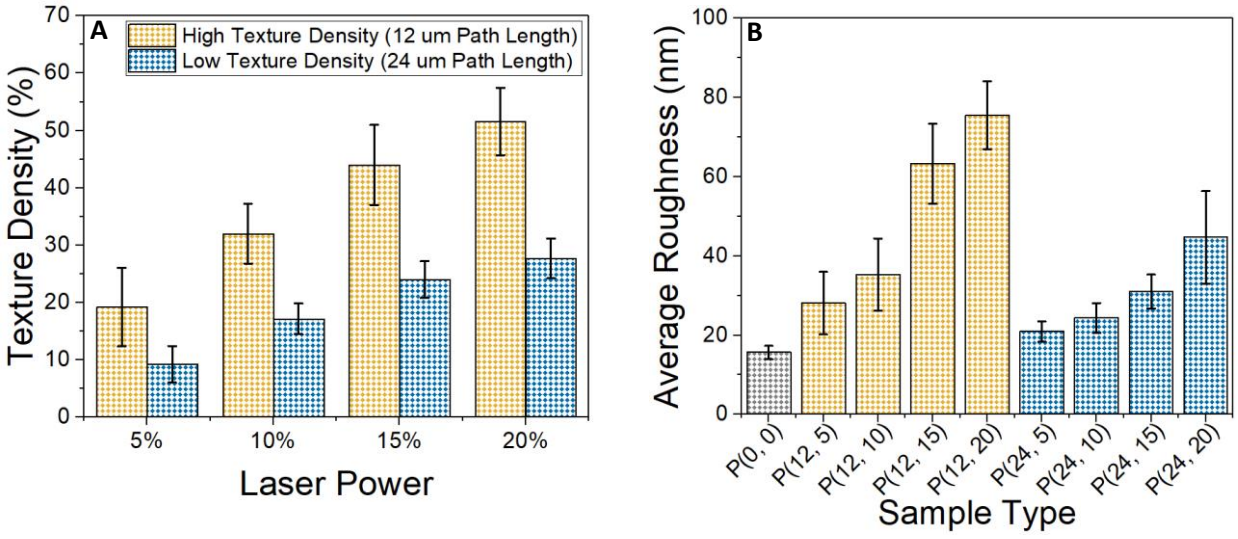

Figure 3.3: Texture density and average surface roughness of surfaces with two different texture path segment length of 24 and 12 μm and four different laser powers: (A) Texture density and (B) average surface roughness of smooth and laser textured stainless steel substrates.

Figure 3.7 shows the images of PDA/PTFE coatings on the smooth (Figure 3.7A1 and A2) and laser textured (Figures 3.7B1-E1 and B2-E2) stainless steel measured by AFM. The wide field of view images (7A1-E1) present the overall look of the PTFE coatings. The texture grooves from higher laser powers were darker (deeper) and more noticeable in the AFM images. Higher magnification images are provided for a closer look at the PTFE particles inside the texture grooves. Figures 3.7C2-E2 showed the textured grooves were fully covered with spindle-like PTFE particles. Also, there was no evidence of coating protrusion inside or on the edge of texture grooves.

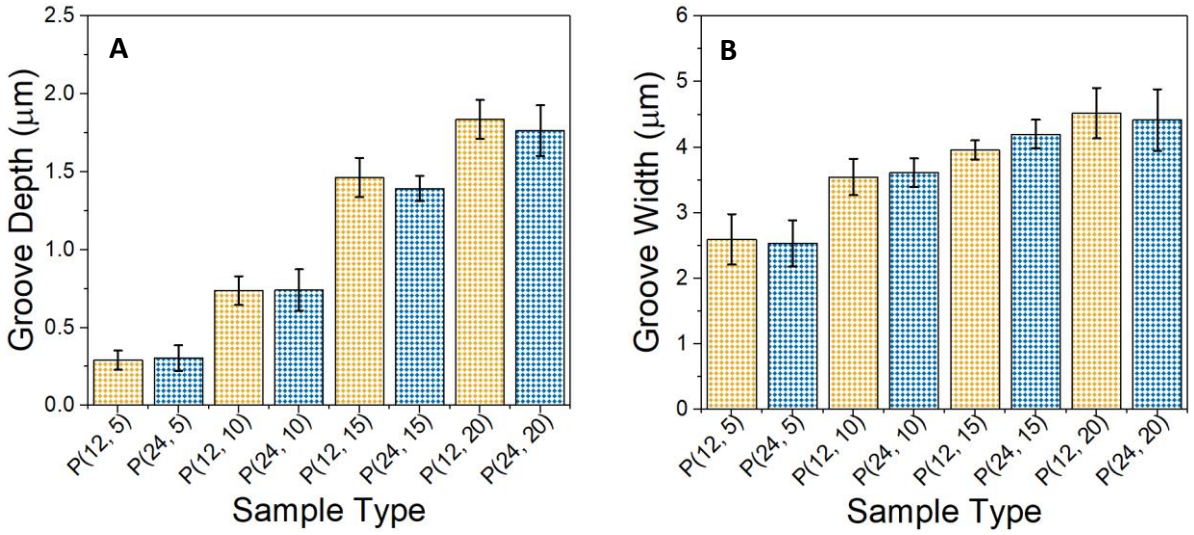

Figure 3.4: Measured groove depth and width of Hilbert curve textures fabricated with different laser powers and texture path segment length: (A) Depth and (B) width.

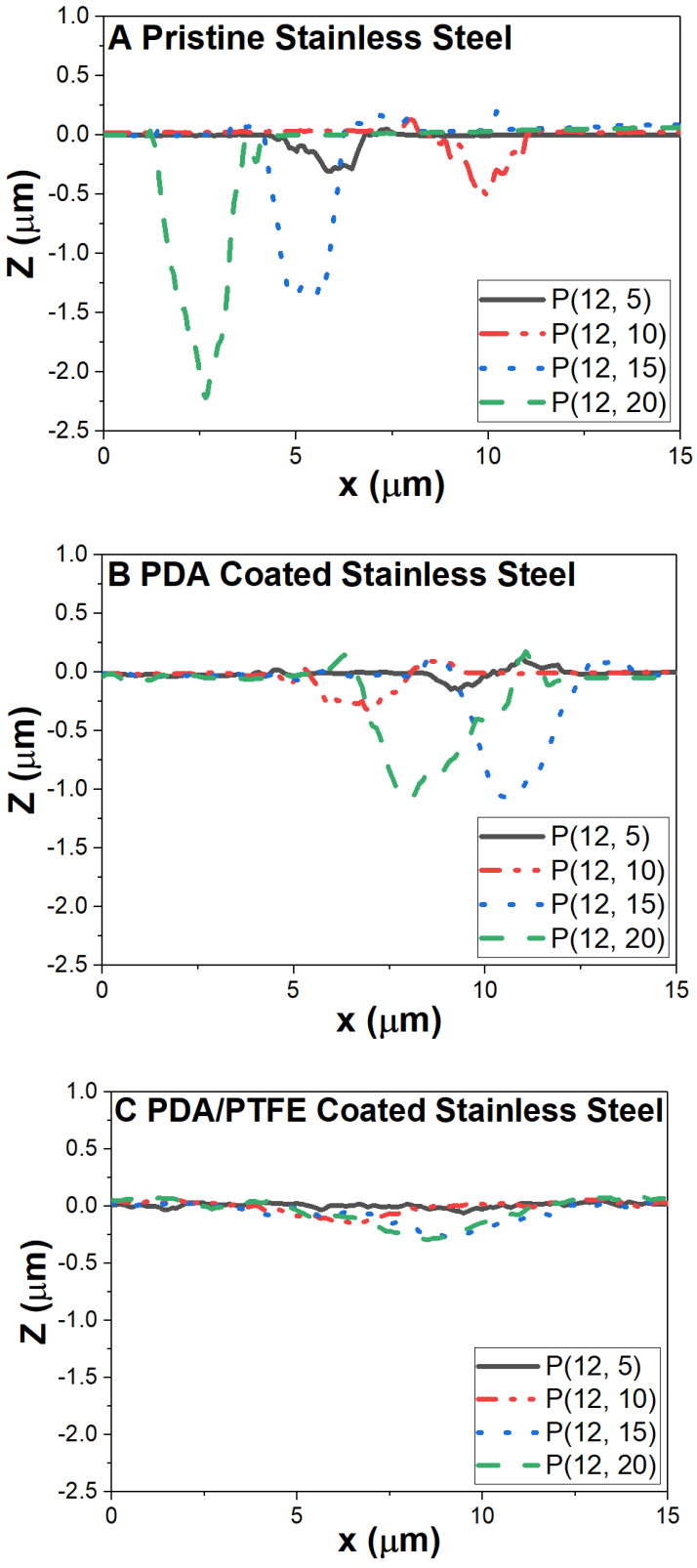

Figure 3.5: Surface topography profile of the textured grooves on (A) pristine, (B) PDA-coated, and (C) PDA/PTFE-coated laser textured stainless steel measured by Dektak.

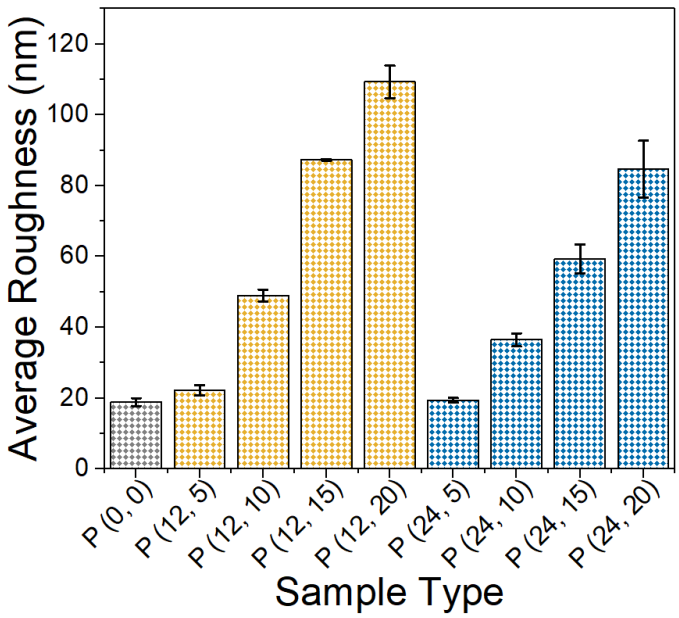

Figure 3.6: Average surface roughness of PDA/PTFE coatings on smooth and laser textured stainless steel.

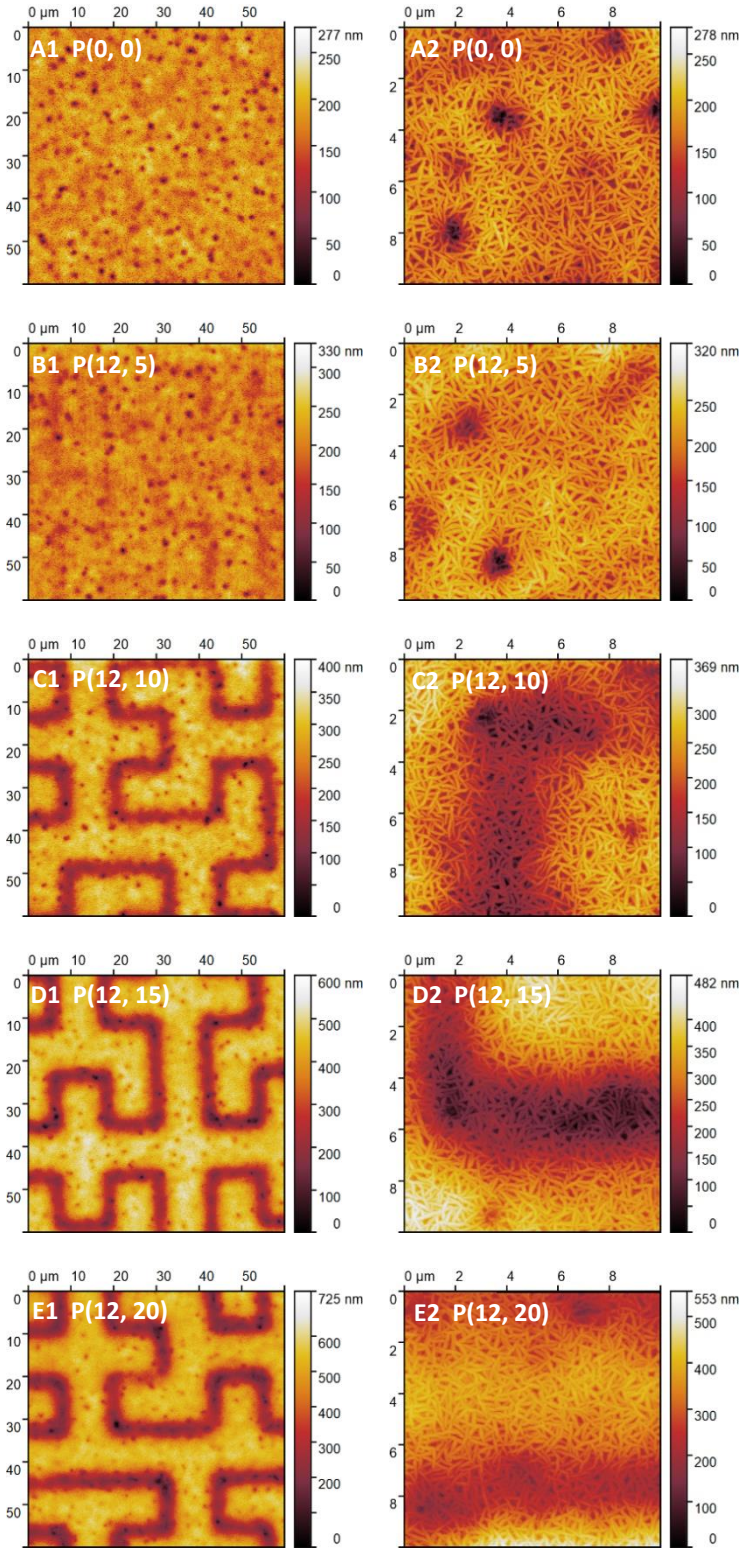

Figure 3.7: AFM images of PDA/PTFE coatings on smooth and laser textured stainless steel with two scan sizes. The texture path segment length is 12 µm in all images and the laser power is: (A1) and (A2) 0, (B1) and (B2) 5%, (C1) and (C2) 10%, (D1) and (D2) 15%, and (E1) and (E2) 20%.

3.4.2 Tribological Test Results

Figure 3.8 illustrates the COF of the PDA/PTFE coatings on smooth and laser textured substrates during the durability tests. As shown, the coatings on laser textured stainless steel had smaller COF than coatings on smooth stainless steel over the test duration. Several peaks existed on the COF graph of samples associated with laser textured stainless steel (pointed with arrows of the same color as each curve). These peaks might represent the points where the coatings were recovered from failure. In other words, although the counterface ball reached the stainless steel, the PTFE stored inside the textured grooves replenished the wear track, and as a result, the complete failure was delayed. This is confirmed by the XPS analysis of the wear track on the PDA/PTFE coating on the P(12, 15) sample after failure shown in Figure 3.9. As shown, F1s and C1s peaks typically present in PTFE were found inside the wear track. This confirms that the durability test results were valid because if the sharp peaks were the failure point, the substrate would have been over rubbed by the counterface ball, and hence, Fe would be the dominant element in the XPS analysis. The close-up looks at the first 150 cycles during which the control sample failed show a step increase in the COF curve during the first few cycles (Figure 3.8C and 3.8D) (pointed with arrows of the same color as each curve). This step increase happened when the counterface ball compacted the loosely connected rough PTFE coating particles, which led to smoother coatings and higher contact area and thus increased COF. Most of the COFs for coatings on laser textured substrates experienced a second step increase on their graphs. The second step possibly happened when the counterface ball compacted the PTFE stored inside the texture grooves. After this point, the COF remained flat and steady until the sharp peaks occurred.

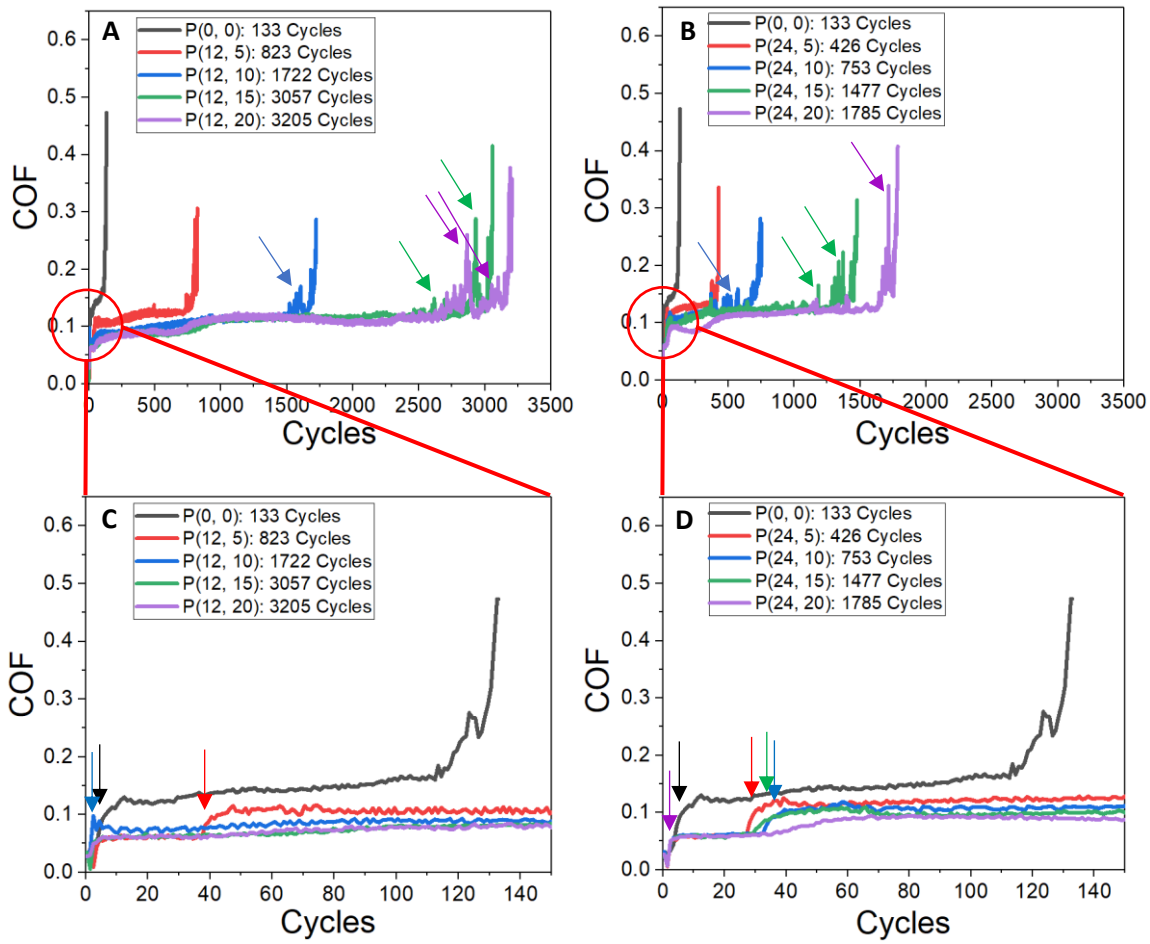

Figure 3.8: COF of the PDA/PTFE coatings on smooth and laser textured stainless steel substrates during the durability tests: Texture path segment length of (A) 12 μm, (B) 24 μm, (C) and (D) zoom-in plots of the first 150 cycles of (A) and (B), respectively.

Figure 3.10 shows the tribological test results. As shown in Figure 3.10A, laser texturing the stainless steel substrates significantly improved the durability of the PDA/PTFE coatings from 140 cycles for PDA/PTFE on smooth stainless steel to almost 3,500 cycles for PDA/PTFE on laser textured stainless steel (25 times improvement). Generally, samples with high laser power had longer durability than samples with low laser power. This is because higher laser power made the texture grooves deeper and wider with more PTFE stored inside the grooves. It also led to a larger surface roughness, which provided the interlocking for the coating. Both of these factors played a part in the remarkably improved durability of the textured samples. While

the largest improvement of durability life for PTFE coatings reported in the previous studies was only up to 8 times, this study showed 25 times improvement in the durability life of thin PTFE coatings.

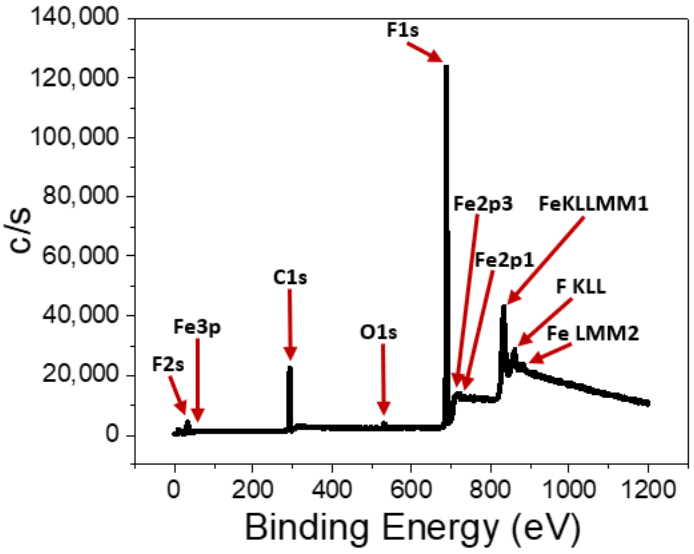

Figure 3.9: XPS analysis of elements inside the wear track after durability test failure on sample P(12, 15).

As shown in Figure 3.10B, the PDA/PTFE coatings on the laser textured stainless steel had a lower COF than the one on smooth stainless steel due to the less contact area between counterface ball and coatings. In addition, coatings on substrates with high texture density had a lower COF than coatings on substrates with low texture density. This is mainly because the counterface ball was in contact with the smoother area on samples having low texture density than samples having high texture density.

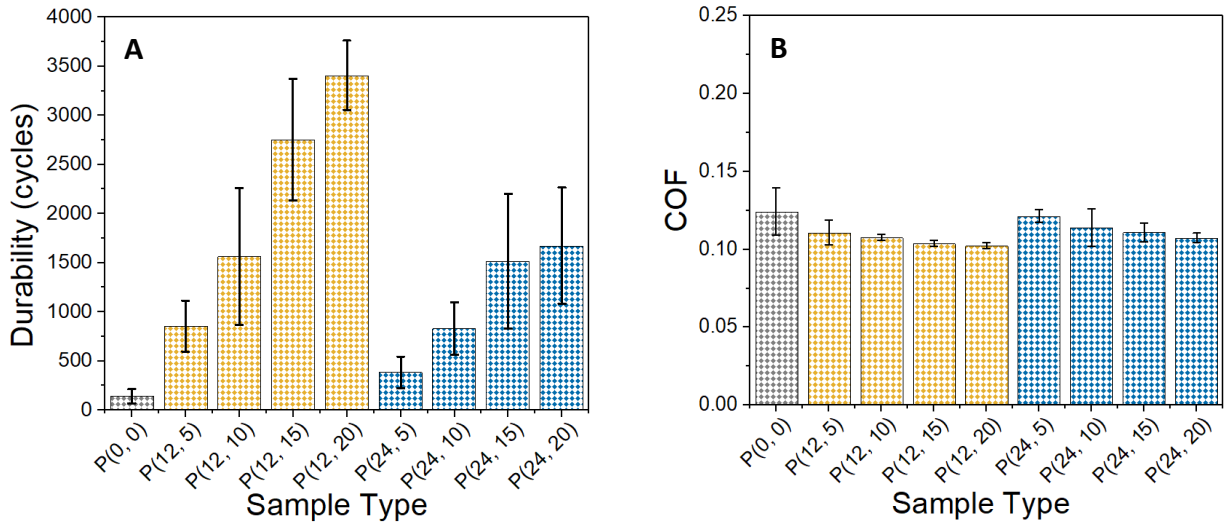

Figure 3.10: Tribological test results: (A) Durability and (B) COF of PDA/PTFE coatings on smooth and laser textured stainless steel.

Figure 3.11 illustrates the optical images of the ball counterfaces and the wear tracks of the PDA/PTFE coatings on the smooth and laser textured stainless steel substrates after the durability tests. There was only a small amount of PTFE residue inside the wear track of the coating on the smooth substrate (arrows on Figure 3.11A2-A3), indicating global delamination has occurred. As shown in Figure 3.12, the wide and flat wear track profile on the smooth substrate was consistent with global delamination. Moreover, the amount of transferred PTFE on the counterface ball for test on the coated smooth substrate was relatively high even though it had short wear life. In contrast, the wear tracks on the coated laser textured substrates had no sign of global delamination. As a consequence of longer durability (testing duration), the width of the wear track enlarged as the laser power used to fabricate the laser textured substrates increased, so did the amount of transferred PTFE on the counterface ball. The surface topography profiles of the wear tracks on the coated laser textured substrates (Figure 3.12) were curved and only the center part of the coating was removed, indicating the laser textures can provide interlocking to prevent PDA/PTFE coatings from global delamination.

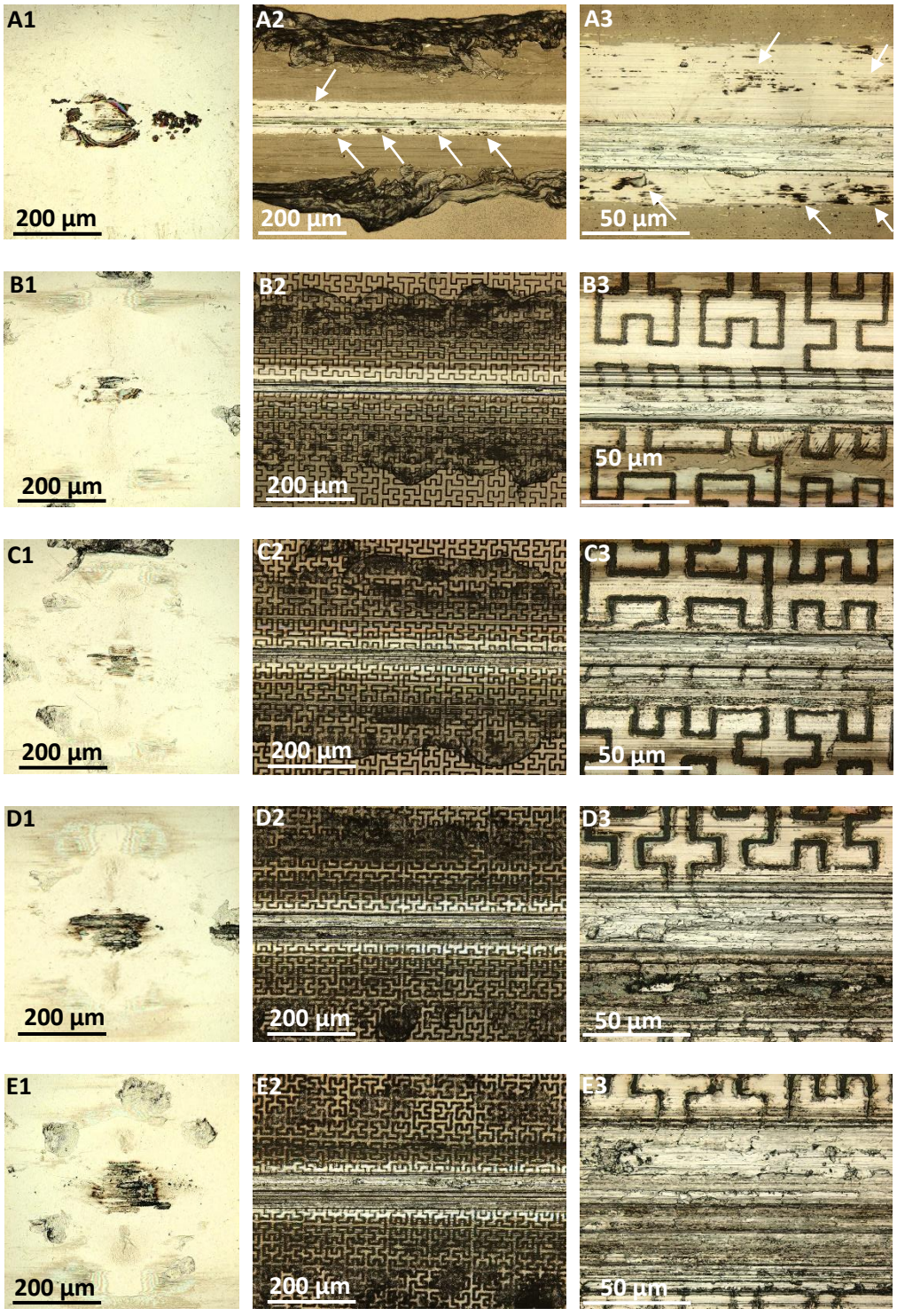

Figure 3.11: Optical images of the counterface balls and wear tracks: (A1)–(E1) counterface balls and (A2)–(E2) wear tracks after the durability test on PDA/PTFE coatings on smooth and laser textured stainless steel with the texture path segment length of 12 µm and LP of (A) 0, (B) 5%, (C) 10%, (D) 15%, and (E) 20%. (A3)–(E3) are zoom-in images of (A2)–(E2). The arrows in (A2) and (A3) point to small amounts of PTFE residue inside the wear track.

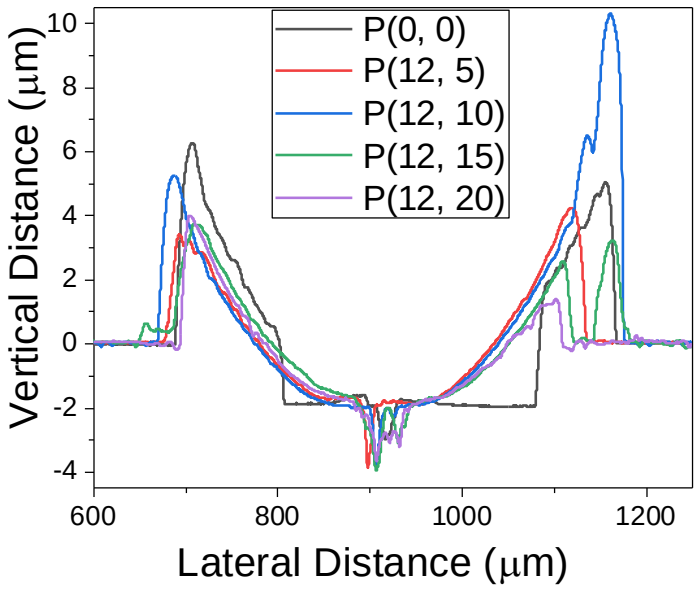

Figure 3.12: Surface topography profiles of the wear tracks after the durability test on the PDA/PTFE coatings on smooth and laser textured stainless steel substrates.

Figures 3.13 and 3.14 present the wear tracks of progressive tests with an increasing number of testing cycles on the coated smooth and laser textured substrates, respectively, to uncover the wear mechanism of PDA/PTFE coatings. PTFE residue inside the wear tracks on the smooth substrate explained the global delamination regardless of the number of cycles that the counterface ball had rubbed the coating (Figure 3.13). Even though there was relatively less transferred PTFE on the counterface ball after 25 cycles, delamination inside the wear track was noticeable. Also, the wear tracks on the smooth substrates were wide and flat from the beginning of the test until the coating failed at 85 cycles and the substrate was worn. In contrast, the wear track on the laser textured surfaces (Figure 3.14) was not obvious when tested for 150 cycles, while it became wider and deeper as the test ran for more cycles indicating an abrasive wear mechanism. After 1,600 cycles of the test (failure cycle of this sample), the substrate was exposed, and the textures were damaged. As discussed before, the progressive tests also showed that the PTFE from inside the textured grooves transferred to the worn top surface of the wear

track (arrows in Figures 3.14A3 and 3.14B3). After the counterface ball rubbed the coating halfway for 850 cycles (Figure 3.14C2 and C3), the texture grooves started to become shallower until they completely vanished, and the coating failed after 1,600 cycles of the test (Figure 3.14G2 and G3). During the testing, the PTFE stored inside the texture grooves got picked up by the counterface ball and transferred back to the wear track, making the test last longer. Also, the amount of transferred PTFE on the counterface ball was minimum until 500 cycles and it increased gradually until the failure of the test, indicating that PTFE was replenished at a relatively constant rate.

Figure 3.15 presents the wear track profiles corresponding to the progressive tests in Figures 3.13 and 3.14. As discussed above, the wear tracks on the coated smooth substrates were wide and flat indicating the global delamination of PTFE, while the wear tracks on the coated laser textured substrates were curved indicating abrasive wear. Also, the depths of the wear tracks on the smooth substrates were almost the same from 25 cycles to 85 cycles. The depth of the wear tracks on the coated laser textured substrate, however, increased as the test continued from 150 cycles to 1,600 cycles. The grooves on the wear track profile associated with 85 cycles on smooth and 1,500 cycles on laser textured substrates indicated the failure point where the counterface ball contacted the stainless steel substrate.

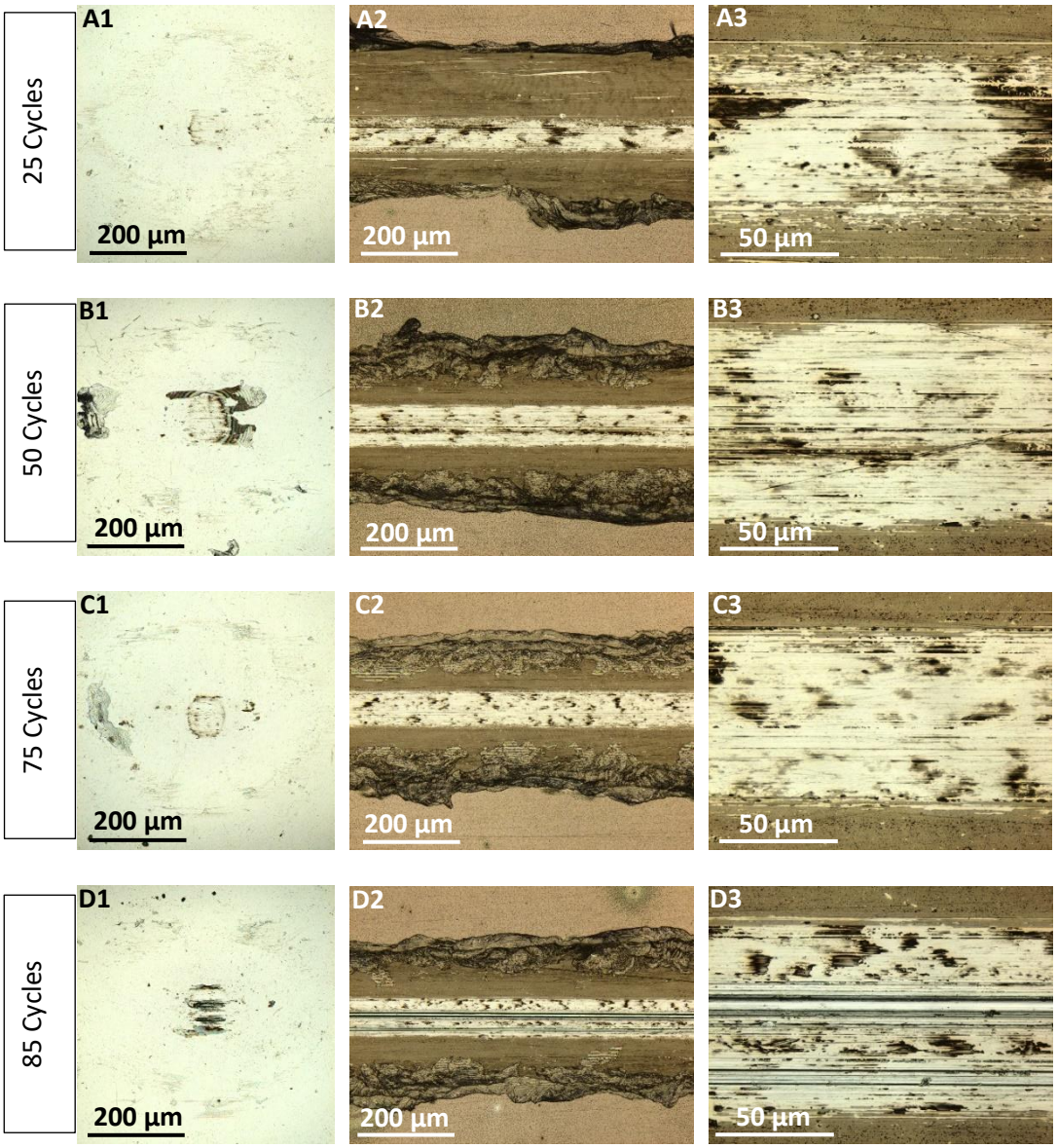

Figure 3.13: Optical images of the counterface balls and wear tracks: (A1)–(D1) counterface balls and (A2)–(D2) wear tracks after progressive test on the PDA/PTFE coatings on smooth stainless steel. (A3)–(D3) are zoom-in images of (A2)–(D2).

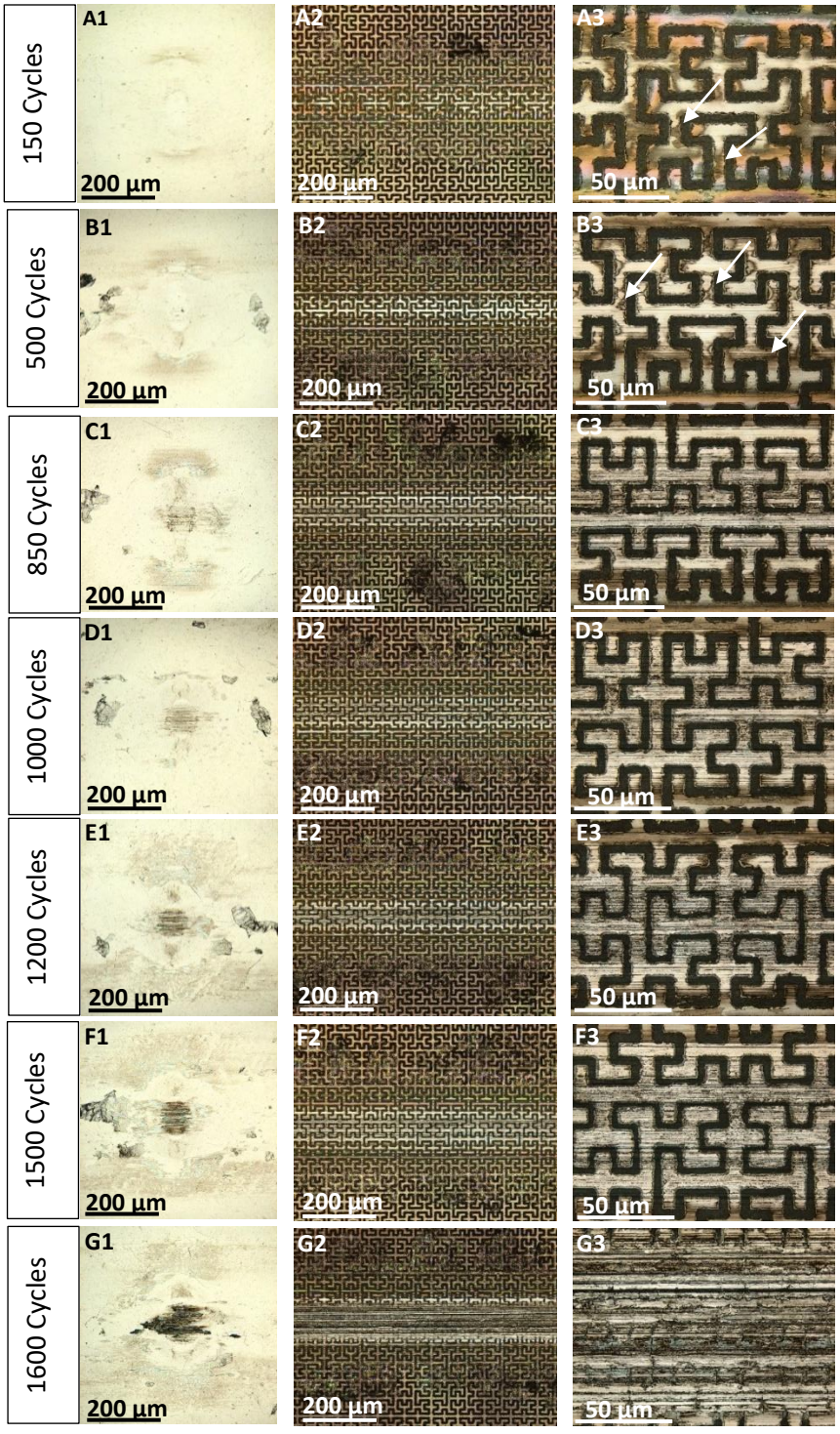

Figure 3.14: Optical Images of the counterface balls and wear tracks: (A1)–(G1) counterface balls, and (A2)–(G2) wear tracks after progressive tests on the PDA/PTFE coatings on laser textured stainless steel. (A3)–(G3) are zoom-in images of (A2)–(G2). The arrows in (A2) and (A3) point to small amounts of PTFE residue inside the wear track. The arrows in (A3) and (B3) point to the PTFE coating transferred from inside the textured grooves to the worn top surface of the wear track.

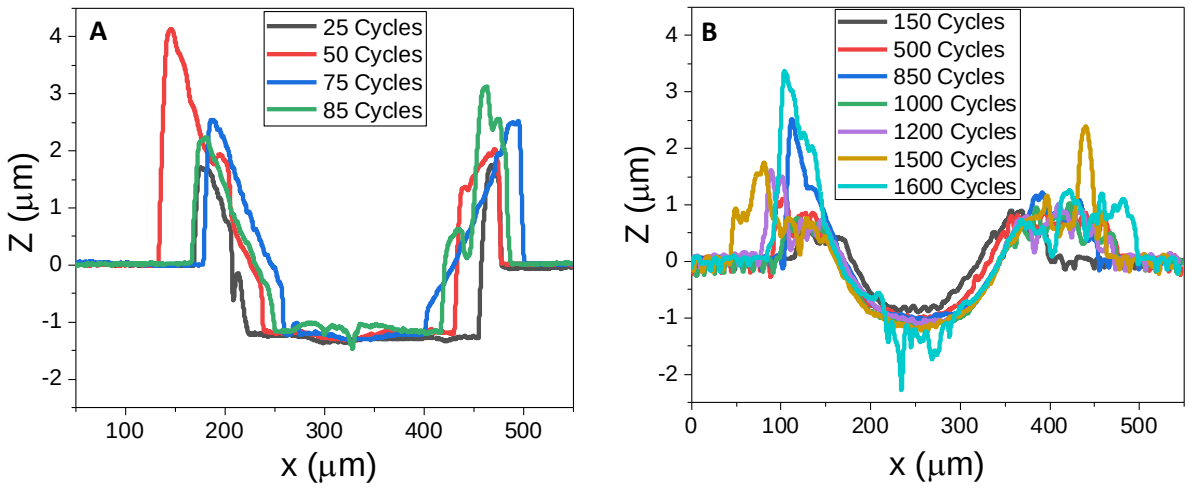

Figure 3.15: Surface topography profile of the wear tracks on the PDA/PTFE coatings on (A) smooth and (B) laser textured stainless steel from progressive tests in Figures 3.14 and 3.15.

3.5 Conclusion

Stainless steel substrates were laser textured with Hilbert curves of two different texture path segment lengths using four different laser powers. Higher laser powers resulted in deeper and wider laser texture grooves, as well as larger average surface roughness. Laser power and texture path segment length both significantly changed texture density. Polydopamine/ polytetrafluoroethylene (PDA/PTFE) was coated on smooth and laser textured stainless steel. Coatings on laser textured substrates had larger surface roughness and showed significantly longer durability with coatings on P(12, 20) having the longest durability of 3,500 on average compared to coatings on smooth substrates which had the durability of only 140 cycles on average. However, a laser power of 15% was selected as the desirable laser power since the 20% laser power resulted in surface debris. In addition, coatings on laser textured substrates had a slightly lower COF than coatings on smooth substrates. Moreover, laser texturing the substrates prevented the global delamination inside the wear track and PTFE stored in the textured grooves replenished the PTFE to the top surface of the wear track. These results suggested that the

Hilbert curve texture can be used to significantly extend PDA/PTFE coating wear life while lowering the COF.

3.6 Acknowledgements

This work was supported by the National Science Foundation under Grants CMMI-1563227 and OIA-1457888. Any opinions, findings, and conclusions or recommendations expressed in this material are those of the authors and do not necessarily reflect the views of the National Science Foundation. The authors thank the use of the Arkansas Nano and Bio Materials Characterization Facility for the use of the XPS system.

References

[1] G. Mariani, "Selection and application of solid lubricants as friction modifiers," in *Lubricant Additives*: CRC Press, 2017, pp. 99-115.

[2] H. Unal, A. Mimaroglu, U. Kadıoglu, and H. Ekiz, "Sliding friction and wear behaviour of polytetrafluoroethylene and its composites under dry conditions," *Materials & Design,* vol. 25, no. 3, pp. 239-245, 2004.

[3] C. Donnet and A. Erdemir, "Solid lubricant coatings: recent developments and future trends," *Tribology Letters,* vol. 17, no. 3, pp. 389-397, 2004.

[4] S. Beckford and M. Zou, "Wear resistant PTFE thin film enabled by a polydopamine adhesive layer," *Applied surface science,* vol. 292, pp. 350-356, 2014.

[5] Y. Jiang, D. Choudhury, M. Brownell, A. Nair, J. A. Goss, and M. Zou, "The effects of annealing conditions on the wear of PDA/PTFE coatings," *Applied surface science,* vol. 481, pp. 723-735, 2019.

[6] C. Miller, D. Choudhury, and M. Zou, "The effects of surface roughness on the durability of polydopamine/PTFE solid lubricant coatings on NiTiNOL 60," *Tribology Transactions,* vol. 62, no. 5, pp. 919-929, 2019.

[7] J. Ou, J. Wang, Y. Qiu, L. Liu, and S. Yang, "Mechanical property and corrosion resistance of zirconia/polydopamine nanocomposite multilayer films fabricated via a novel non-electrostatic layer-by-layer assembly technique," *Surface and interface analysis,* vol. 43, no. 4, pp. 803-808, 2011.

[8] J. Ou, L. Liu, J. Wang, F. Wang, M. Xue, and W. Li, "Fabrication and tribological investigation of a novel hydrophobic polydopamine/graphene oxide multilayer film," *Tribology Letters,* vol. 48, no. 3, pp. 407-415, 2012.

[9] Z. Wu, Y. Xing, P. Huang, and L. Liu, "Tribological properties of dimple-textured titanium alloys under dry sliding contact," *Surface and Coatings Technology,* vol. 309, pp. 21-28, 2017.

[10] A. Rosenkranz, L. Reinert, C. Gachot, and F. Mücklich, "Alignment and wear debris effects between laser-patterned steel surfaces under dry sliding conditions," *Wear,* vol. 318, no. 1-2, pp. 49-61, 2014.

[11] A. Borghi, E. Gualtieri, D. Marchetto, L. Moretti, and S. Valeri, "Tribological effects of surface texturing on nitriding steel for high-performance engine applications," *Wear,* vol. 265, no. 7-8, pp. 1046-1051, 2008.

[12] Y. Xing, J. Deng, Z. Wu, and F. Wu, "High friction and low wear properties of laser-textured ceramic surface under dry friction," *Optics & Laser Technology,* vol. 93, pp. 24-32, 2017.

[13] B. Mao, A. Siddaiah, Y. Liao, and P. L. Menezes, "Laser surface texturing and related techniques for enhancing tribological performance of engineering materials: A review," *Journal of Manufacturing Processes,* vol. 53, pp. 153-173, 2020.

[14] L. Rapoport *et al.*, "Friction and wear of MoS_2 films on laser textured steel surfaces," *Surface and Coatings Technology,* vol. 202, no. 14, pp. 3332-3340, 2008.

[15] T. Hu, Y. Zhang, and L. Hu, "Tribological investigation of MoS_2 coatings deposited on the laser textured surface," *Wear,* vol. 278, pp. 77-82, 2012.

[16] C. G. Guleryuz and J. E. Krzanowski, "Mechanisms of self-lubrication in patterned TiN coatings containing solid lubricant microreservoirs," *Surface and Coatings Technology,* vol. 204, no. 15, pp. 2392-2399, 2010.

[17] A. Voevodin and J. Zabinski, "Laser surface texturing for adaptive solid lubrication," *Wear,* vol. 261, no. 11-12, pp. 1285-1292, 2006.

[18] A. Wang, J. Xia, Z. Yang, and D. Xiong, "A novel assembly of MoS_2-PTFE solid lubricants into wear-resistant micro-hole array template and corresponding tribological performance," *Optics & Laser Technology,* vol. 116, pp. 171-179, 2019.

[19] H. Fan, Y. Su, J. Song, H. Wan, L. Hu, and Y. Zhang, "Design of “double layer” texture to obtain superhydrophobic and high wear-resistant PTFE coatings on the surface of Al_2O_3/Ni layered ceramics," *Tribology International,* vol. 136, pp. 455-461, 2019.

[20] C. Lu, P. Shi, J. Yang, J. Jia, E. Xie, and Y. Sun, "Effects of surface texturing on the tribological behaviors of PEO/PTFE coating on aluminum alloy for heavy-load and long-performance applications," *Journal of Materials Research and Technology,* vol. 9, no. 6, pp. 12149-12156, 2020.

Chapter 4

Laser Surface Texturing of Both Thin Polytetrafluoroethylene Coatings and Stainless Steel Substrates for Improving Tribological Properties

4.1 Abstract

Hilbert curve patterns were laser-textured on both stainless steel substrates and polytetrafluoroethylene (PTFE) thin coatings by applying 15% and 5% of the 2.3-W full laser power, respectively. The nanomechanical and tribological behavior of both smooth and laser-textured PTFE coatings on both smooth and laser-textured stainless steel substrates were studied. It was found that laser-texturing thin PTFE coatings reduced the hardness of PTFE coatings and prevented the coating from tearing under nanoindenter scratches. Furthermore, laser-texturing on both PTFE coatings and the stainless steel substrate improved the coating wear life 29 times compared to the wear life of the control sample without any laser textures.

4.2 Introduction

Polytetrafluoroethylene (PTFE) is a polymer composed of carbon and fluorine atoms and is popular for its distinguished properties such as thermal resistance, chemical stability, low surface energy, and low maintenance cost [1, 2]. The polymer is chemically inert due to the strong C–F bonds between the carbon and fluorine atoms of the PTFE [3]. Among all of the desirable properties, PTFE has a low coefficient of friction (COF), which makes its coating a great solid lubricant for surfaces that are in rubbing contact [4]. Besides low friction, PTFE's other properties, including corrosion resistance, drag reduction, superhydrophobicity, and self-cleaning, make the lubricant exceptional for industrial applications [5].

One major downside of PTFE, when used as a coating, is its low wear resistance, which limits its tribological applications [6]. However, laser-texturing of hard metal and metal composite substrate surfaces was found to improve the wear resistance of the PTFE coatings deposited on them [7-11]. For example, laser-texturing the Hilbert curve pattern on stainless steel showed significant improvement in the durability of thin polydopamine (PDA)/PTFE coatings [11]. Micropatterns on the surfaces produced by laser-texturing function as solid lubricant reservoirs and/or wear debris traps that prolong the wear life of the lubricant coating [11]. The roughness created by the textures also provided interlocking to the PTFE coating, thus preventing coating global delamination [12].

While laser surface texturing is capable of providing precise control of the micro/nanopatterns and is environmentally friendly, it has rarely been used to texture PTFE coatings for tribological application. Most studies on laser-texturing of PTFE were on texturing bulk PTFE or PTFE sheets and were for improving surface hydrophobicity by altering the micro/nanostructure of PTFE particles [3, 13-19]. Liang et al. laser machined PTFE surfaces and presented a fibrous homogeneous and heterogeneous surface structure after laser machining. They also suggested a hair-like structure for laser-treated PTFE that was positively affected by laser fluence [16]. Kietzig et al. demonstrated that increasing laser power increased the density and length of hair-like structures [17]. Li et al. applied femtosecond laser treatment on PTFE sheets and fabricated rough microstructures to obtain superhydrophobic surfaces for oil and water separation [13]. Toosi et al. fabricated biaxial and uniaxial nano and micro patterns on PTFE surfaces and showed that PTFE hydrophobic morphologies depend on the laser parameters [14]. Also, Fan et al. laser textured submicron grooves on PTFE surfaces and showed that the intervals between textured grooves affected the superamphiphobicity of PTFE surfaces [15].

Only one study was found that investigated both the superhydrophobicity and the wear resistance of laser-textured PTFE coating on laser-textured Al_2O_3/Ni composites. A 5-time improvement in the wear life of the laser-textured PTFE coating on the laser-textured surface compared to the smooth PTFE coating on a smooth surface was reported [5]. However, in that study, only simple laser texture patterns of dimples and grooves were investigated and the coating had a very large thickness of 30 μm. Furthermore, the texture depths on the coating and substrate were very large, 20 and 55 μm, respectively. Additionally, no adhesive underlayer was used. It has been shown that using polydopamine (PDA) as an adhesive underlayer significantly improves the adhesion of PTFE coatings to the substrate and hence increases its wear life by reducing coating global delamination [20].

The objective of the current study is to understand the effect of laser-texturing shallow grooves on both the substrates and very thin (1.5 μm-thick) PDA/PTFE coatings on the coating tribological properties. Hilbert curve was chosen because it is a single, continuous curve that doesn't cross over itself, which makes the texturing process efficient and the resulting texture uniform. The pattern also combines the benefit of both parallel and perpendicular grooves so that lubricant can remain entrapped for longer periods, which could benefit situations where servicing worn components is expensive or difficult. Additionally, the anisotropic arrangement of the grooves helps ensure that the contact area for wear involves both parallel and perpendicular grooves. In this study, the same Hilbert curve pattern was used to laser-texture the stainless steel substrate and the thin PTFE coating, and the wear and friction of the smooth and laser-textured PTFE coatings on smooth and laser-textured stainless steel substrate were investigated.

4.3 Materials

316 stainless steel substrates (25.4 mm × 25.4 mm × 0.76 mm in size) and Cr steel balls (6.35 mm in diameter) were purchased from McMaster-Carr, IL, USA. Grit 320 sandpaper, 6 μm polycrystalline diamond suspension, and 0.06 μm amorphous colloidal silica suspension were purchased from Buehler, IL, USA. Dopamine hydrochloride and tris (hydroxymethyl) aminomethane were purchased from Sigma Aldrich, MO, USA. Also, aqueous PTFE dispersion (Teflon Dispersion DISP30) with 60 wt% of PTFE was purchased from Fuel Cell Earth, TX, USA.

4.4 Methods

4.4.1 Sample Preparation

Stainless steel substrates were polished to mirror-finish in three steps with sandpaper, diamond suspension, and colloidal silica suspension for 2 min, 12 min, and 15 min, respectively, using an AutoMet 250 Grinder-Polisher (Buehler, IL, USA) with a head speed of 60 rpm, a base speed of 150 rpm, and normal load of 6 N. Stainless steel was chosen as the substrate because it is a commonly used material in many applications. The polished samples were then laser-textured using an A5 Series femtosecond laser (Oxford Lasers Ltd., UK) with 15% of the 2.3-W full laser power, 600 Hz laser frequency, and 1200 R.A. divider. Next, samples were washed in deionized (DI) water plus detergent, acetone, and isopropyl alcohol in a sonication bath for 20 min each. Then, PDA/PTFE coatings were deposited on the stainless steel substrates using a previously reported procedure [21, 22]. Briefly, PDA was deposited on smooth and laser-textured stainless steel substrates at a temperature of 60 ˚C in a rocking bath containing dopamine hydrochloride mixed with a tris buffer solution. A rocking rate of 25 rpm and a

rocking angle of 7° for 45 min was used. In this step, the pH of the solution was brought to 8.5 using Trizma base mixed with DI water. Finally, PTFE was coated on PDA deposited stainless steel substrates using a dip coater (KSV Dip Coater, MD, USA) with a dipping and withdrawal speed of 10 mm/min, and soaking time of 1 min [23]. PDA/PTFE coated stainless steel samples were then heated at 120 °C and 300 °C and annealed at 372 °C for 4 min each. Hilbert curve pattern was laser-textured on the resulting PTFE coating with 5% of the 2.3-W full laser power. In addition, for performing nanoindentation and nanoscratch tests, square areas of 150 μm × 150 μm were laser-textured on the PTFE coatings using the same laser parameters.

4.4.2 Sample Characterization

A 3D laser scanning confocal microscope (VK-X260, Keyence Corporation) was used to measure the surface of smooth and laser-textured substrates and image the wear tracks and the counterface balls after the durability tests. An atomic force microscope (AFM, Dimension Icon, Bruker) having a ScanAsyst air AFM tip (Bruker) with a 0.4 N/m spring constant was used to measure the surface morphology and surface roughness of PDA/PTFE coatings. A stylus contact profilometer (Dektak 150, Bruker Nano Surfaces) was used to measure the coating thickness and the profile of wear tracks after durability and progressive wear tests. X-ray photoelectron spectroscopy (PHI Versaprobe XPS system, Physical Electronics) was used to analyze the surface chemistry of PTFE coatings with and without laser texturing. A nanoindenter (TriboIndenter, Hysitron) equipped with a spheroconical indenter with a 5-μm-radius diamond tip was used to perform indentations to a maximum load of 100 μN with loading and unloading rates of 2.5 μN/s and a holding time of 2.5 s. These indentations were used to measure the modulus of elasticity and hardness of the smooth and laser-textured (LT) PTFE coatings. Additionally, the nanoindenter and the 5-μm-radius diamond tip were used to perform load-

controlled scratch tests at maximum loads of 1000 μN, 2000 μN, and 3000 μN with an 8-μm scratch length.

4.4.3 Tribology Testing

A tribometer (UMT-3, Bruker) was used to conduct linear reciprocating wear tests with a ball-on-plate configuration. Cr steel balls with 6.35 mm diameter and 0.221 μm average root mean square surface roughness were used as the counterfaces. This material was selected because it is commonly used in industrial applications. Smooth and laser-textured PDA/PTFE coatings on smooth and laser-textured stainless steel substrates were used as the plates. Figure 4.1 shows the test setup and optical images of the counterface ball. The tests were run with 2 N normal loads, 5 mm stroke length, and 10 mm/s sliding speed. Friction forces greater than 0.65 was set to be the failure criteria and the temperature and humidity were kept constant at 25 ◦C and 25%, respectively.

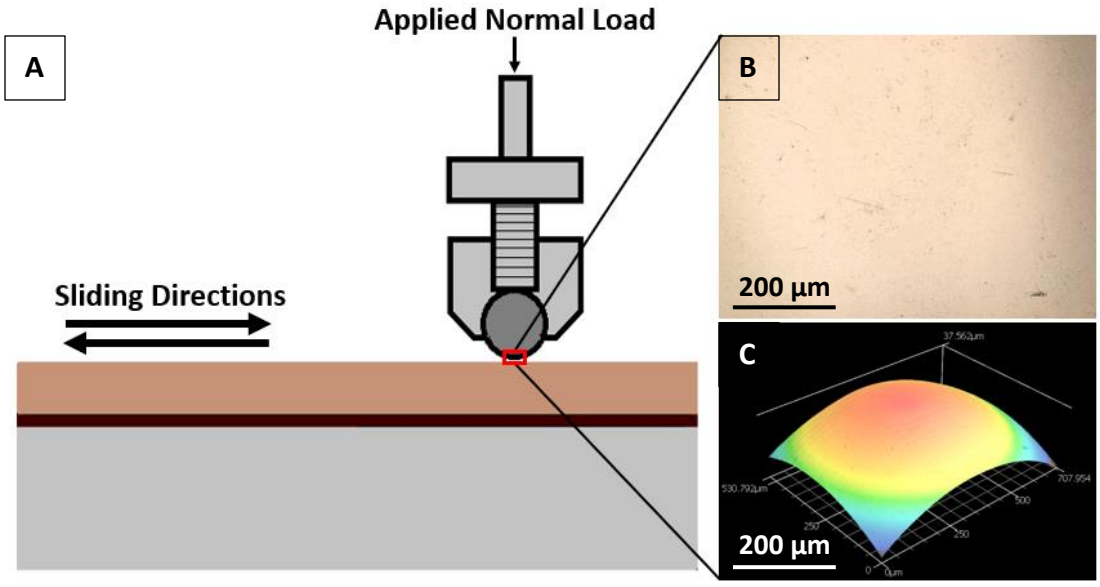

Figure 4.1: Tribological test setup and optical images of the Cr-Steel counterface ball: A) ball-on-plate configuration, B) 2D optical image of the counterface ball with the curvature removed, and C) 3D optical image of the counterface ball.

4.5 Results and Discussions

4.5.1 Coating Surface Topography and Roughness

Four types of samples, i.e., smooth and laser-textured PTFE coatings on smooth and laser-textured stainless steel substrates, were fabricated and labeled as shown in Table 4.1. Figure 4.2 shows the schematics of sample types in Table 4.1. Hilbert curve patterns were laser-textured on stainless steel substrates and PTFE coatings. Laser power of 15% of the 2.3-W full laser power was used for laser-texturing the hard stainless steel substrates. This laser parameter resulted in textured grooves with 1.27 ± 0.4 μm depth and 5.0 ± 0.6 μm width on the substrates. The average surface roughness of smooth stainless steel and laser-textured stainless steel was measured as 0.08 ± 0.01 μm and 0.17 ± 0.06 μm, respectively.

Table 4.1: List of different sample types.

Sample Label	Substrate	Underlayer	Top layer
SS/PDA/PTFE	Smooth stainless steel	PDA	Smooth PTFE
SS/PDA/LT PTFE	Smooth stainless steel	PDA	Laser-textured PTFE
LT SS/PDA/PTFE	Laser-textured stainless steel	PDA	Smooth PTFE
LT SS/PDA/LT PTFE	Laser-textured stainless steel	PDA	Laser-textured PTFE

To avoid affecting the spindle-like structure of PTFE nanoparticles, a very low laser power of 5% of the 2.3-W full laser power was used for laser-texturing the PTFE coating. Figure 4.3 illustrates the AFM images of the surface topography of PTFE coatings of the four sample types. The surface profile of the PTFE coating topography at the horizontal line in each AFM image is plotted in Figure 4.3E. The average surface roughness of PTFE coatings of the

SS/PDA/PTFE, LT SS/PDA/PTFE, SS/PDA/LT PTFE, and LT SS/PDA/LT PTFE samples measured from the AFM images was 40.85 nm, 105.44 nm, 73.35 nm, and 111.17 nm, respectively. As expected, the roughness was higher for the samples with the substrate textured.

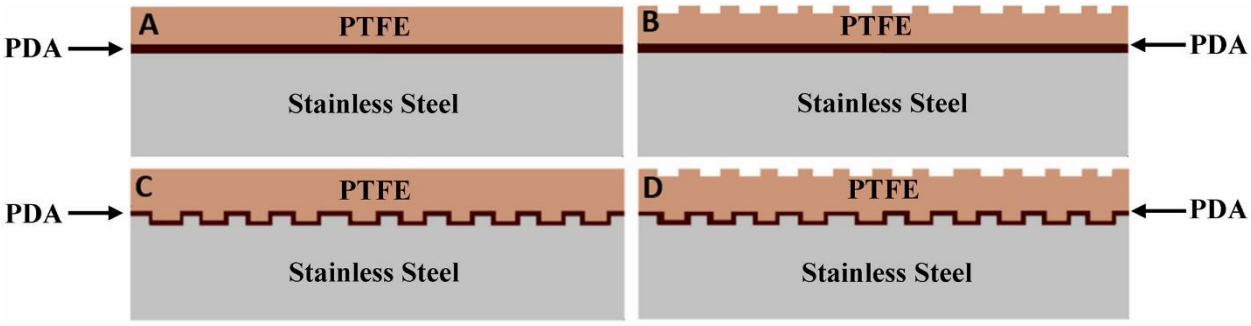

Figure 4.2: Schematic of different sample types (Not to scale): A) SS/PDA/PTFE, B) SS/PDA/LT PTFE, C) LT SS/PDA/PTFE, and D) LT SS/PDA/LT PTFE.

It is interesting to observe that the morphology of the laser-textured PTFE coating (Figure 4.3B) is quite different from that of the PTFE coating on the laser-textured substrate (Figure 4.3C). As shown in Figure 4.3E, the PTFE along the Hilbert curve on the SS/PDA/LT PTFE sample (lighter color in Figure 4.3B) was about 120 nm taller than the remaining PTFE areas that were not affected by the laser. In contrast, the PTFE over the Hilbert curve patterned on the LT SS/PDA/PTFE substrate was deeper (darker color in Figure 4.3C). This is due to the texture grooves on the surface of stainless steel substrates. PDA and PTFE would deposit inside the grooves resulting in a deeper surface topography than the areas outside the grooves [11]. However, it should be noted that the surface profile was less than 300 nm deep compared to the measured depth of 1.27 μm for texture grooves on stainless steel. This is due to the existence of PTFE inside the texture grooves [11]. On the other hand, on SS/PDA/LT PTFE sample, the PTFE coating was bumped up about 100 nm in the areas affected by laser energy.

Also, it can be seen that when both stainless steel substrate and PTFE were laser-textured (Figure 4.3D), the surface profile depth was decreased to 200 nm (Figure 4.3E) because of the combined effects of the texture grooves on the substrate and the raising up of the coating by the laser texturing of the coating. Although the texture patterns on the PTFE coatings were not completely lined up with those on the stainless steel substrate because the latter was covered by the PDA/PTFE coatings, comparing Figure 4.3D with Figures 4.3B and C suggests that the texture patterns on PTFE coatings overlapped the texture pattern on the stainless steel substrates since the texture pattern in Figure 4.3D does not have a clear and sharp border like the texture pattern in Figures 4.3B and C. As a result, overlapping the texture patterns on the PTFE coating with that on the stainless steel substrate decreased the overall depth of surface profile on LT SS/PDA/LT PTFE sample compared to that on LT SS/PDA/PTFE (Figure 4.3E).

Figure 4.4 shows representative AFM images of the PTFE and LT PTFE coating surfaces and particle size analysis results based on three AFM images of each coating type. The results were obtained using a custom MATLAB script that allowed the user to measure the length and width of 100 PTFE particles in each image (Figures 4.4A2 and 4.4B2). All measured data were collected in the boxplots in Figures 4.4C1 and 4.4C2. Statistical difference between each dataset was calculated using a two-tailed paired *t*-test of each length and width data pair. The means of both length and width were found to be significantly different with a $p < 0.0001$. As shown in Figures 4.4C1, and 4.4C2, the average lengths of the spindle-like PTFE particles on the laser-textured area were longer while the average widths were narrower. This could be due to the heat from the laser beam. Applying heat on PDA/PTFE coating increases the length of spindle-like PTFE particles and combines them to form a cross-network structure [21]. The networks formed by longer PTFE particles required more space than those formed by shorter PTFE particles.

Therefore, they protruded and bumped up compared to the coating not affected by the laser beam. That is why the line profile of LT PTFE in Figure 4.3E was higher than that of the neighboring areas.

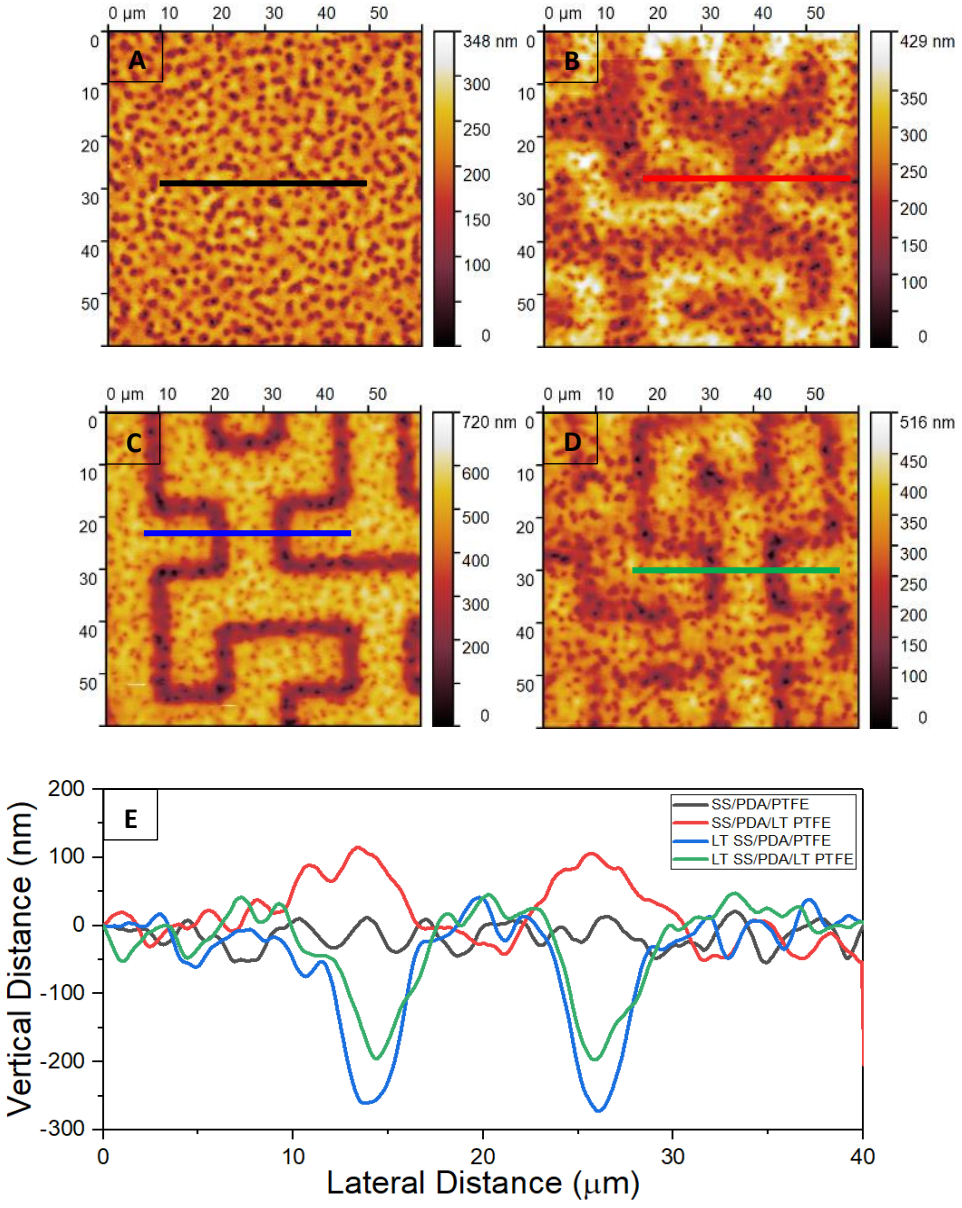

Figure 4.3: AFM images of surface topography of PTFE coatings in: A) SS/PDA/PTFE, B) SS/PDA/LT PTFE, C) LT SS/PDA/PTFE, D) LT SS/PDA/LT PTFE, and E) profile of PTFE topography across the lines on images A-D.

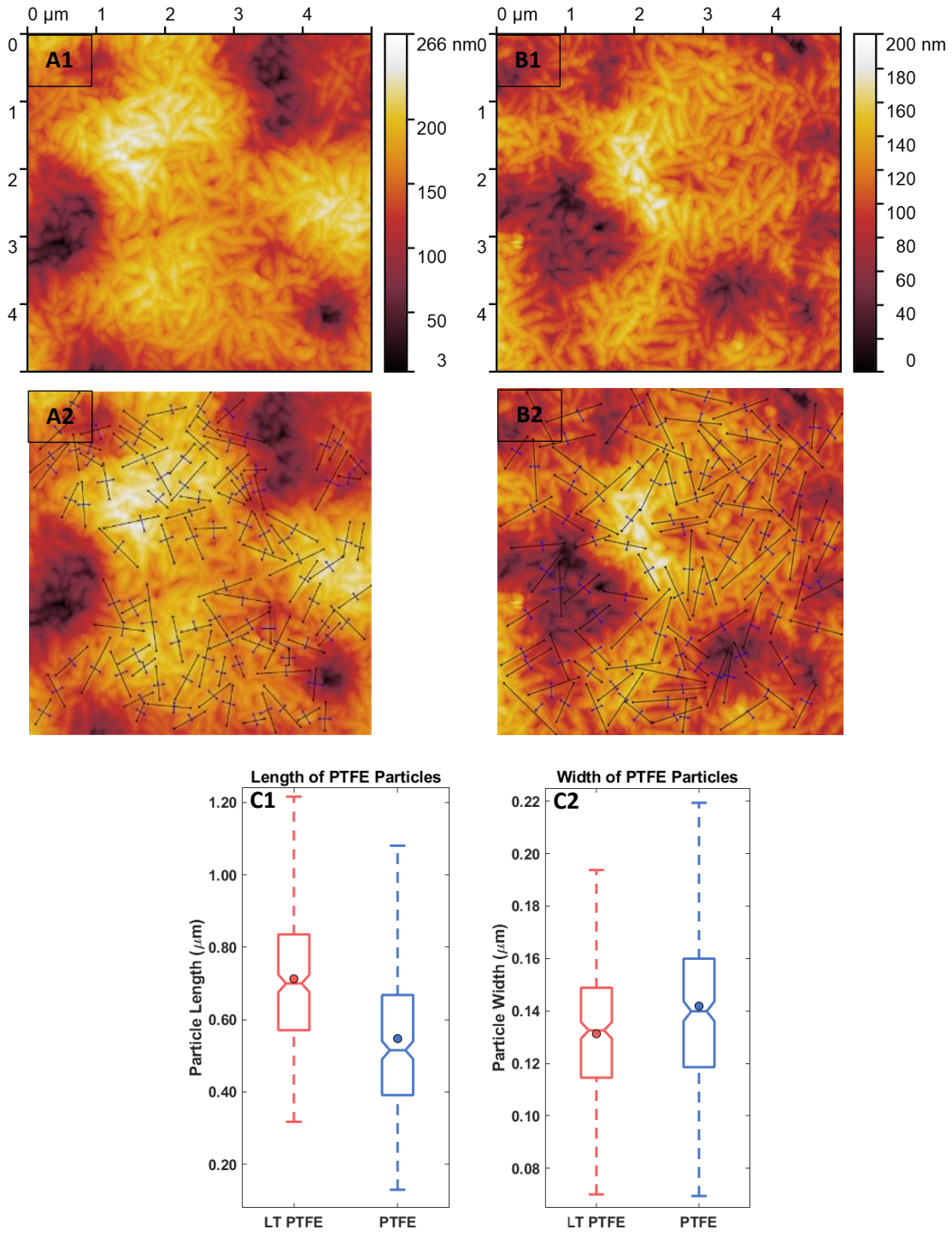

Figure 4.4: AFM images of PTFE and LT PTFE coatings and PTFE particle size analysis: A1 and B1) AFM images and A2 and B2) AFM images with labeled particle lengths and widths of the PTFE and LT PTFE coatings, respectively, and boxplots of particle C1) length and C2) width of the PTFE and LT PTFE coatings, respectively.

4.5.2 The effect of Laser Texturing on the Coating Chemistry

XPS analysis was performed on SS/PDA/PTFE and SS/PDA/LT PTFE samples to investigate the effect of laser-texturing on the surface chemistry of PTFE. As shown in Figure 4.5, both samples had the same photoelectron energy peaks meaning that the surface material on both PTFE and LT PTFE coatings had the same elemental and chemical composition. Hence, it could be concluded that laser-texturing the PTFE coating did not affect its chemical bonds because of the very low laser power used.

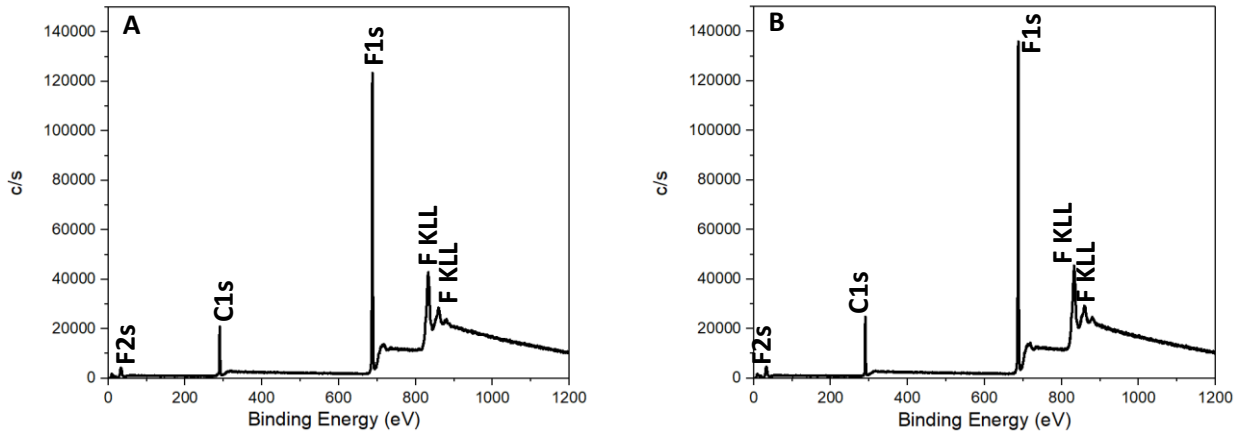

Figure 4.5: XPS spextra of PTFE and laser textured PTFE coatings: A) SS/PDA/PTFE and B) SS/PDA/LT PTFE.

4.5.3 The effect of Laser Texturing on the Mechanical Properties and Scratch Resistance of the Coatings

To further investigate the effect of laser-texturing on the PTFE coating, the mechanical properties of PTFE and laser-textured PTFE were measured through nanoindentation. As shown in Figure 4.6A, laser-texturing significantly reduced the hardness but did not significantly change the modulus of elasticity of PTFE coating. Figure 4.6B the load-displacement curves of five indentations performed on PTFE and LT PTFE. LT PTFE deformed more easily than PTFE

under loading, and greater plastic deformation was observed for LT PTFE after unloading. It can be concluded that laser-texturing the PTFE coating made it less resistant to plastic deformation. The variations in the Young's modulus and hardness of the coatings were caused by the porous nature of the coatings.

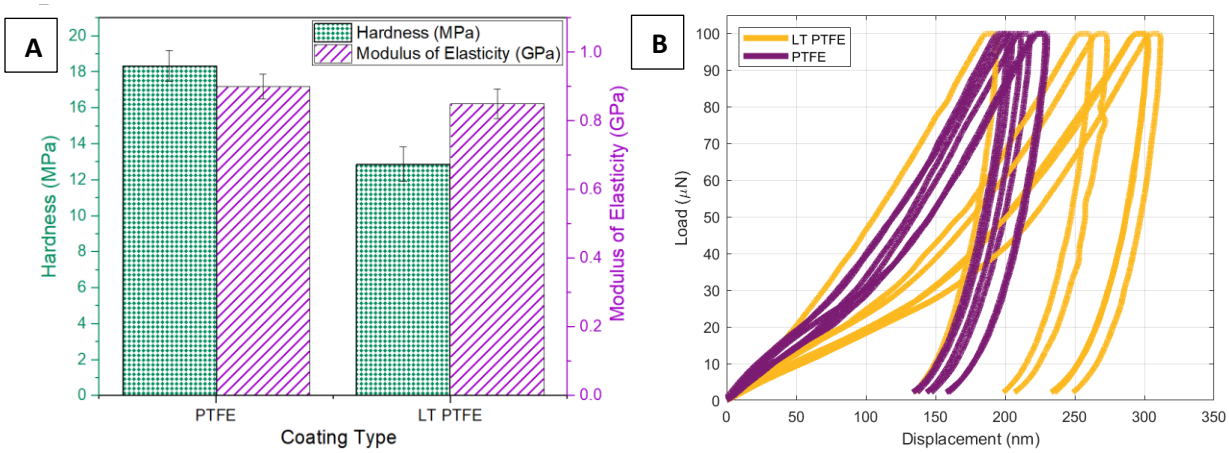

Figure 4.6: Hardness, modulus of elasticity, and load-displacement curves from indentations on SS/PDA/PTFE and SS/PDA/LT PTFE coatings: A) hardness and modulus of elasticity and B) load-displacement curves.

Scratch tests were performed on PTFE coatings of SS/PDA/PTFE and SS/PDA/LT PTFE samples using a 5-μm-radius diamond indenter at normal loads of 1000 μN, 2000 μN, and 3000 μN. Figure 4.7 shows the displacement curves during scratch. In Figure 4.7, the first 10 s of the plots (10 s–20 s) correspond to the loading period where the normal load was applied at constant rates of 100, 200, and 300 μN/s and the tip did not move laterally. From t = 20 s to t = 50 s, the constant normal load of 1000 μN, 2000 μN, or 3000 μN was held, and the tip scratched on the surface at a constant velocity of 0.27 μm/s and for a length of 8 μm. From t = 50 s to t = 60 s, the load was reduced to zero with a constant unloading rate equal to the loading rate. As shown in Figures 4.7A and B, the displacement of the LT PTFE coating on the SS/PDA/LT PTFE sample was larger than the displacement of the PTFE coating on the SS/PDA/ PTFE sample at 1000 μN

and 2000 μN loads. As discussed before, the LT PTFE coating was softer than the PTFE coating and hence it could be displaced easier during loading. The reduced hardness of the LT PTFE coating enabled it to be compacted more effectively than the PTFE coating. However, the LT PTFE coating showed less displacement than the PTFE coating throughout the scratches at 3000 μN load (Figure 4.7C, t = 20 s to t = 50 s).This can be explained from the SEM images of the coatings after scratch in Figure 4.8.

Figures 4.8A3 and 4.8B3 show that, at 3000 μN scratch load, the PTFE coating on the SS/PDA/PTFE sample failed, but the LT PTFE coating on the SS/PDA/LT PTFE sample did not. During the 3000 μN scratches on the PTFE coating (Figure 4.8A3), the indenter tip tore the coating and exposed the stainless steel substrate, thus resulting in a larger displacement than that of the SS/PDA/LT PTFE sample, as shown in Figure 4.7C. In contrast, the improved compaction of the LT PTFE coating on the SS/PDA/LT PTFE sample enabled a resilient layer of coating near the substrate to withstand these higher-load scratches and prevented contact between the tip and stainless steel substrate (Figure 4.8B3). This enhanced scratch resistance of the LT PTFE coating was attributed to the better-compactable PTFE nanostructures that result from laser texturing. The compaction of PTFE has previously been shown to improve its tribological performance during nanoindenter scratch testing [24].

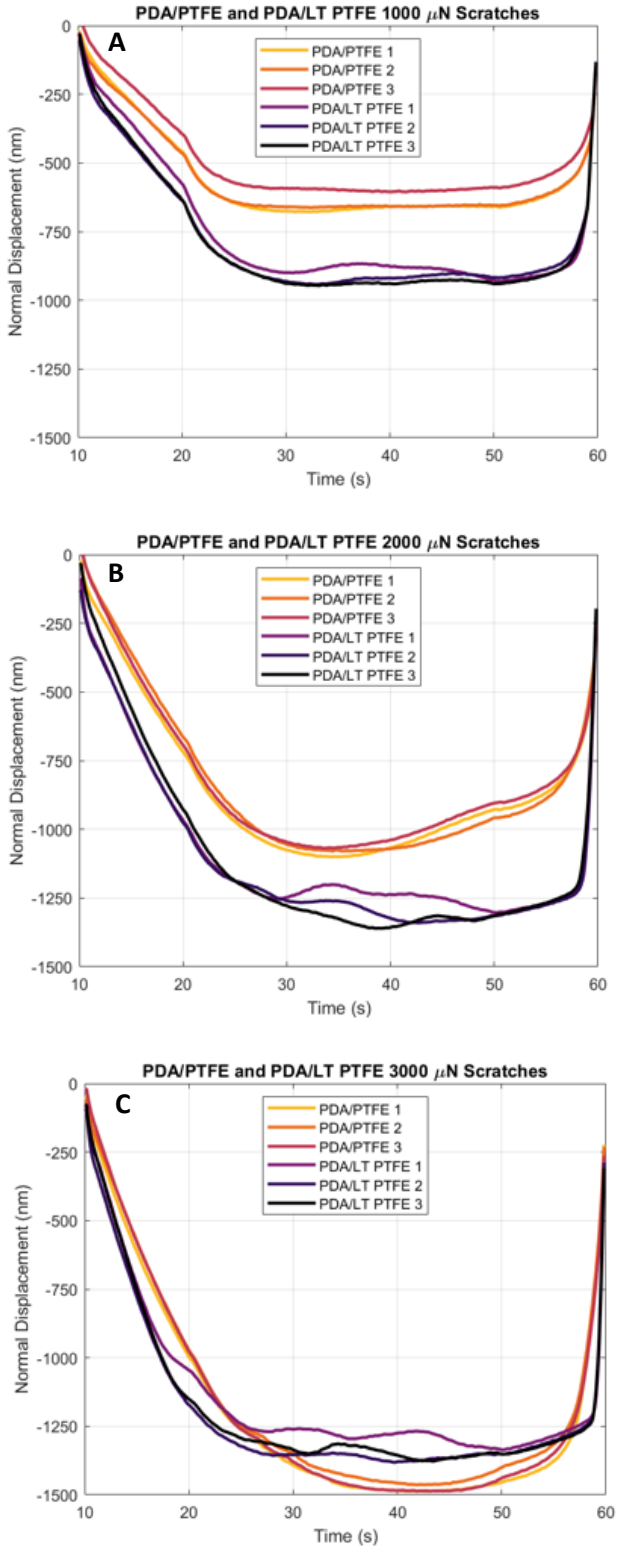

Figure 4.7: Normal displacement vs. time for the nanoindenter scratches performed on SS/PDA/PTFE and SS/PDA/LT PTFE coatings using a 5 μm diamond indenter: A) 1000 μN normal load, B) 2000 μN normal load, and C) 3000 μN normal load.

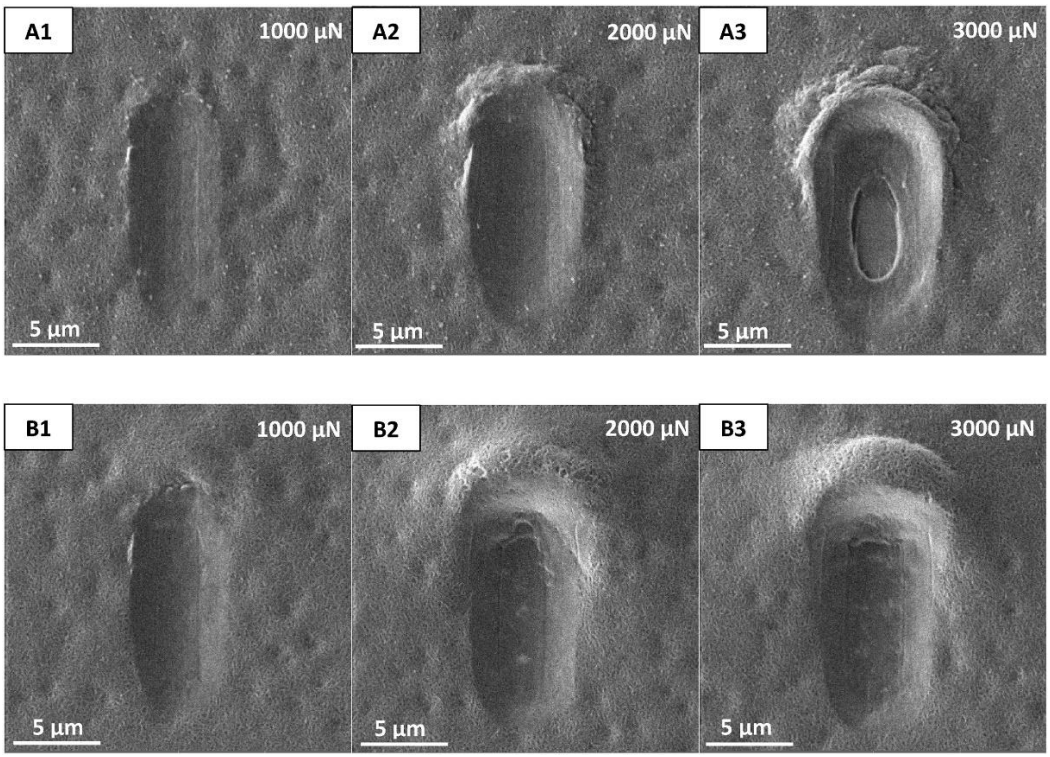

Figure 4.8: SEM images of the nanoindenter scratches performed on A) SS/PDA/PTFE and B) SS/PDA/LT PTFE coatings with: A1, B1) 1000 µN normal load, A2, B2) 2000 µN normal load, and A3, B3) 3000 µN normal load.

4.5.4 The effect of Laser Texturing on the Coating Tribological Properties

Figure 4.9 shows the tribological test results. It can be seen from Figure 4.9A that the PTFE coatings without laser texturing on the smooth substrate had the shortest wear life of 101 cycles. Laser texturing the PTFE coating and the substrate increased the coating wear life to 614 and 1977 cycles, respectively. Notably, laser texturing both the coating and the substrate increased the coating wear life to about 2900 cycles, which is 29 times that of the untextured PTFE coating on the smooth substrate. These improvements can be explained by surface roughness caused by laser texturing. Laser texturing the PTFE coating slightly increased the coating surface roughness and thickness on the Hilbert curves. This led to more compaction of the coating along the Hilbert curves and thus increased coating durability. It should be noted that

compaction played a major role in forming a durable coating that is more resistant to wear regardless of the initial coating hardness. The lower initial hardness caused the LT PTFE coating to deform more easily initially and compacted more due to being taller than the neighboring untextured areas, which led to better wear resistance. Also, the heat from the laser beam elongated the PTFE nanoparticles and improved their network connectivity, resulting in a more cohesive coating. Therefore, the LT PTFE coating was more resistant to wear.

Laser-texturing the substrate has been shown to provide a reservoir for the PTFE lubricant and helped recover the tests from failure [11]. The roughness created by the textures on the substrate also provided interlocking to the PTFE coating and thus prevented coating global delamination [11].

Figure 4.9B illustrates that the samples with a laser-textured substrate, laser-textured PTFE, or both had a slightly lower COF than the samples without laser texturing (SS/PDA/PTFE). The representative COF graphs of each sample type are presented in Figure 4.9C. The sharp increase at the end of each graph represents the coating failure. There was an increase in the COF of the SS/PDA/PTFE sample immediately after the test began and well in advance of when the coating failed with a sharp COF increase. In comparison, this COF increase was delayed for samples with either laser-textured PTFE or stainless steel substrate, which happened around 300 cycles. This increase in the COF was due to compacting loosely connected PTFE particles by the counterface ball [11]. Since laser-textured samples had rougher surfaces, they experienced this increase later than the SS/PDA/PTFE sample.

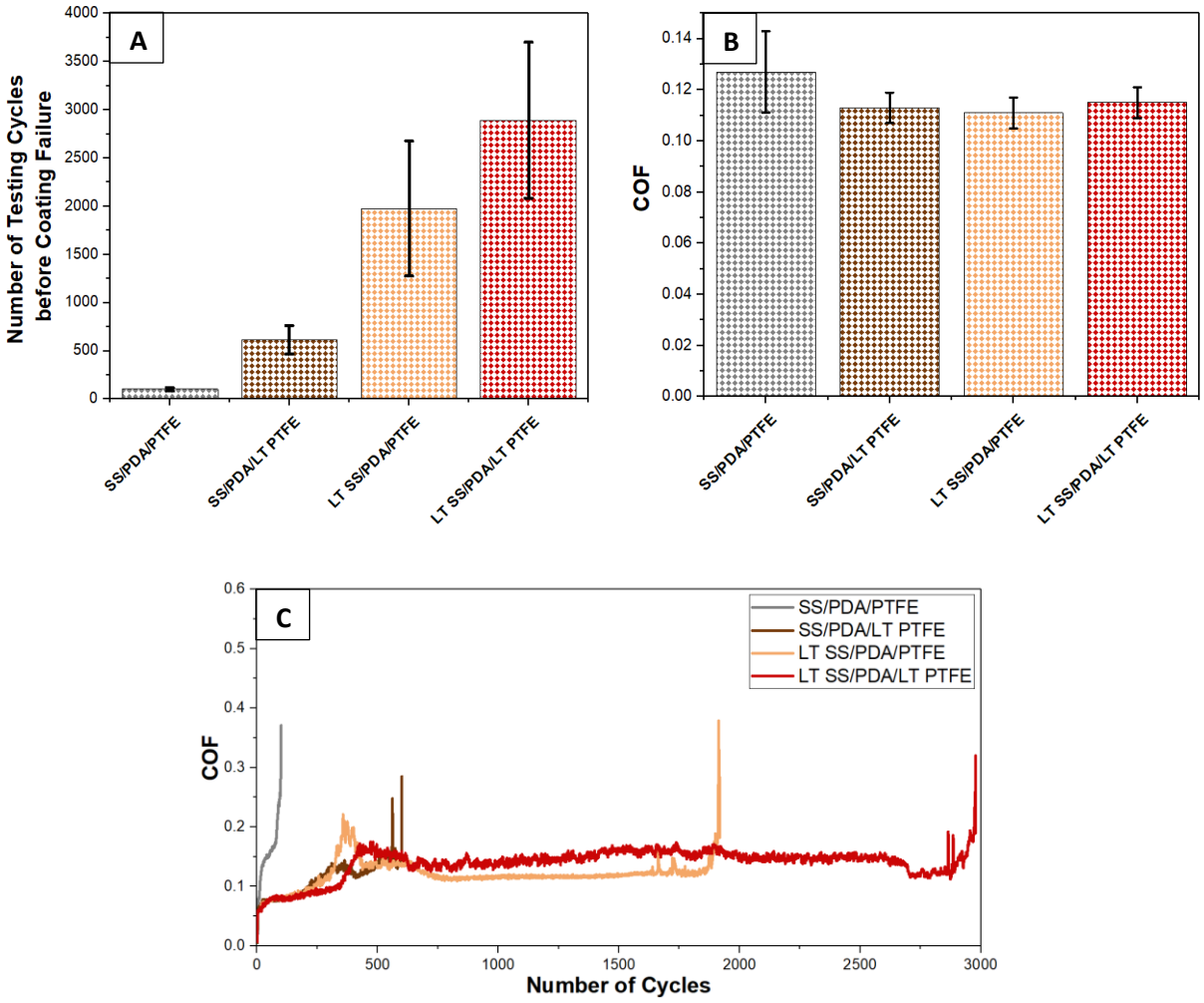

Figure 4.9: Durability and COF of smooth and laser-textured PTFE coatings with PDA underlayer on smooth and laser-textured stainless steel substrates: A) Number of testing cycles before coating failure, B) average COF over the test duration, and C) representative COF as a function of the number of testing cycles during the durability tests.

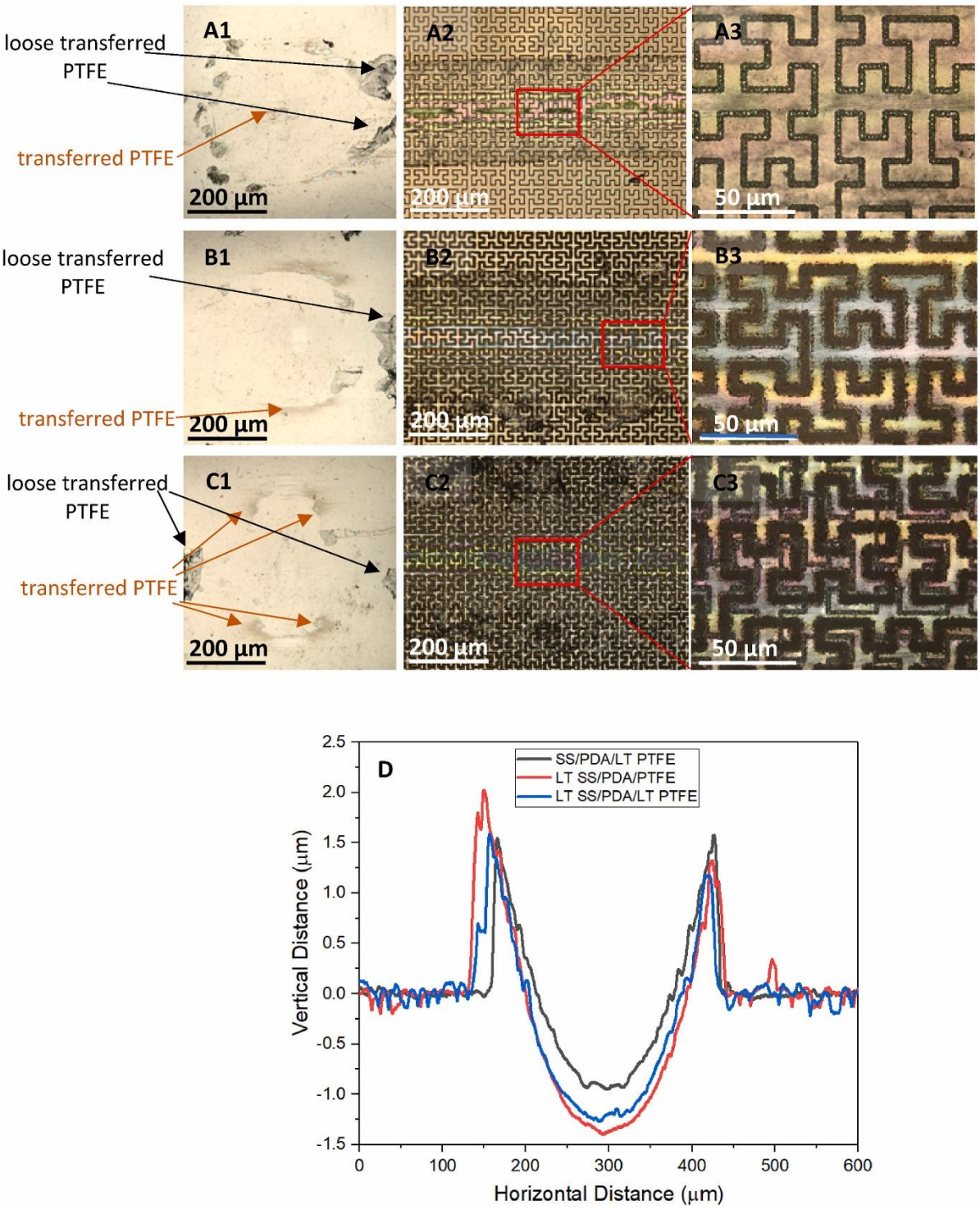

Figure 4.10: Optical images of the counterface balls and wear tracks after 400-cycle progressive tests for: A) SS/PDA/LT PTFE, B) LT SS/PDA/PTFE, C) LT SS/PDA/LT PTFE (A3-C3: Zoom-in images of the red boxes on A2-C2), and D) profile of the wear tracks shown in A-C. (For interpretation of the references to color in this figure legend, the reader is referred to the Web version of this article.)

Figures 4.10 to 4.12 show the optical images of counterface ball and wear tracks after 400-cycle progressive tests, 900-cycle progressive tests, and tests conducted to coating failure, respectively. On the SS/PDA/LT PTFE sample, the PTFE coating was barely rubbed off after 400 cycles and it was compacted by the counterface ball since LT PTFE was soft. Hence, the laser-textured pattern was not rubbed off and there was some loose transferred PTFE on the counterface ball and only a slight amount of transferred PTFE at the center of the ball (Figure 4.10A). This sample failed after 614 cycles at which the laser-textured pattern was rubbed off and a large amount of PTFE was transferred to the center of the counterface ball (Figure 4.12B). Also, there was no loose transferred PTFE on the counterface ball after test failure since the loose material might have been transferred back to the wear track at some point during the test.

For the LT SS/PDA/PTFE sample, after 400 cycles, the PTFE coating was plowed from the center to the sides of the wear track and the substrate was slightly exposed at the center of the wear track (Figure 4.10B2). This led to a slight increase in the COF, as shown in Figure 4.9C. However, the test did not fail because PTFE stored inside the texture grooves replenished the wear track and brought the COF back to a low level. This can be seen in the image of the wear track after 900 cycles (Figure 4.11A). This sample failed after 1977 cycles of testing when all PTFE stored inside the texture grooves were rubbed off and transferred to the counterface ball (Figure 4.12C).

A combination of the phenomena observed from the SS/PDA/LT PTFE sample and the LT SS/PDA/PTFE sample was observed for the LT SS/PDA/LT PTFE sample after 400 cycles. PTFE was compacted and plowed to the sides of the wear track which slightly diminished the laser-textured pattern on PTFE. Therefore, no obvious PTFE was transferred to the center of the counterface ball, however, there was some loose transferred PTFE surrounding the contact area

of the counterface ball. These loose PTFE might transfer back to the wear track later during the test to repair the wear (Figure 4.10C). After 900 cycles, the laser-textured pattern of the PTFE was less visible and some PTFE was transferred to the center of the counterface ball. The substrate was almost exposed but the texture grooves on the substrate were still filled with PTFE (Figure 4.11B) that would replenish the wear track and recover the test (Figure 4.9C). Also, some loose PTFE materials were transferred to the counterface ball (Figure 4.11B1) due to the counterface scratched part of the soft laser-textured PTFE not interlocked in the texture grooves. This sample failed after 2893 cycles at which point the laser-textured patterns on both stainless steel substrate and PTFE were completely removed in the wear track, and the PTFE was rubbed off and transferred to the counterface ball (Figure 4.12D). It should be noted that although this sample ran much more number of cycles than other samples, the width of the wear track on this sample is the same as on SS/PDA/LT PTFE and LT SS/PDA/PTFE samples. This shows the effectiveness of Hilbert curve textured grooves in preventing coating wear and global delamination.

The profiles of the wear tracks in Figures 4.10 to 4.12 illustrate that the depth of the wear tracks increased as the number of tribology test cycles increased. Also, Figure 4.12A indicates global delamination of the SS/PDA/PTFE sample, and unlike the textured samples, a large amount of loose PTFE was transferred to the counterface ball (Figure 4.12A1).

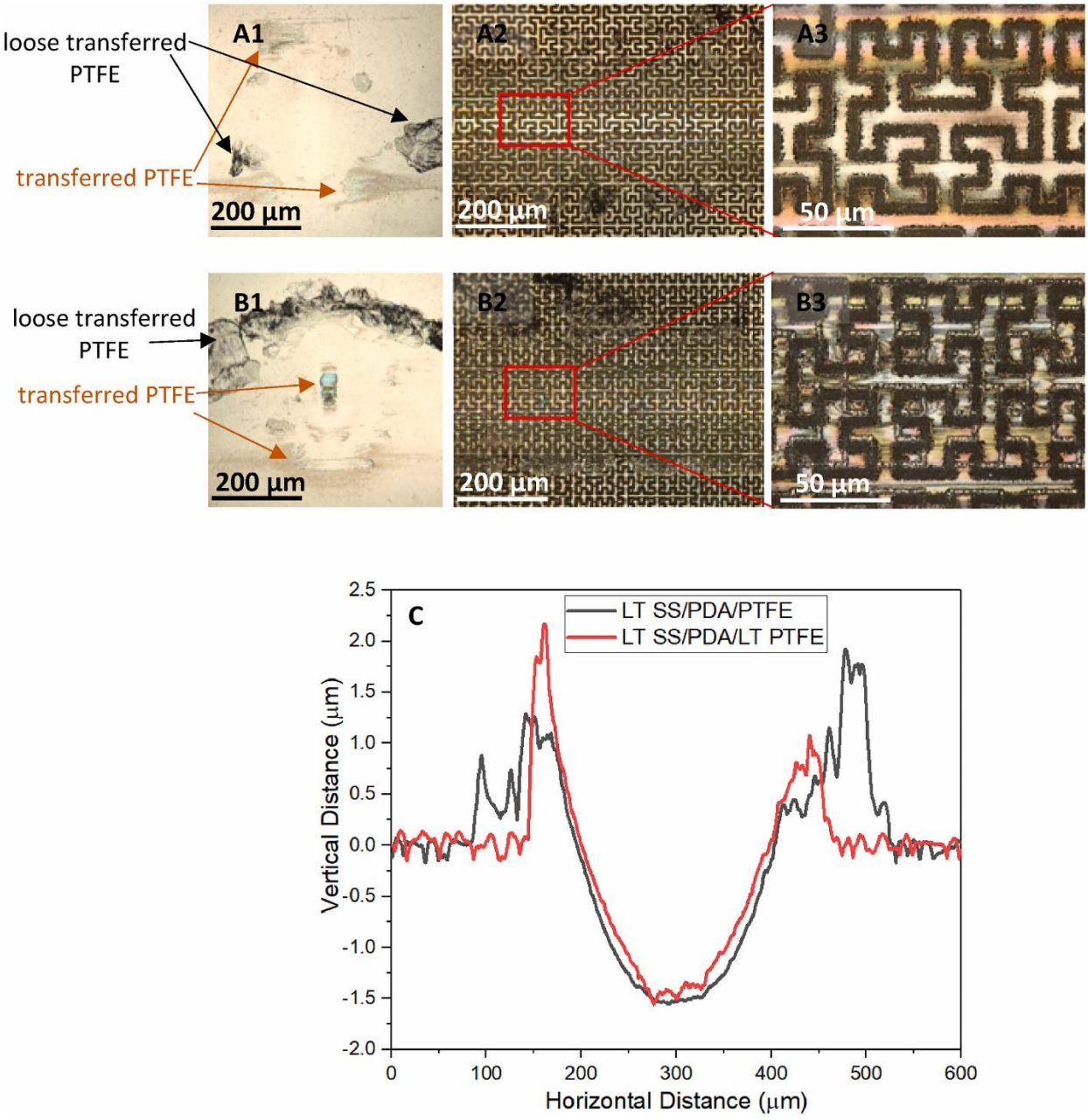

Figure 4.11: Optical images of the counterface balls and wear tracks after 900-cycle progressive tests for: A) LT SS/PDA/PTFE, B) LT SS/PDA/LT PTFE (A3-B3: Zoom-in images of the red boxes on A2-B2), and C) profile of the wear tracks shown in A and B. (For interpretation of the references to color in this figure legend, the reader is referred to the Web version of this article.)

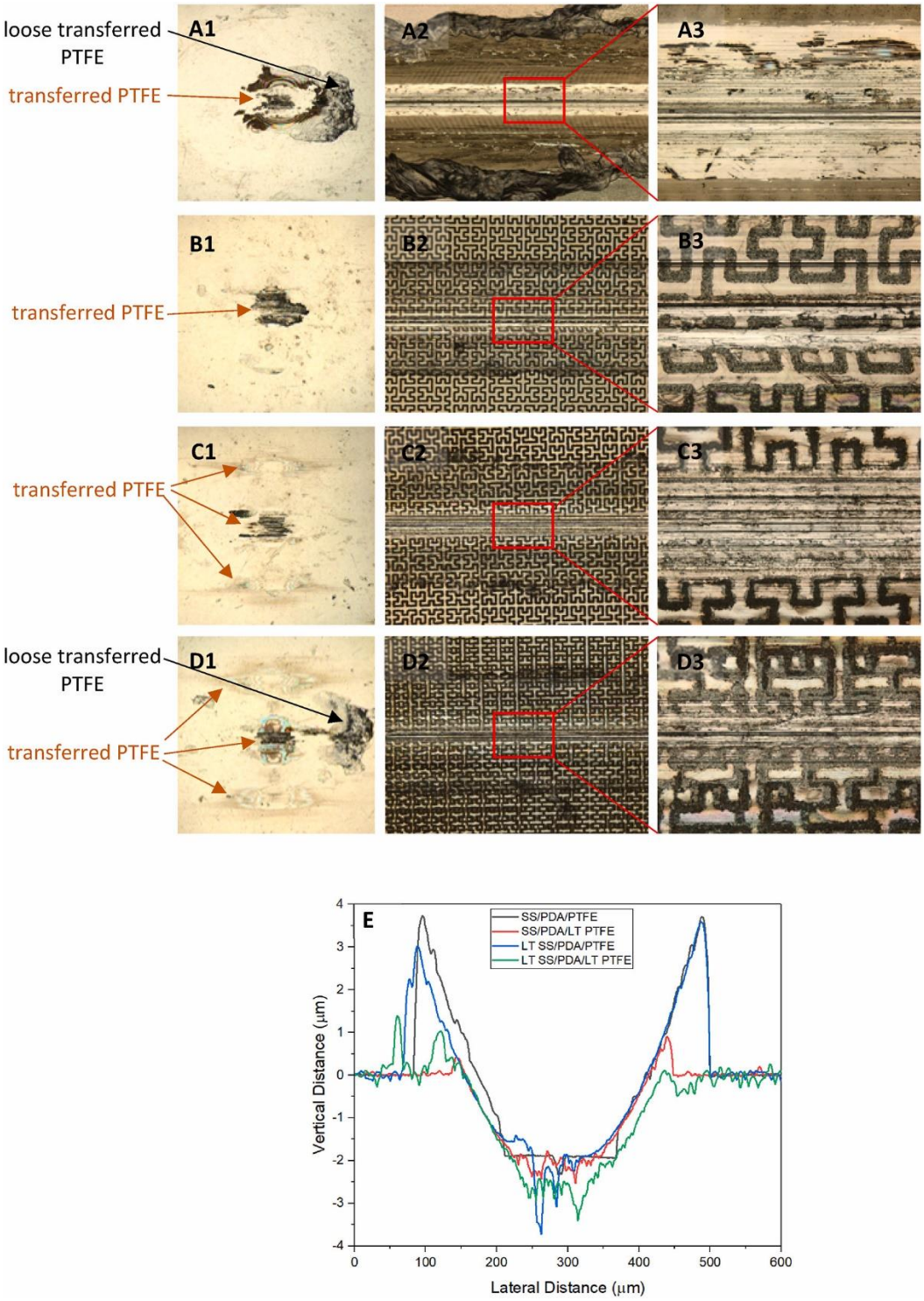

Figure 4.12: Optical images of the counterface balls and wear tracks after test failure for: A) SS/PDA/PTFE, B) SS/PDA/LT PTFE, C) LT SS/PDA/PTFE, D) LT SS/PDA/LT PTFE (A3-D3: Zoom-in images of the red boxes on A2-D2), and E) profile of the wear tracks shown in A-D. (For interpretation of the references to color in this figure legend, the reader is referred to the Web version of this article.)

Figure 4.13 demonstrates the SEM images and EDS elemental maps of the wear tracks after tribology tests to failures. As presented in the EDS maps of iron, Fe, and fluorine, F, the wear track on SS/PDA/PTFE sample (where the fluorine from the coating is mostly removed) had the largest width (Figure 4.13A). This data confirms the wide and flat wear track profile in Figure 4.12E that represented the global delamination of the coating inside the wear track. It can be observed that laser texturing stainless steel substrate and/or PTFE coating significantly decreased the wear track width and prevented the coating's global delamination despite their longer testing duration (Figure 4.13B-D). Laser texturing reduced the wear track width by protruding (for LT PTFE, Figure 4.13B and D) and/or recessing (for LT SS, Figure 4.13C and D) the surface. The protruded laser-textured areas of PTFE (arrow positions in Figures 4.13B and D resulted in a higher contact pressure and increased the compaction in these areas, which led to more coherent coating. The recessed laser-textured areas of SS (arrow positions in Figure 4.13C and D) increased the surface roughness and interlocking between the coating and the substrate. They also stored PTFE that replenished and recovered the removed PTFE above grooves within the wear track. It can be seen that laser texturing the stainless steel substrate resulted in a narrower wear track after testing more cycles than laser texturing the PTFE coating. Therefore, it was more effective than laser texturing the PTFE coating.

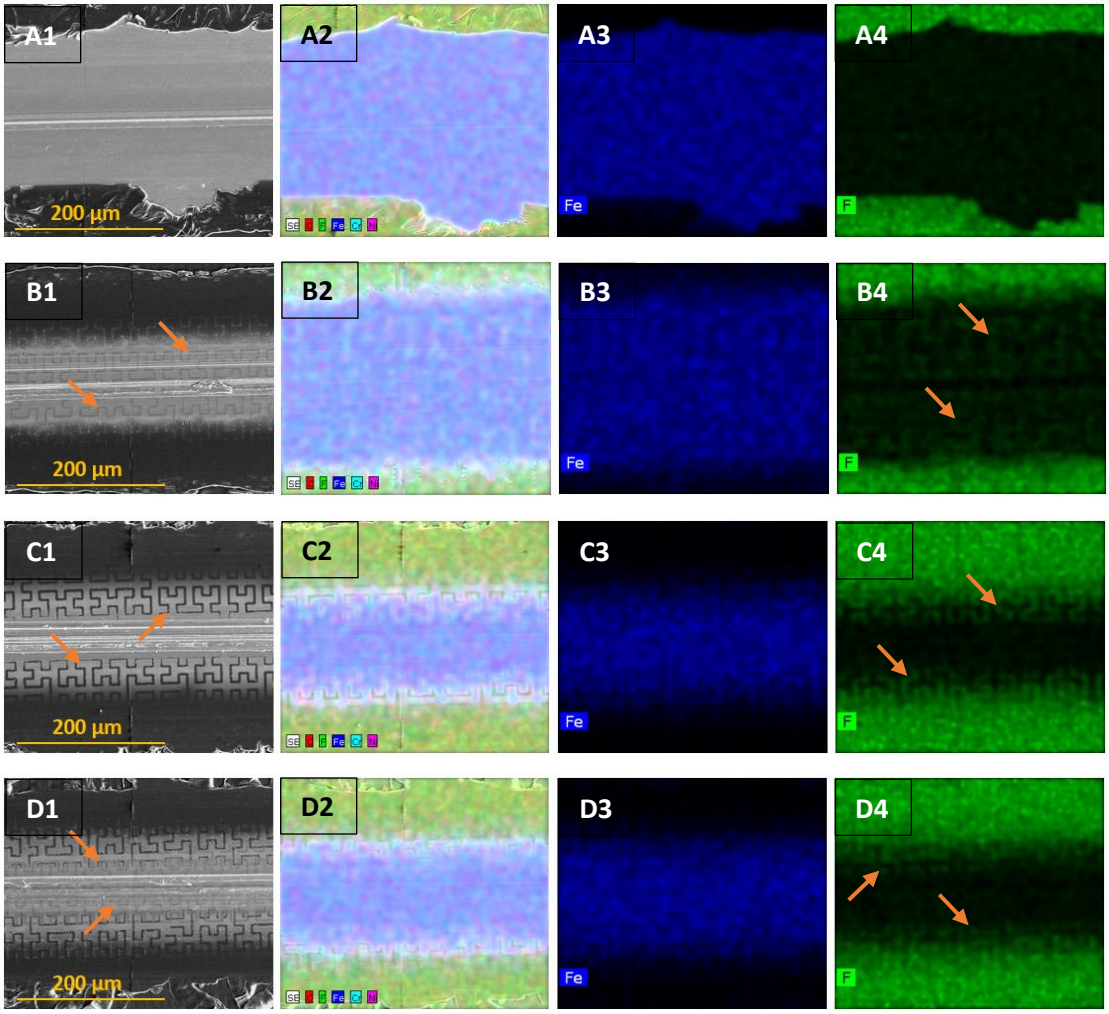

Figure 4.13: SEM images (A1-D1), EDS elemental maps (A2-D2), EDS map of iron (A3-D3), and EDS map of fluorine (A4-D4) of wear tracks after test failure for: A) SS/PDA/PTFE (113 cycles), B) SS/PDA/LT PTFE (601 cycles), C) LT SS/PDA/PTFE (1918 cycles), and D) LT SS/PDA/LT PTFE (2809 cycles).

4.6 Conclusion

Stainless steel substrates and PTFE thin coatings were laser-textured with 15% and 5% of the 2.3-W full laser power, respectively. The coating surfaces were characterized and the mechanical and tribological behaviors of the smooth and laser-textured PTFE on smooth and laser-textured stainless steel were studied. It was shown that laser-texturing both the substrate and the PTFE increased the surface roughness of the PTFE coating. Laser-texturing PTFE

bumped up the coating and made the coating softer without changing its chemical bonds. This resulted in a smaller hardness of the laser-textured PTFE compared to smooth PTFE. Consequently, laser-textured PTFE was compacted more than smooth PTFE at various loads during nanoscratch tests. Also, it was shown that better compactable laser-textured PTFE coating had better coating cohesion during the nanoscratch tests at higher loads, while PTFE without laser texture was torn by the indenter tip. The tribology test results showed that laser-texturing the PTFE coating or the stainless steel substrate improved the wear life of the PDA/PTFE coating over 6 times and 19 times, respectively, while laser-texturing both improved the wear life of the PDA/PTFE coating about 29 times. Also, laser-texturing prevented PDA/PTFE coatings from global delamination.

Authors Statement

Firuze Soltani-Kordshuli: Conceptualization, Writing-original draft, Methodology, Validation, Formal Analysis, Investigation, Visualization. **Charles Miller:** Conceptualization, Writing-review & editing, Investigation, Visualization. **Nathaniel Harris:** Conceptualization, Writing-review & editing, Formal Analysis, Visualization. **Min Zou:** Writing-Review & Editing, Methodology, Supervision, Funding acquisition.

Declaration of Competing Interest

The authors declare that they have no known competing financial interests or personal relationships that could have appeared to influence the work reported in this paper.

Data Availability

Data will be made available on request.

4.7 Acknowledgment

This work was supported by the National Science Foundation under Grants CMMI-1563227 and OIA-1457888. Any opinions, findings, and conclusions or recommendations expressed in this material are those of the authors and do not necessarily reflect the views of the National Science Foundation. The authors thank the use of the Arkansas Nano and Bio Materials Characterization Facility for the use of the XPS system. The authors also acknowledge the support from the Open Access Publishing Fund administered through the University of Arkansas Libraries.

References

[1] H. Unal, A. Mimaroglu, U. Kadıoglu, and H. Ekiz, "Sliding friction and wear behaviour of polytetrafluoroethylene and its composites under dry conditions," *Materials & Design*, vol. 25, no. 3, pp. 239-245, 2004.

[2] D. L. Burris and W. G. Sawyer, "Improved wear resistance in alumina-PTFE nanocomposites with irregular shaped nanoparticles," *Wear,* vol. 260, no. 7-8, pp. 915-918, 2006.

[3] A. Riveiro *et al.,* "Influence of laser texturing on the wettability of PTFE," *Applied Surface Science,* vol. 515, p. 145984, 2020.

[4] F. Soltani-Kordshuli *et al.,* "Tribological behavior of the PDA/PTFE+ Cu-SiO2 nanoparticle thin coatings," *Surface and Coatings Technology,* vol. 409, p. 126852, 2021.

[5] H. Fan, Y. Su, J. Song, H. Wan, L. Hu, and Y. Zhang, "Design of “double layer” texture to obtain superhydrophobic and high wear-resistant PTFE coatings on the surface of Al2O3/Ni layered ceramics," *Tribology International,* vol. 136, pp. 455-461, 2019.

[6] S. Beckford, Y. Wang, and M. Zou, "Wear-resistant PTFE/SiO2 nanoparticle composite films," *Tribology Transactions,* vol. 54, no. 6, pp. 849-858, 2011.

[7] I. Etsion, "State of the art in laser surface texturing," *J. Trib.,* vol. 127, no. 1, pp. 248-253, 2005.

[8] L. Rapoport *et al.,* "Friction and wear of MoS2 films on laser textured steel surfaces," *Surface and Coatings Technology,* vol. 202, no. 14, pp. 3332-3340, 2008.

[9] C. G. Guleryuz and J. E. Krzanowski, "Mechanisms of self-lubrication in patterned TiN coatings containing solid lubricant microreservoirs," *Surface and Coatings Technology,* vol. 204, no. 15, pp. 2392-2399, 2010.

[10] A. Voevodin and J. Zabinski, "Laser surface texturing for adaptive solid lubrication," *Wear,* vol. 261, no. 11-12, pp. 1285-1292, 2006.

[11] F. Soltani-Kordshuli, N. Harris, and M. Zou, "Tribological behavior of polydopamine/polytetrafluoroethylene coating on laser textured stainless steel with Hilbert curves," *Friction,* Research Article 2022, doi: 10.1007/s40544-022-0671-0. Research Article *In Press*

[12] C. Miller, D. Choudhury, and M. Zou, "The effects of surface roughness on the durability of polydopamine/PTFE solid lubricant coatings on NiTiNOL 60," *Tribology Transactions,* vol. 62, no. 5, pp. 919-929, 2019.

[13] W. Li, Q. Yang, F. Chen, J. Yong, Y. Fang, and J. Huo, "Femtosecond laser ablated durable superhydrophobic PTFE sheet for oil/water separation," in *Second International Conference on Photonics and Optical Engineering*, 2017, vol. 10256: International Society for Optics and Photonics, p. 102563O.

[14] S. F. Toosi, S. Moradi, S. Kamal, and S. G. Hatzikiriakos, "Superhydrophobic laser ablated PTFE substrates," *Applied Surface Science*, vol. 349, pp. 715-723, 2015.

[15] W. Fan, J. Qian, F. Bai, Y. Li, C. Wang, and Q.-Z. Zhao, "A facile method to fabricate superamphiphobic polytetrafluoroethylene surface by femtosecond laser pulses," *Chemical Physics Letters*, vol. 644, pp. 261-266, 2016.

[16] F. Liang, J. Lehr, L. Danielczak, R. Leask, and A.-M. Kietzig, "Robust non-wetting PTFE surfaces by femtosecond laser machining," *International journal of molecular sciences*, vol. 15, no. 8, pp. 13681-13696, 2014.

[17] A.-M. Kietzig, J. Lehr, L. Matus, and F. Liang, "Laser-induced patterns on metals and polymers for biomimetic surface engineering," in *Laser Applications in Microelectronic and Optoelectronic Manufacturing (LAMOM) XIX*, 2014, vol. 8967: SPIE, pp. 9-16.

[18] K. T. Ahmmed, C. Patience, and A.-M. Kietzig, "Internal and external flow over laser-textured superhydrophobic polytetrafluoroethylene (PTFE)," *ACS Applied Materials & Interfaces*, vol. 8, no. 40, pp. 27411-27419, 2016.

[19] A. Riveiro *et al.*, "Laser texturing to control the wettability of materials," *Procedia CIRP*, vol. 94, pp. 879-884, 2020.

[20] S. Beckford and M. Zou, "Wear resistant PTFE thin film enabled by a polydopamine adhesive layer," *Applied surface science*, vol. 292, pp. 350-356, 2014.

[21] Y. Jiang, D. Choudhury, M. Brownell, A. Nair, J. A. Goss, and M. Zou, "The effects of annealing conditions on the wear of PDA/PTFE coatings," *Applied surface science*, vol. 481, pp. 723-735, 2019.

[22] Y. Zhao and M. Zou, "Experimental investigation of the wear mechanisms of thin PDA/PTFE coatings," *Progress in Organic Coatings*, vol. 137, p. 105341, 2019.

[23] A. Abe, D. Choudhury, and M. Zou, "Improved tribological performance of PDA/PTFE thin coatings with silica nanoparticles incorporated into the PDA underlayer," *Journal of Tribology*, pp. 1-22, 2021.

[24] C. Miller and M. Zou, "Microscale friction and deformation behavior of polydopamine/polytetrafluoroethylene-coated 60NiTi from nanoscratch tests," *Thin Solid Films*, vol. 743, p. 139079, 2022.

Chapter 5

Conclusions and Future Work

5.1 Conclusions

This dissertation study focused on improving the adhesion and wear life of PTFE coatings on stainless steel substrates. To improve the adhesion of the PTFE coating, an adhesive PDA underlayer was used, resulting in PDA/PTFE coatings. Various approaches were then explored to improve the wear life of these coatings. Durability and progressive wear tests were conducted to evaluate the tribological (friction and wear) properties of the PDA/PTFE coatings.

First, the effect of adding Cu-SiO_2 core-shell nanoparticles (NPs) to the PTFE top layer of PDA/PTFE coatings was studied. Cu-SiO_2 core-shell NPs were added to the PTFE top layer in three low concentrations of 0.005 wt%, 0.0075 wt%, and 0.01 wt%, and the tribological behavior of the resulting coatings was evaluated. The results of this study showed that incorporating low concentrations of Cu-SiO_2 core-shell NPs into the PTFE top layer increased the wear life of PDA/PTFE coatings. In particular, the PDA/PTFE + 0.0075 wt% NP coating had the longest wear life, which was twice that of the PDA/PTFE coating without NPs. It was also found that adding Cu-SiO_2 core-shell NPs improved the surface morphology of the coating, making it less porous, more coherent and interconnected, and smoother. Additionally, this study showed that the addition of NPs eliminated global delamination during durability tests and improved the adhesion of the PTFE transfer film to the counterface ball.

Next, the effect of laser surface texturing the stainless steel substrate on the wear and friction of PDA/PTFE coatings was investigated. Before coating PDA/PTFE, Hilbert curve

patterns with two different texture path segment lengths (12 μm and 24 μm) were laser textured on stainless steel substrate using four different laser powers of 5%, 10%, 15%, and 20 % of 2.6 watts. This resulted in nine types of substrates with different texture densities (texture area coverage). It was shown that higher laser powers resulted in deeper and wider texture grooves leading to larger average surface roughness. Also, PDA/PTFE coatings on laser-textured substrates had larger surface roughness and showed significantly longer wear life. Among all, PDA/PTFE coating on P(12, 20), i.e., laser-textured stainless steel substrate with a segment path length of 12 μm and laser power of 20% of 2.6 watts, had the longest wear life of 3500 cycles that is 25 times the wear life of the coating on a smooth substrate. Even though the laser power of 20% contributed to the longest wear life of the PDA/PTFE coating, the laser power of 15% was selected as the desirable laser power for laser texturing the stainless steel substrate since the laser power of 20% resulted in surface debris. Moreover, it was shown that coatings on laser-textured substrates had lower COF during the tribology tests. Laser texturing prevented global delamination inside the wear tracks, allowing the stored PTFE inside the grooves to replenish the PTFE inside the wear track, leading to the significantly improved wear life of the coating.

Lastly, the effect of laser texturing on both the stainless steel substrate and the PTFE top layer was examined. Hilbert curve patterns were laser textured on the surface of hard stainless steel and soft PTFE coatings with laser powers of 15% and 5% of 2.3 watts, respectively. The coating surface, mechanical properties, and tribological behavior of smooth and laser-textured PTFE coatings on smooth and laser-textured substrates were studied. It was shown that laser texturing the substrate and the PTFE coating increases the surface roughness of PDA/PTFE coatings. Also, laser texturing the PTFE coating made it softer (having smaller hardness), increased the length of PTFE particles, and bumped up the coating without affecting its chemical

bonds. During the nanoscratch tests, softer laser-textured PTFE was compacted more than smooth PTFE which resulted in a better coating adhesion at higher loads. This fact prevented the laser-textured coating from tearing up by the indenter tip. Furthermore, laser texturing PTFE coating and stainless steel substrate increased the wear life of PDA/PTFE coating by 6 times and 19 times, respectively. Laser texturing both PTFE coating and stainless steel substrate increased the wear life of PDA/PTFE coatings by 29 times while preventing global delamination inside the wear track.

In summary, adding Cu-SiO_2 core-shell NPs to the PTFE top layer, and laser texturing the stainless steel substrate and/or the PTFE coating can significantly extend the wear life of PDA/PTFE coatings without increasing the COF. These methods could be promising for a wide range of industries that use PTFE coatings since applying these methods can help reduce costs and improve performance. Overall, the findings of this dissertation signify a step forward in the development of new methods for improving the tribological properties of PTFE coatings.

5.2 Future Work

PTFE is a commonly used solid lubricant in different industries because of its low COF, chemical resistance, and high-temperature stability. While this dissertation provided different methods to improve the wear resistance of PTFE coatings, there is always room for further improvement in terms of wear life and adhesion.

Adding novel Cu-SiO_2 core-shell NPs to the PTFE top layer demonstrated a significant improvement in the wear life of PDA/PTFE coatings. The next step can be synthesizing PDA-coated Cu-SiO_2 core-shell NPs and incorporating them into the PTFE top layer. The adhesion properties of PDA can improve the bonding of the core-shell NPs to the PTFE particles and

therefore makes a more interconnected coating. Also, incorporating these core-shell NPs into the PDA under layer, as well as both the PDA under layer and PTFE top layer is essential to be studied in future research. This can help understand the optimum layer structure and NP distribution to achieve the best coating performance. Furthermore, it is suggested to study the effect of different synthesis parameters including the size, concentration, and surface chemistry of the Cu-SiO_2 core-shell NPs on the performance of PDA/PTFE coatings. Moreover, investigating different environmental and operating conditions on the long-term wear life and stability of PDA/PTFE coatings is of great importance for understanding their performance in real-world applications.

Laser texturing the stainless steel substrates has contributed to promising improvements in the wear life and wear resistance of PDA/PTFE coatings. Laser texturing the Hilbert curve pattern on the surface of stainless steel substrates can result in inconsistent texture grooves over a large area on the surface due to its relatively complicated pattern and can be a time-consuming process. Therefore, it is suggested to investigate laser texturing the several other patterns on the surface of stainless steel to find an optimum texture pattern that provides more consistency and less texturing time in comparison with the Hilbert curve patterns. Laser texturing each pattern can result in a surface with unique properties and can provide different advantages and disadvantages. It is important to consider the properties of stainless steel substrate and PDA/PTFE coatings to choose the best texture pattern. Besides, the laser parameters including laser power, laser frequency, and beam speed play an important role in the size and shape of the resulting texture grooves. It is suggested to investigate the combination of different laser parameters in future studies and find the most suitable ones for laser texturing stainless steel that is supposed to be coated with PDA/PTFE. Another topic that can be studied in future works is

the type of laser used such as CO_2, fiber, and diode laser on the resulting texture grooves. All of these variables can help achieve the best texture grooves on the surface of stainless steel substrates and therefore result in an ultimately improved PTFE-coated surface for industrial applications.

Also, laser surface texturing on the soft PTFE coatings needs further investigation. For future works, studying the effect of different laser parameters on the tribological, mechanical, and chemical properties of PTFE coatings can be an interesting and important topic. In the current dissertation, only one specific combination of laser power and laser frequency was used to laser texture the PTFE coatings. Examining different laser parameters (power, frequency, and speed) on the resulting surface textures as well as the different properties of PTFE coatings need to be studied. Moreover, since the thickness of PTFE coatings can play an important role, it is suggested to study the effect of laser texturing on PTFE coatings with different thicknesses and understand how coating thickness can affect the resulting textures.